SAND2015-8473PE

Exceptional service in the national interest

Sandia National Laboratories

Impacts of Microstructural Variability on Mechanical Response

Gustavo M. Castelluccio

Postdoctoral Appointee, Sandia National Laboratories

September 25th 2015,
University of New Mexico

U.S. DEPARTMENT OF ENERGY

National Nuclear Security Administration

Sandia National Laboratories is a multi-program laboratory managed and operated by Sandia Corporation, a wholly owned subsidiary of Lockheed Martin Corporation, for the U.S. Department of Energy's National Nuclear Security Administration under contract DE-AC04-94AL85000. SAND NO. 2011-XXXXP

Big challenges require new materials

Material innovation process

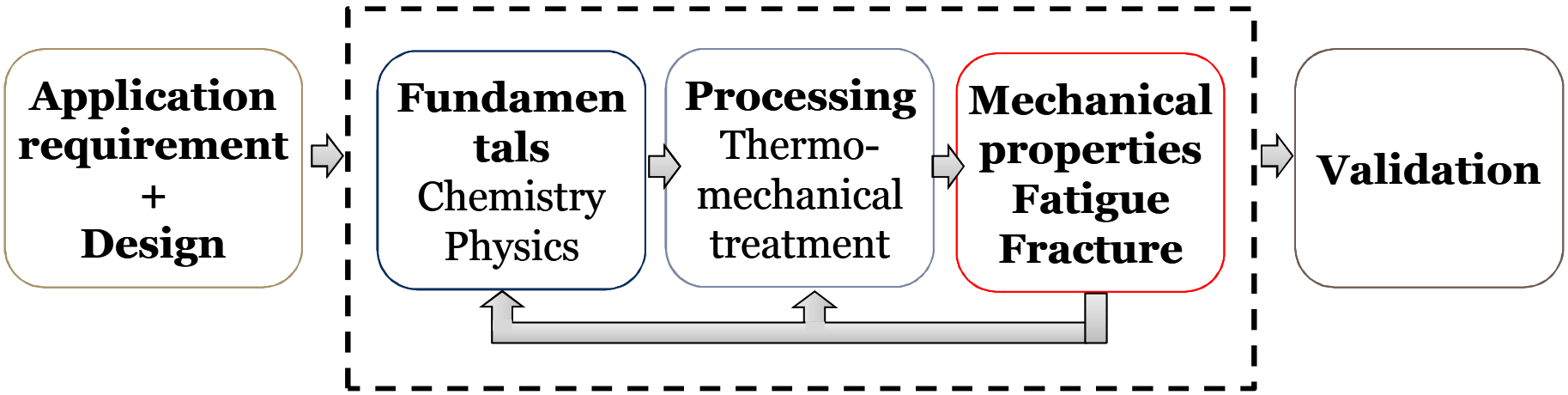

The key to success is to integrate knowledge into efficient design strategies

Sandia National Laboratories

Challenge

Design modeling frameworks to optimize the mechanical response as a function of microstructural attributes.

Key aspects:

1. Quantify the mechanical response driving force.

2. Determine an adequate domain to assess the driving force.

Agenda

- Mesoscale Modeling of Microstructurally Small Fatigue Cracks

- Mesoscale-sensitive crystal plasticity models

- Sources of Variability in Components

Georgia Tech

[1] Woodruff School of Mechanical Engineering

[2] Materials Science and Engineering

Sandia National Laboratories

Mesoscale Modeling of Microstructurally Small Fatigue Cracks

Gustavo M. Castelluccio

David L. McDowell[1,2]

Integrated Computational Materials Engineering

Boeing 787

http://www.flickr.com/photos/tsuna72/12608803893

Integrated Computational Materials Engineering

Turbine disks failures

Boeing 767

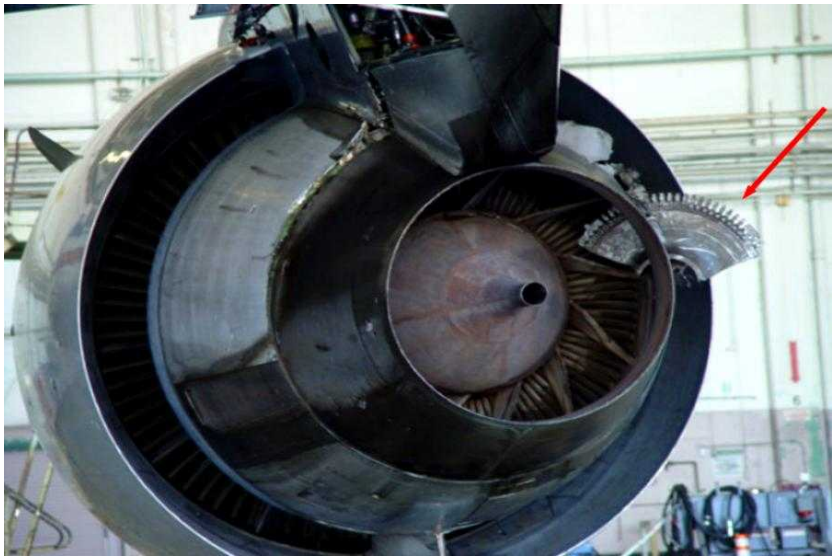

http://webcommunity.ilvolo.it/

Airbus A380

http://www.dailymail.co.uk/

Integrated Computational Materials Engineering

Bimodal microstructure in turbine disks

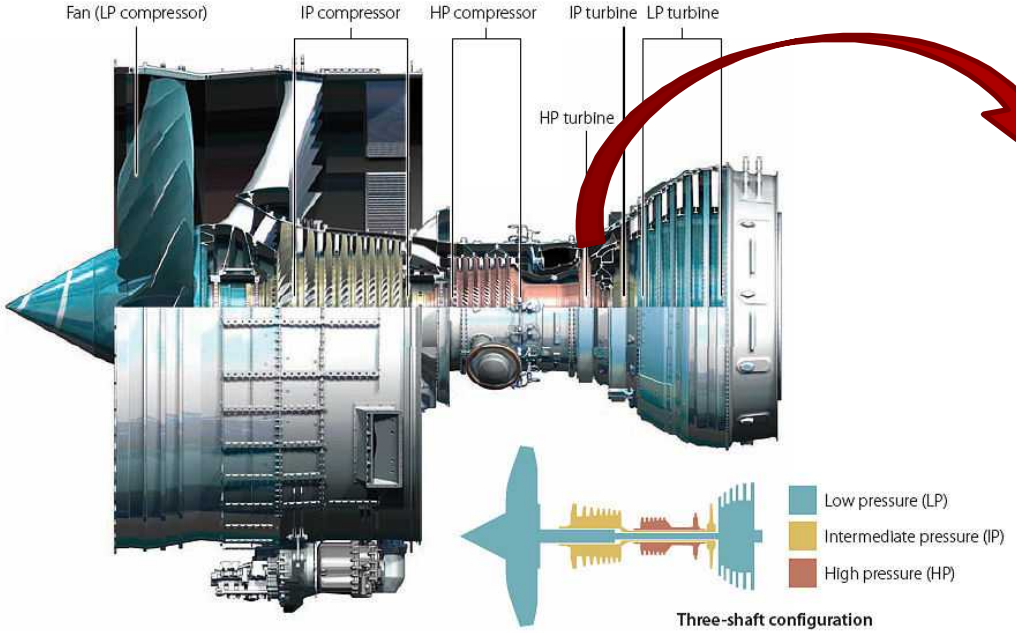

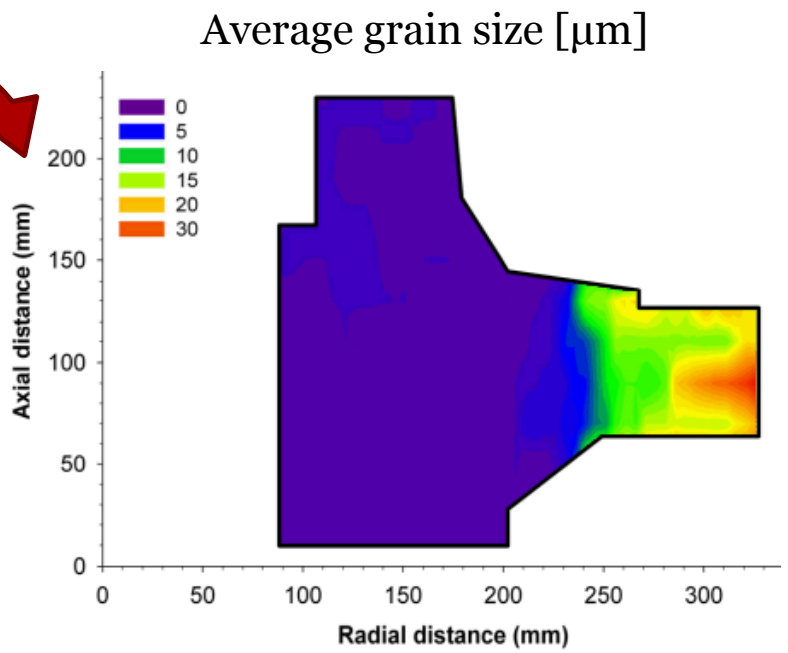

http://aviationtroubleshooting.blogspot.co.uk/2010_11_01_archive.html

Mitchell, R. J. et al. In Superalloys Conference, TMS , 2008.

Early Stages of Fatigue Damage

Microstructurally Small Cracks (MSCs)

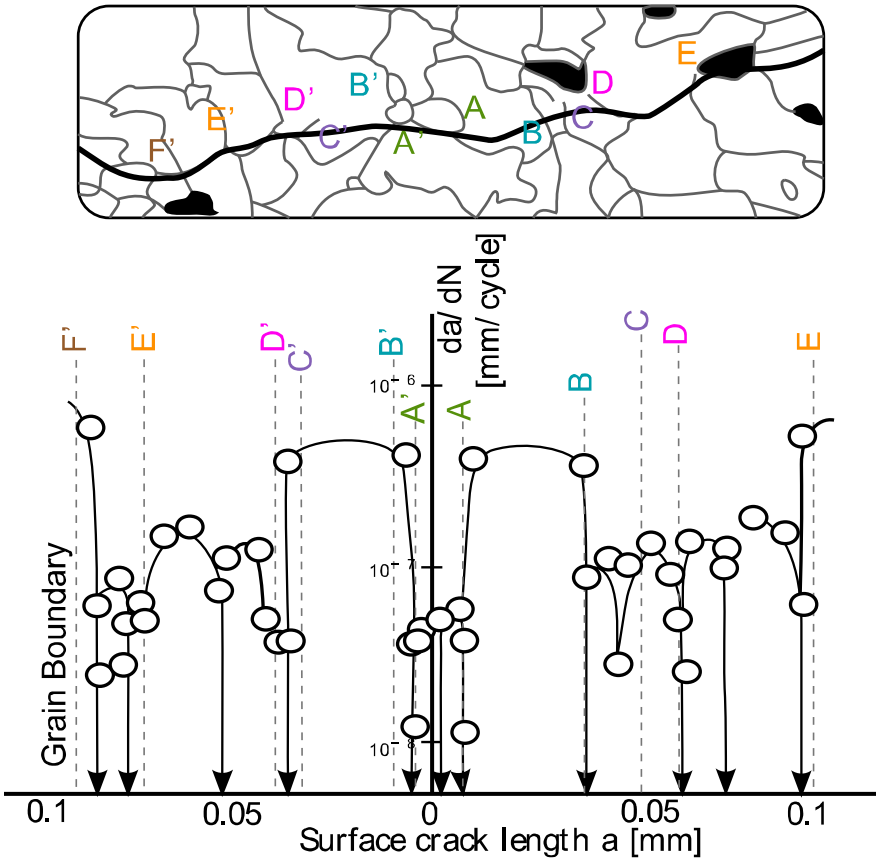

Adapted from **Tokaji K. et al.**, Short Fatigue Cracks, ESIS 13, 85-99, (1992)

Early Stages of Fatigue Damage

Hierarchical approach to estimate fatigue life:

$$N_f = N_{Nuc} + N_{MSC} + N_{PSC} + N_{LC}$$

$$N_{nuc} = \frac{\alpha_g}{d_{gr}} \Delta\gamma^{-2}$$

No single dominant mechanism

$$\left.\frac{da}{dN}\right|_{msc} = \phi\left\langle \Delta CTD - \Delta CTD_{th} \right\rangle$$

Dominated by dislocation emission

$$\left.\frac{da}{dN}\right|_{psc} = C\Delta J^m$$

Dominated by isotropic plasticity

$$\left.\frac{da}{dN}\right|_{lc} = C\Delta K^m$$

Dominated by elasticity

Fatigue Indicator Parameter (FIP)

FIPs quantify transgranular fatigue driving force

Fatemi and Socie (1988)

$$FIP^{\alpha} = \frac{\Delta\gamma^{\alpha}}{2}\left(1 + k\frac{\sigma_n^{\alpha}}{\sigma_y}\right)$$

$$\Delta CTD \propto FIP$$

Castelluccio & McDowell, Int. J. Fract. (2012)

Depends on the environment

$$N_{nuc} = \frac{\alpha_g}{d_{gr}}\left(FIP\right)^{-2}$$

$$\left.\frac{da}{dN}\right|_{MSC}^{\alpha} \approx \phi\left\langle A \cdot FIP^{\alpha}(a) - \Delta CTD_{th}\right\rangle$$

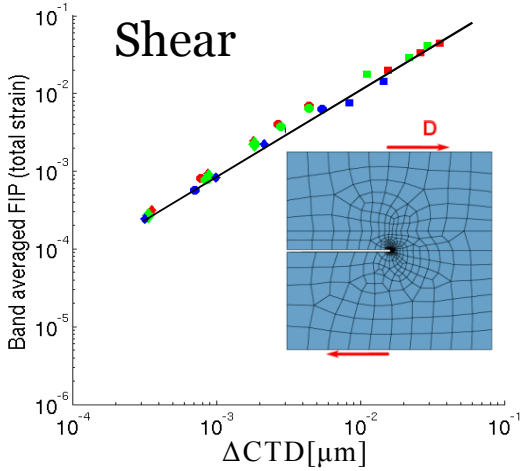

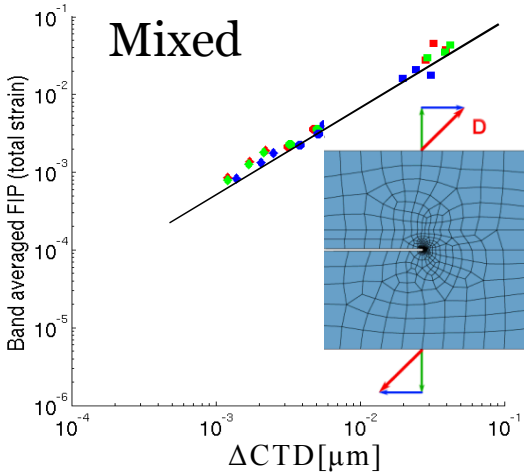

Crystal Plasticity Model

Crystal plasticity + Elastic damage for RR1000 @ 650C

B. Lin et al. Mater. Sci. Eng. A, 527, 3581-87, 2010

- 12 octahedral and 6 cube slip systems
- Isotropic damage coupled with elasticity along critical planes

$$\frac{\dot{\gamma}^{(\alpha)}}{\dot{\gamma}_0} = exp\left[-\frac{F_0}{\kappa\theta}\left\langle 1-\left\langle\frac{\left|\tau^{(\alpha)}-B^{(\alpha)}\right|-S^{(\alpha)}\mu/\mu_0}{\hat{\tau}_o\,\mu/\mu_0}\right\rangle^{p}\right\rangle^{q}\right] sgn(\tau^{(\alpha)}-B^{(\alpha)})$$

$$\dot{S}^{(\alpha)} = \left[h_S - d_D\left(S^{(\alpha)}-S_0^{(\alpha)}\right)\right]\left|\dot{\gamma}^{(\alpha)}\right|$$

$$\dot{B}^{(\alpha)} = h_B\dot{\gamma}^{(\alpha)} - r_D^{(\alpha)}B^{(\alpha)}\left|\dot{\gamma}^{(\alpha)}\right|$$

$$r_D^{(\alpha)} = \frac{h_B\mu_0}{S^{(\alpha)}}\left\{\frac{\mu_0'}{f_c\lambda}-\mu\right\}^{-1}$$

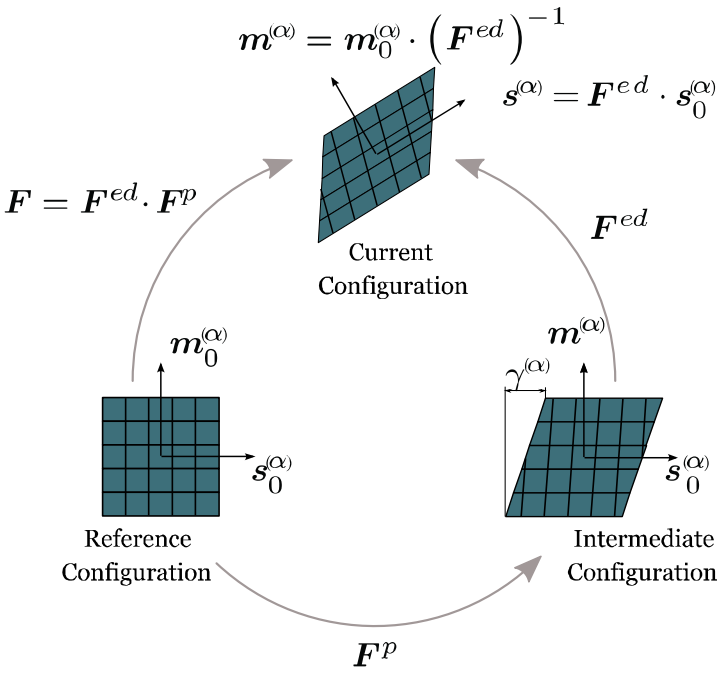

Framework Assumptions

Sandia National Laboratories

Main Assumptions:

1. Perfect crystallographic crack growth (Stage I).

2. A few computed loading cycles for a given crack configuration result in fatigue indicator parameters (FIPs) that correlate with the crack growth within the next grain (albeit neglecting transient cyclic hardening or softening details).

3. FIPs averaged over mesoscale domains are more useful than pointwise computed values: (i) physical process zone and (ii) numerical regularization.

Fatigue Damage Domain

For trangranular failure, FIPs are averaged along bands parallel to slip normal directions.

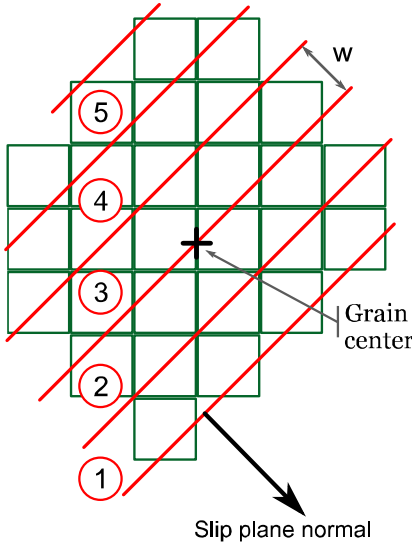

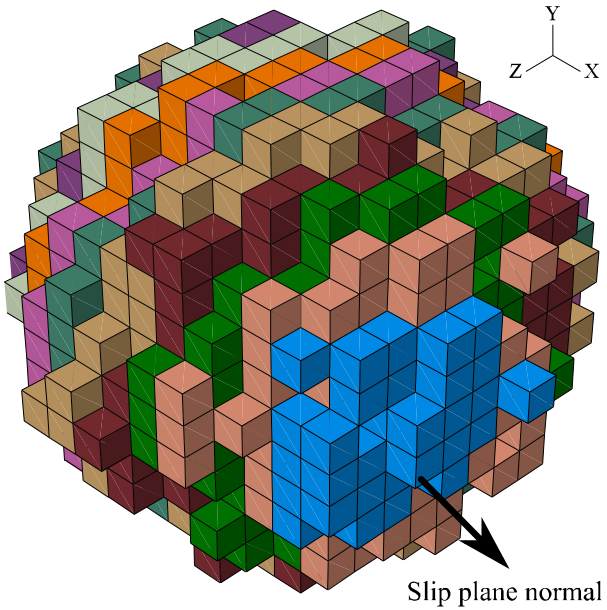

$$\Rightarrow \quad \mathrm{FIP}^{\alpha}_{meso} = Avg(\mathrm{FIP}^{\alpha}) \ per\ band$$

Finite Elements Simulations

- 52 grains (~65 elements)
- 1% strain along Z axis
- Periodic boundaries
- 3375 elements
- R_{ε}=0.1

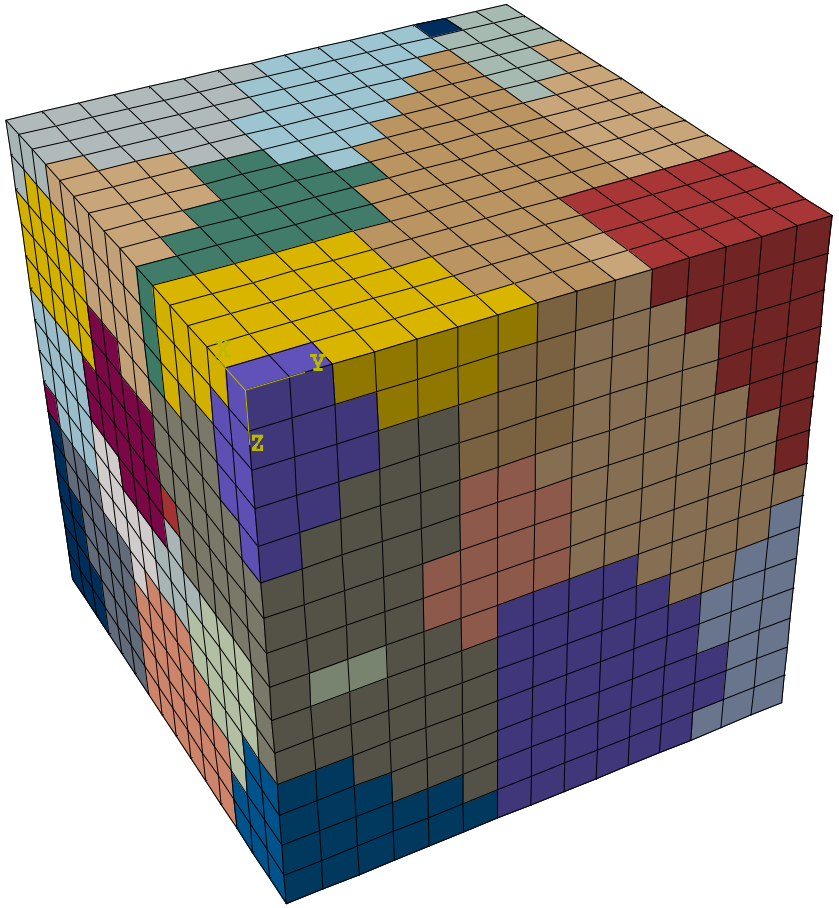

Modeling Crack Nucleation

Statistical characterization of crack nucleation:

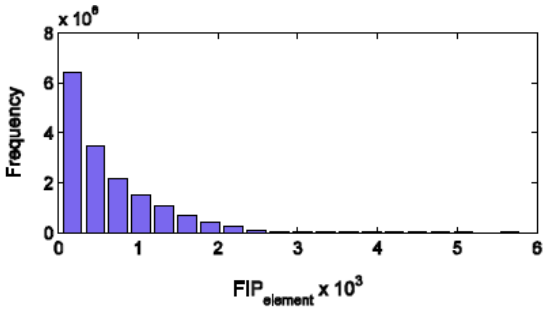

FIP per element

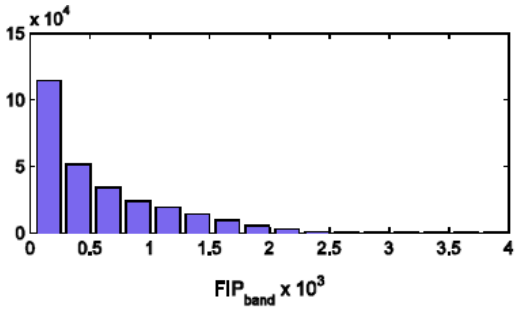

FIP band average

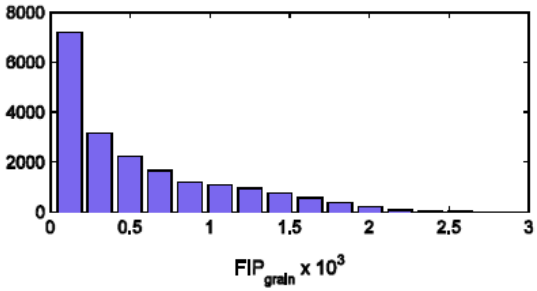

FIP grain Average

Increasing size of the sampling domain

Modeling Crack Nucleation

FIP variability within grains

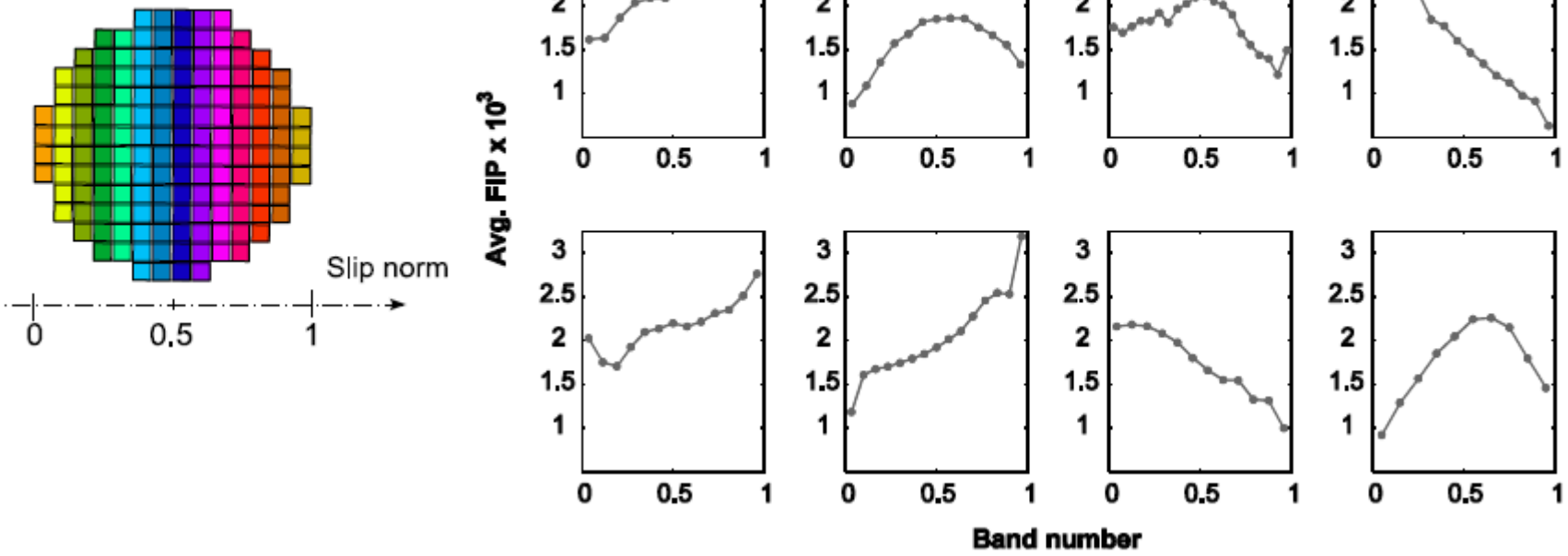

Modeling Crack Nucleation

Non-local grain influence:

Random realizations

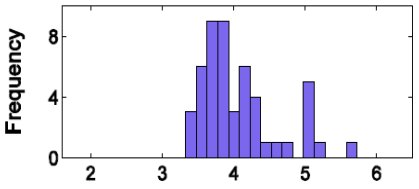

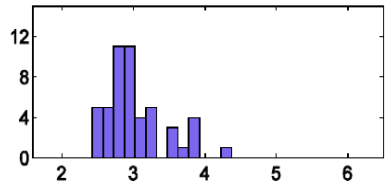

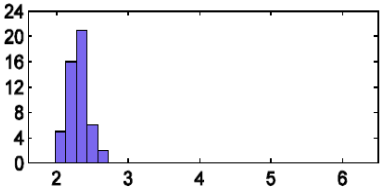

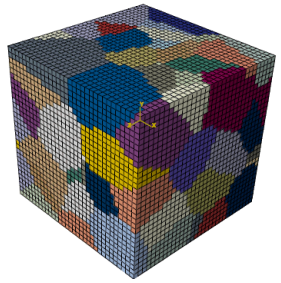

Identical nucleation grain

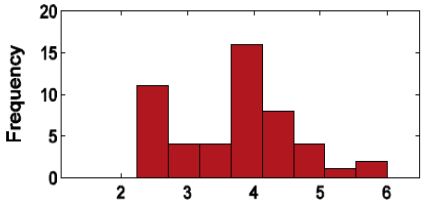

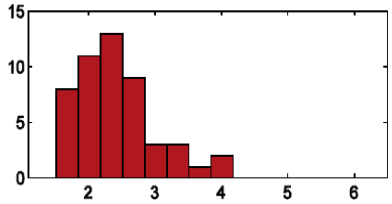

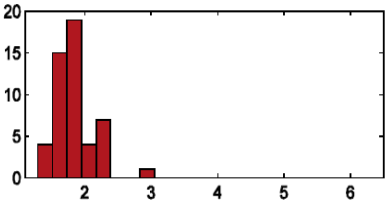

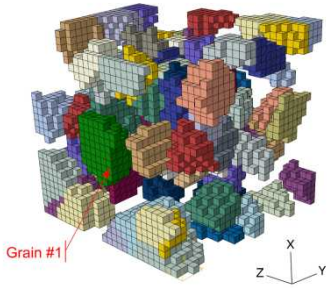

Identical first neighbor grains

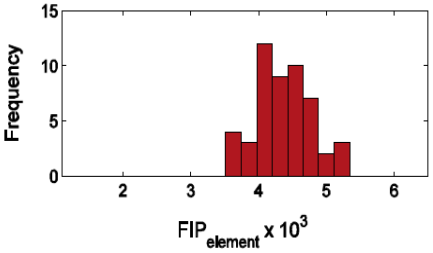

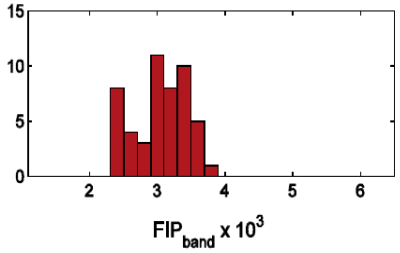

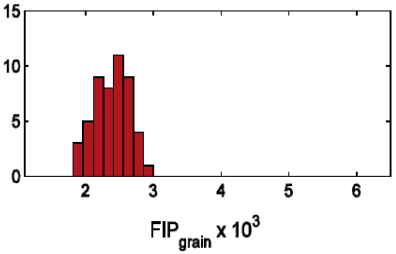

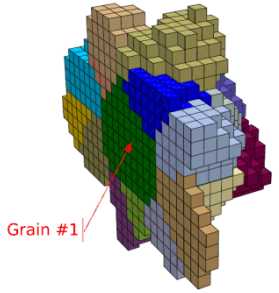

Modeling Crack Growth

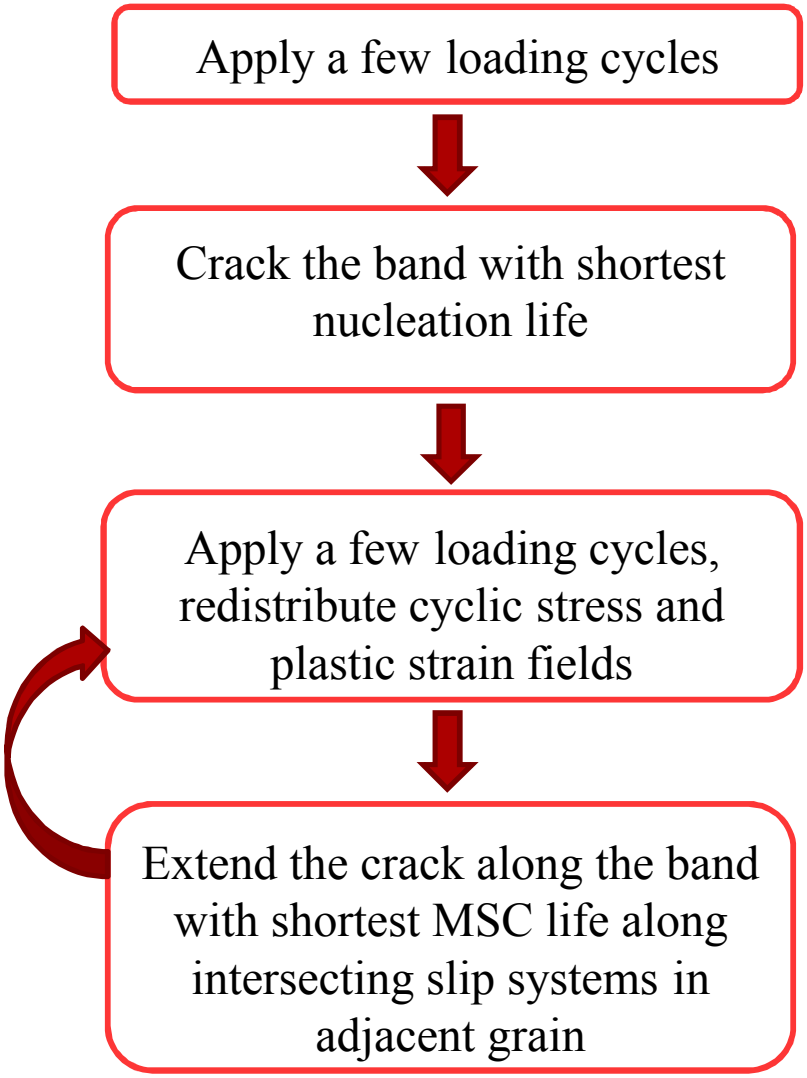

1st grain (Nucleation)

$$N^{\alpha}_{Nuc} = \frac{\alpha_g}{d_{gr}}\left(FIP^{\alpha}_0\right)^{-2} \qquad d_{gr} = D_{st} + \sum_{i}^{n} \omega^i D^i_{nd}$$

Subsequent grains (MSC) (analytical projection)

$$N^{\alpha}_{MSC} = \int_{o}^{d_{gr}} \frac{da}{\phi\left\langle FIP^{\alpha}_o A\left(1 - \frac{1}{2}a^2\right) - \Delta CTD_{th}\right\rangle} - N^{\alpha}_{Hist}$$

$$N^{\alpha}_{MSC} = \frac{1}{\sqrt{c_1 c_2}} \tanh^{-1}\left(d_{gr}\sqrt{\frac{c_2}{c_1}}\right) - N^{\alpha}_{Hist}$$

$$c_1 = 2d^2_{gr}c_2 - \phi\Delta CTD_{th} \qquad c_2 = \frac{\phi A FIP^{\alpha}_0}{2d_{gr}d^{ref}_{gr}}$$

Modeling Crack Growth

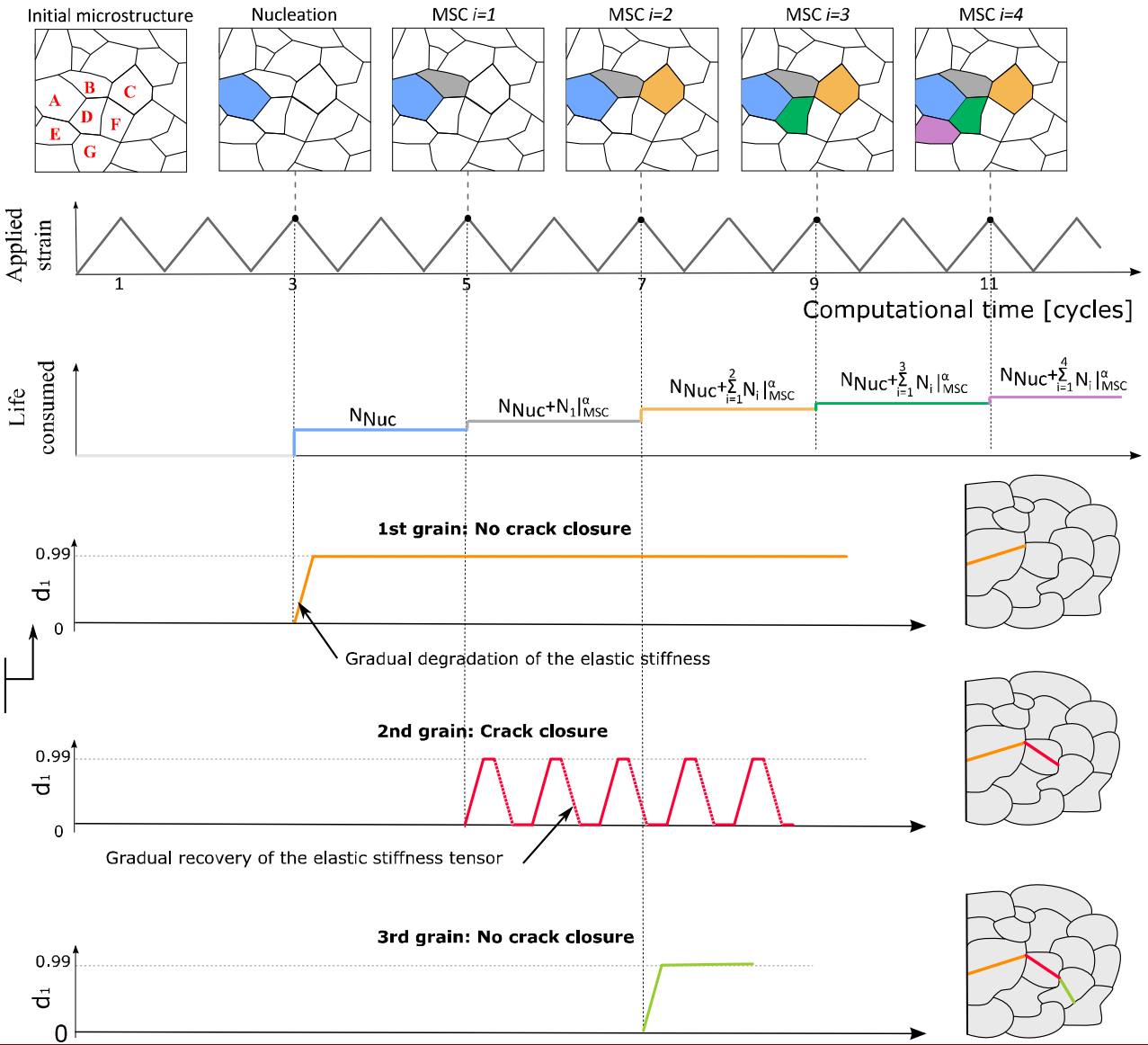

d_1 is proportional to the evolution of the elastic stiffness tensor

Modeling Crack Growth

As large as (ALA) grains

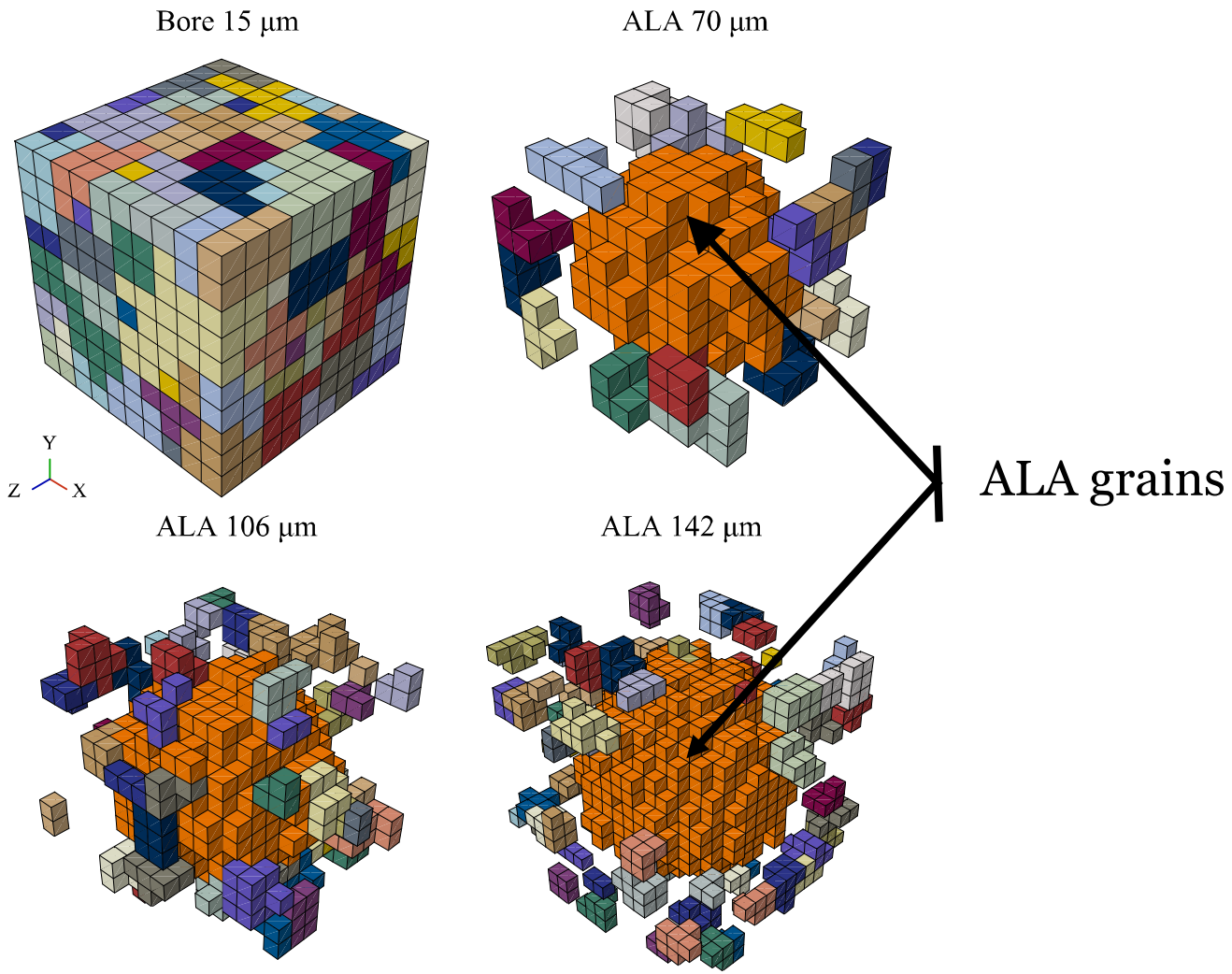

Modeling Crack Growth

Fatigue life predictions for different ALA grain size

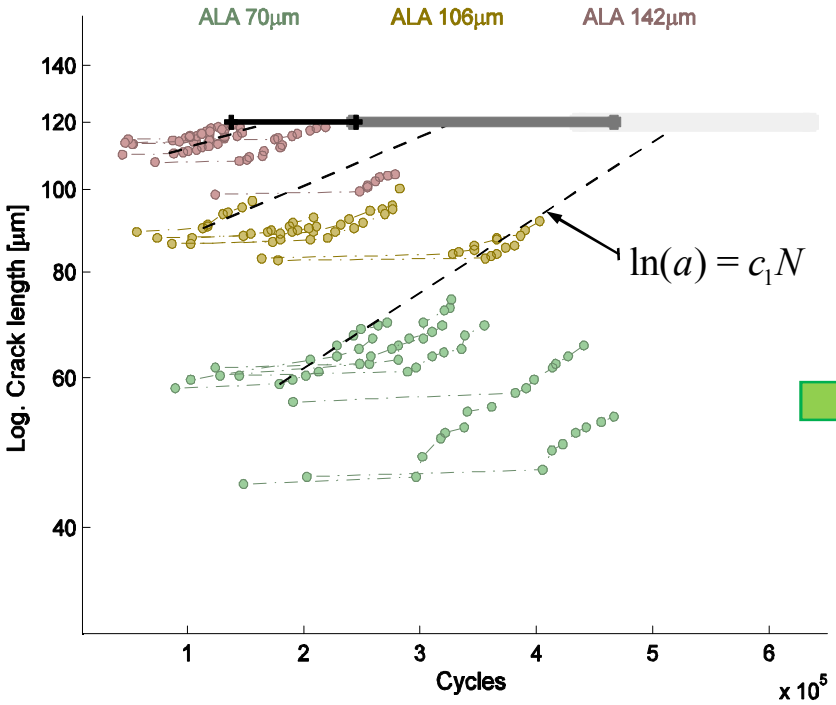

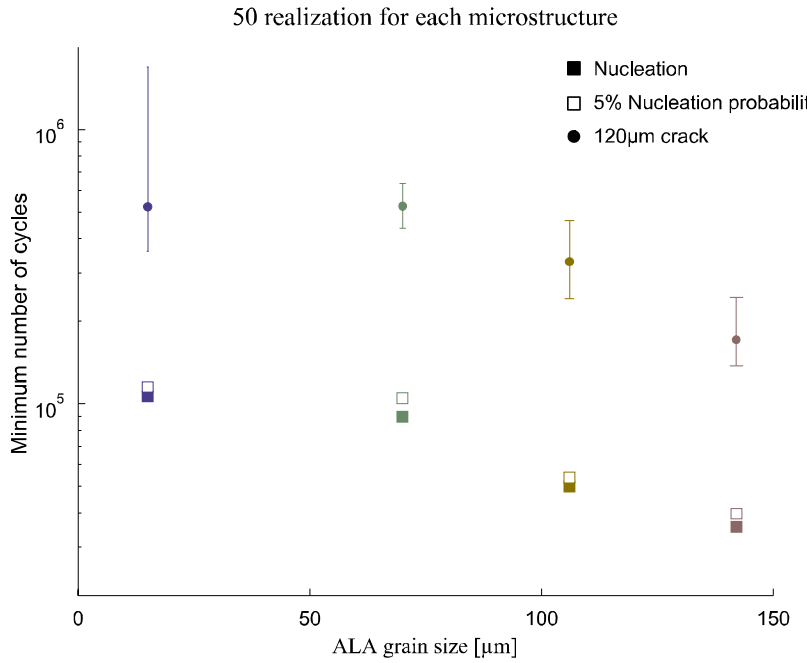

Mesoscale-sensitive crystal plasticity models

Gustavo M. Castelluccio

David L. McDowell

Cyclic Mesoscale Dislocation Structures

Sandia National Laboratories

Approximate dislocation substructures as a function of crystal orientation

[001] promotes double slip (labyrinth) and deformation is carried by screw dislocation on two <111> planes independently.

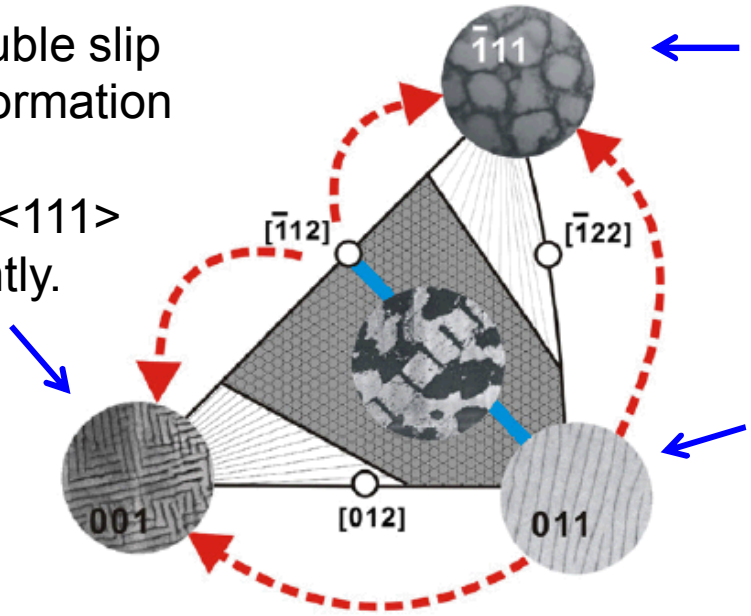

[-111] promotes multiple slip and cross slip leading to cells with low misorientation.

[011] to [-112] promote single slip PSBs and walls and deformation is carried by screw dislocations gliding along <111> plane.

Li et al. 2011. Progress in Materials Science 56 (3): 328–77.

High strain amplitudes and mean stresses and large number of cycles tend to promote cells.

Mesoscale-Sensitive Crystal Plasticity

Sandia National Laboratories

Intergranular

Mesoscale structure constraint and rotation

Atomistic

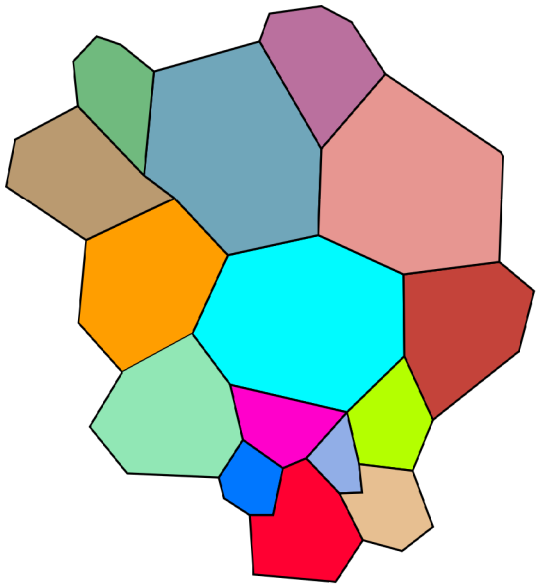

Dislocation bow-outs control dislocation production

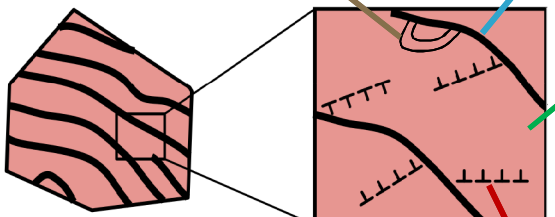

Wall thickness controls back stress softening

Cross slip and annihilation (H-dependent) control dislocation depletion

Pile-ups (H dependent) control isotropic hardening to avoid resolving polar densities within structures.

Mesoscale-Sensitive Crystal Plasticity

The approach includes:

- Dislocation **multiplication**, **annihilation** and **cross slip**.
- **Athermal stress** based on dislocation pile-up.
- **Back stress** based on Eshelby's inclusion approach.
- Physics-based rather than fitting-based.
- Calibration based on single-crystals

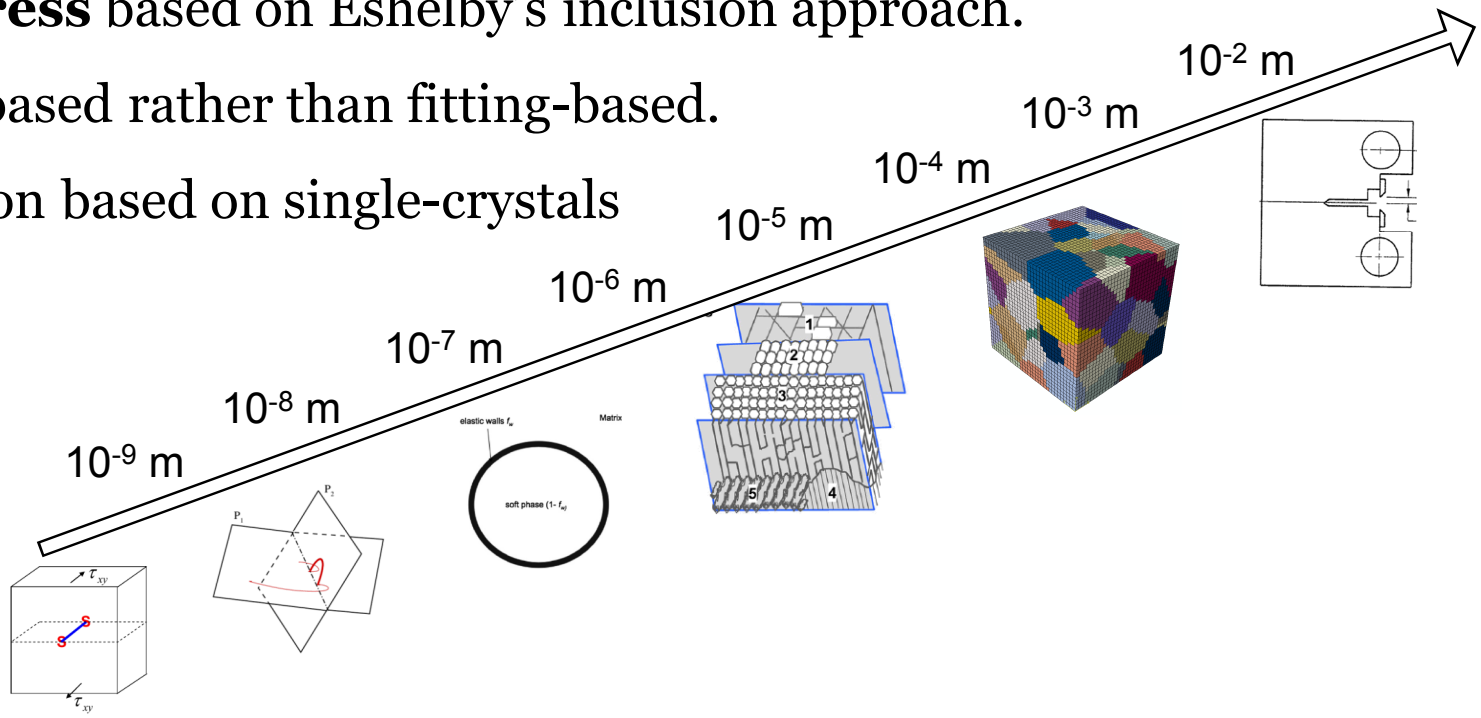

Mesoscale-Sensitive Crystal Plasticity

Sandia National Laboratories

• **Mesoscale frameworks** are feasible computational tools to assess the resistance against fracture and fatigue.

• The key to success is to **simplify** lower length scales and model explicitly those microstructural attributes that control the resistance.

• Experimental and modeling efforts should be balanced to convey efficient **integrated computation approaches**.

Sources of Variability in Components

Gustavo M. Castelluccio
Matthew Brake
John Emery
Joe Bishop

Sources of Uncertainty in Components

Sandia National Laboratories

Microstructural, geometrical and in-service conditions impact the variability of the mechanical response in components

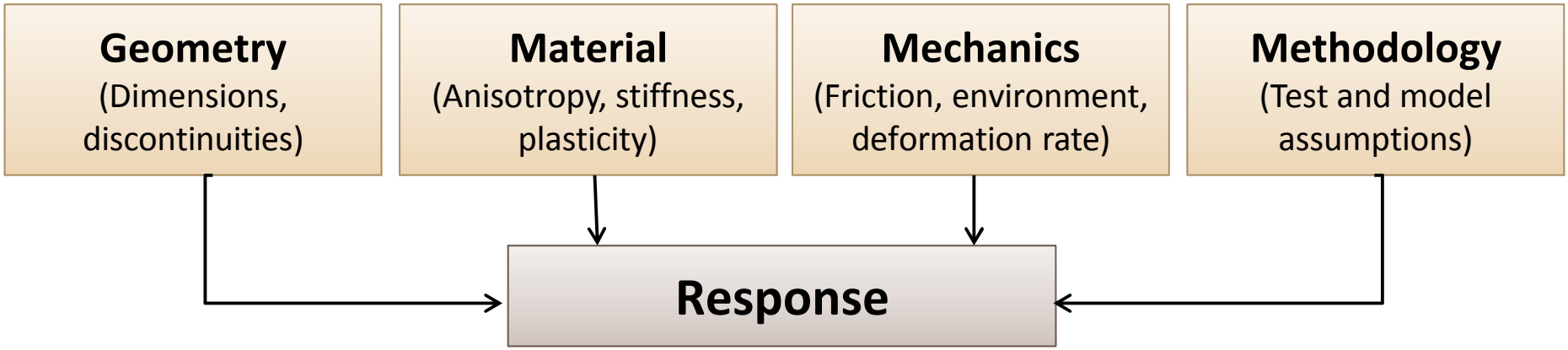

Sources of Uncertainty in Components

Example: Fasteners

- Highly nonlinear: geometry discontinuities, friction, plastic deformation.
- Manufacturing and installation variability.

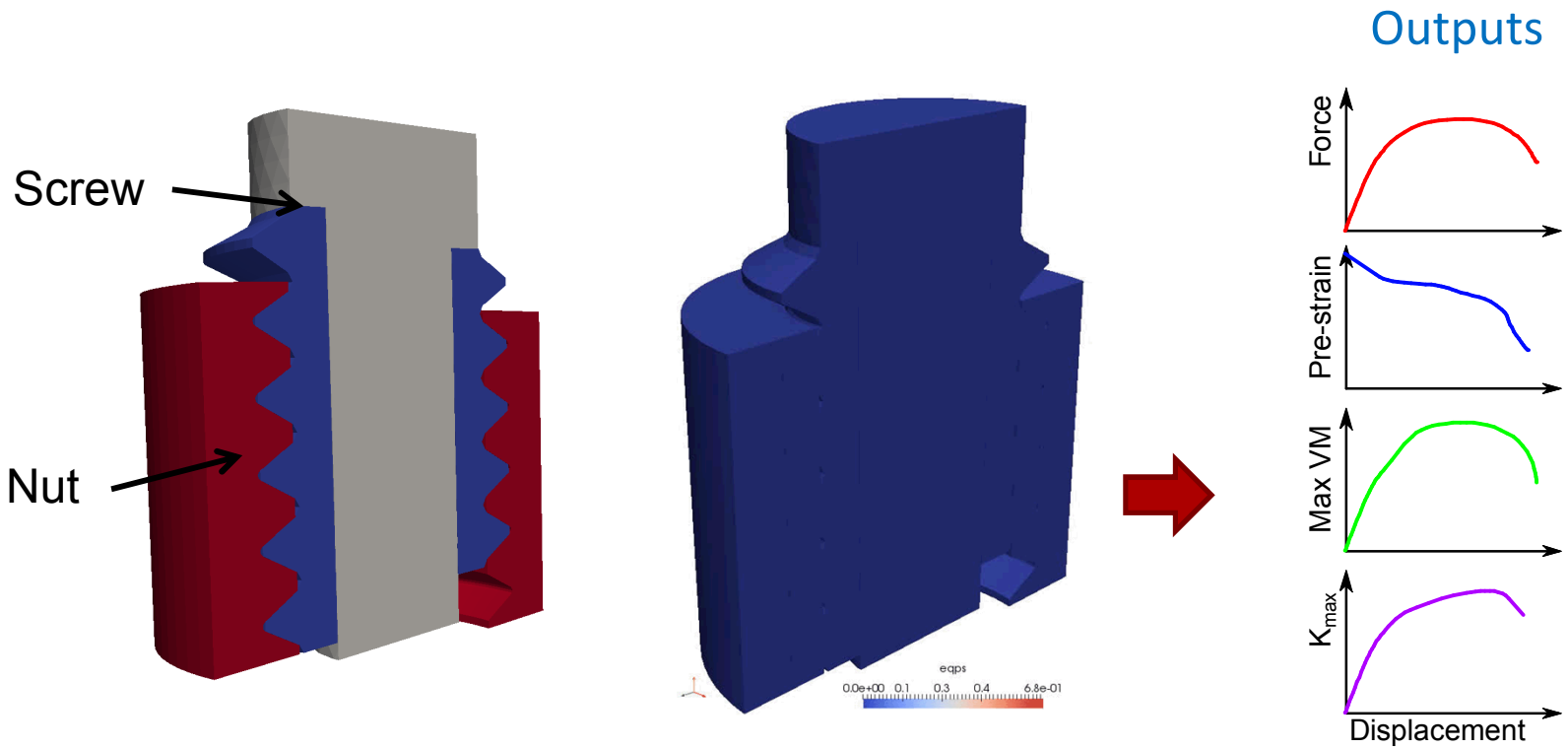

Sources of Uncertainty in Components

Variability induced by friction and pre-loading conditions

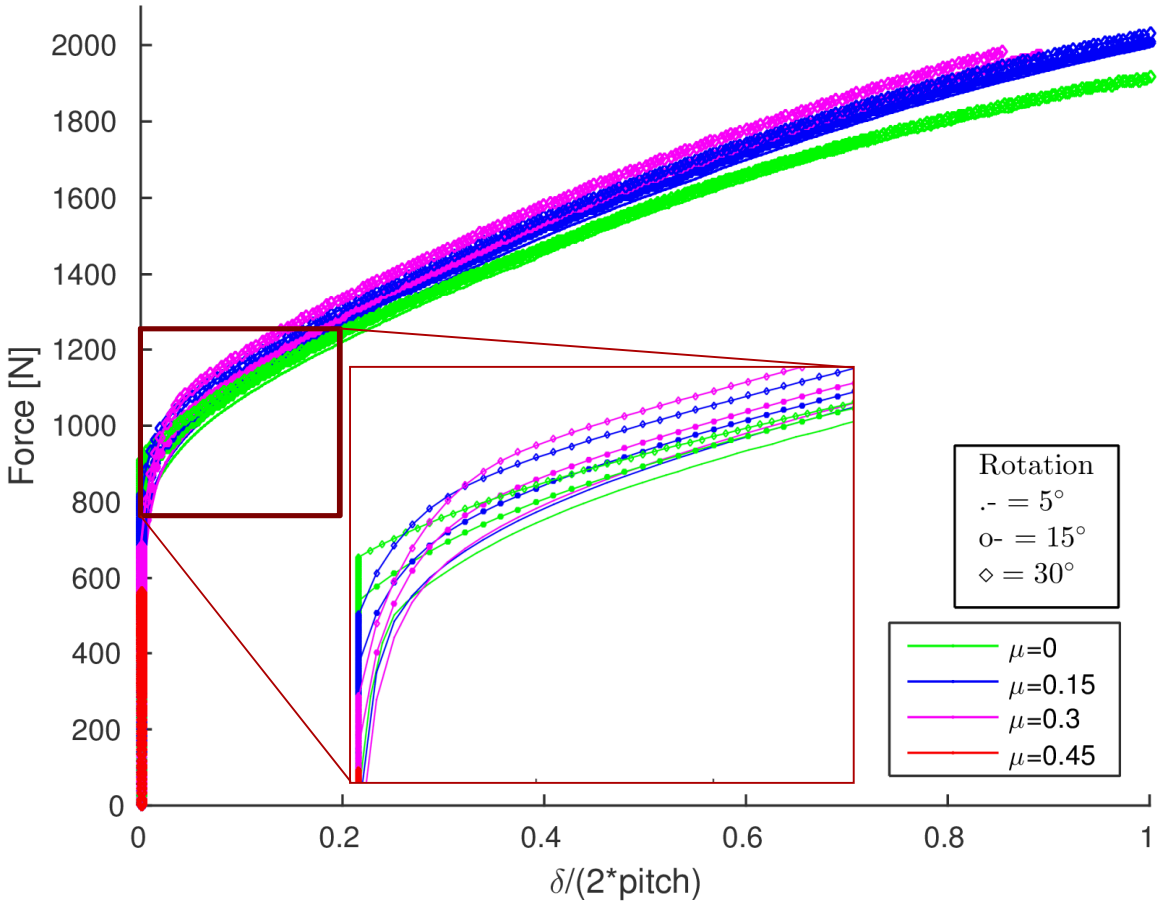

How sensitive is the mechanical response to in-service installation, material or mechanical properties?

Sources of Uncertainty in Components

Example: I-beams
Microstructural attributes induce local variability in the mechanical response.

Initial microstructure

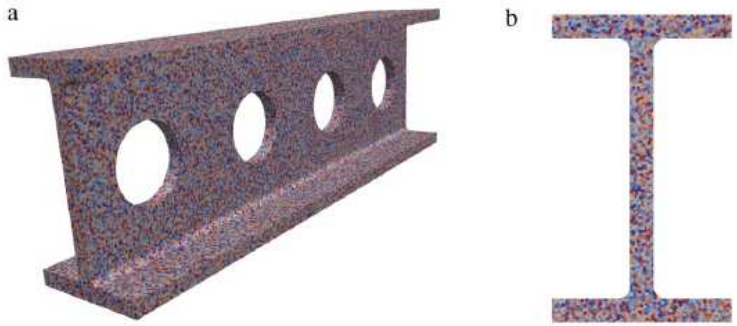

von Mises stress

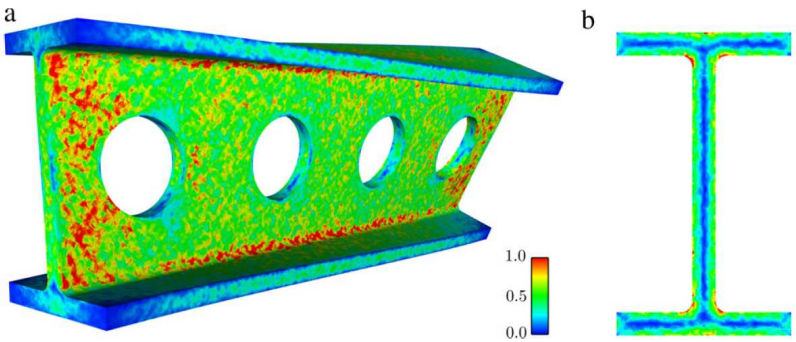

Can we estimate microstructural response without brute force simulations?

Bishop J. et al., Comput. Methods Appl. Mech. Engrg, 287,262-289, (2015)

Sources of Uncertainty in Components

Statistical characterization of mechanical response

$$\mathbf{R}(\mathbf{x}) = \boldsymbol{\mu}(\mathbf{x}) + \mathbf{a}(\mathbf{x})\,\mathbf{Y}(\mathbf{x}) = \begin{pmatrix} \mu_1(\mathbf{x}) \\ \mu_2(\mathbf{x}) \\ \mu_3(\mathbf{x}) \end{pmatrix} + \begin{pmatrix} \sigma_1(\mathbf{x}) & 0 & 0 \\ 0 & \sigma_2(\mathbf{x}) & 0 \\ 0 & 0 & \sigma_3(\mathbf{x}) \end{pmatrix} \begin{pmatrix} Y_1(\mathbf{x}) \\ Y_2(\mathbf{x}) \\ Y_3(\mathbf{x}) \end{pmatrix}$$

$$Y_k(\mathbf{x}) = h_k(G_k(\mathbf{x})) = F_k^{-1} \circ \Phi(G_k(\mathbf{x})),\ k = 1, 2, 3$$

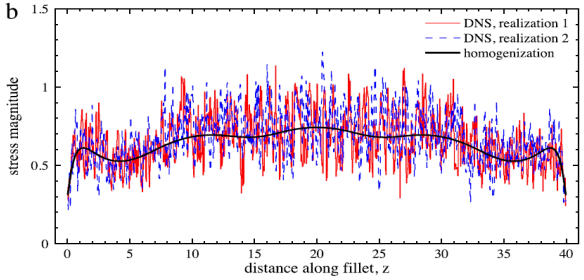

RVE Modeling → **Statistical Characterization** → **Component Response** → **Brute Force Validation**

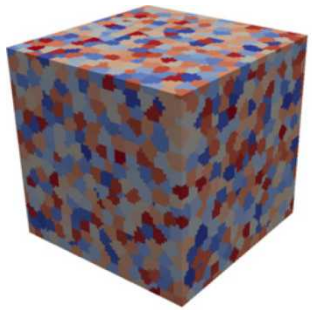

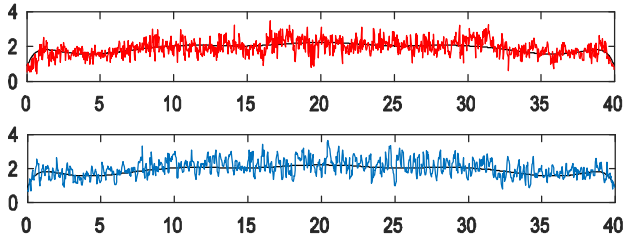

Acknowledgments

G. M. Castelluccio is deeply grateful for the support provided in the last six years by:

- The **Roberto Rocca Program**
- **QuesTek Innovations LLC** and **AFRL under** the Air Force Contract No. FA8650-10-C-5206.
- **Systems Solutions, Inc**. (Technical Monitor: **Dr. Nam Phan, NAVAIR**)
- **Bettis Atomic Power Laboratory** (Technical Monitor: Dr. Clint Geller)
- **Sandia National Laboratories** (Matthew Brake and Diane Peebles)

Collaborations with **UES** and **Rolls Royce** are also acknowledged as part of this program.

Sandia National Laboratories

Questions?

Sandia National Laboratories

Appendix

Crystal plasticity framework

Atomistic scale

$$\dot{\gamma}^{\alpha} = \rho_{s_m}^{\alpha} l_{struct} b \nu_G \exp\left(-\frac{F_0}{k_b T}\left(1 - \left[\frac{\left\langle \left| \tau^{\alpha} - B^{\alpha} \right| - S_0^{\alpha} \right\rangle}{s_t^0 \frac{C_{44}}{C_{44}^0}} \right]^{p} \right)^{q} \right) \operatorname{sgn}\left(\left| \tau^{\alpha} - B^{\alpha} \right| - S_0^{\alpha} \right)$$

$$\dot{\rho}_{s_m}^{\alpha} = \underbrace{\frac{k_{multi}}{b l_{struct}} \left| \dot{\gamma}^{\alpha} \right| - \frac{2 y_s}{b} \rho_{s_m}^{\alpha} \left| \dot{\gamma}^{\alpha} \right|}_{\text{Essmann \& Mughrabi (1979)}} \underbrace{- \Upsilon \frac{2 \left| \dot{B}^{\alpha} \right|}{\mu b d_{struct}}}_{\text{Castelluccio}} + \underbrace{\frac{d_{struct}}{d_0 t_0} \left(\rho_{s_m}^{\zeta} e^{\left(-V_{cs} \frac{\tau_{III} - \tau^{\alpha}}{k_B T} \right)} - \rho_{s_m}^{\alpha} e^{\left(-V_{cs} \frac{\tau_{III} - \tau^{\zeta}}{k_B T} \right)} \right)}_{\text{Verdier, Fivel and Groma (1998)}}$$

$$S^{\alpha} = S_0^{\alpha} + \alpha^{*} \frac{\mu b}{d_{struct}} + \mu b \left(A_{\alpha\alpha} \rho_{s_m}^{\alpha} \right)^{1/2}$$

$$\tau_{III} = \frac{\mu b}{4 \pi y_s}$$ Brown (2001)

$$V_{cs} = V_{cs}(\tau)$$

$$d_{struct} = K \mu b \tau^{-1}$$ Sauzay (2011)

k_{multi} ⇔ 2 ->PSB-Laby, 1 ->Cell

$$l_{struct} = \eta d_{struct}, \eta \approx 1 - 20$$

$$\Upsilon = 1 \Leftrightarrow \begin{cases} dB > 0 \,\&\, 0 > \dot{\gamma} \\ dB < 0 \,\&\, 0 < \dot{\gamma} \end{cases}$$

$$\left(A_{ii} \right)^{\sim 0.5} \square\, 0.35$$

$$\mu = \mu(T, \mathbf{C}, c_H)$$ Wen (2011)

Determination of parameters

Constants from atomistic models (values and sensitivity)

$\nu \approx 1\times10^{12}$ $\quad b \approx 2.5\times10^{-10} m$ $\quad C_{11}, C_{12}, C_{44}, C_{44}^0$

$\tau_{III} \cong \dfrac{\mu b}{4\pi y_s}$

$y_s \approx y_s(SFE)$

S_0^{α}

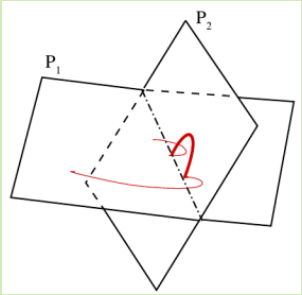

Expected hydrogen influence: **High**

F_0

s_t^0

$0 < p < 1{,}1 < q < 2$

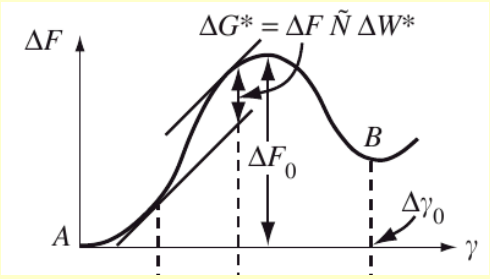

Expected hydrogen influence: **Medium**

A_{ij}

dislocation interaction coefficients

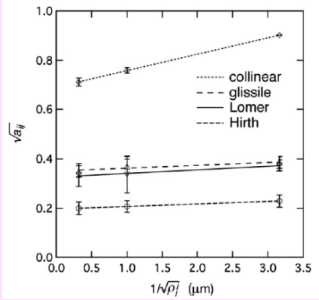

Expected hydrogen influence: **medium-?**

$V_{cs} = 20 - 1800b^3$

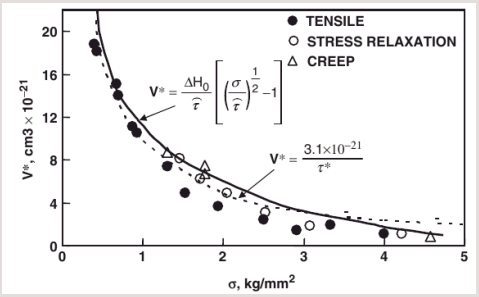

Expected hydrogen influence: **low--?**

Athermal stress formulations

Mesoscale

$$\dot{B}^{\alpha} = \left[\frac{f_w}{1-f_w}\frac{2\mu\left(1-2S_{1212}\right)}{\left(1+4\mu S_{1212} f_{Hill}\right)}\right]\mathbf{D}^{p} : \left(s^{\alpha}\otimes m^{\alpha}\right),$$

$\dot{B}^{\alpha}$: Back stress rate

$\mathbf{D}^{P}$: Plastic rate of deformation tensor

Eshelby tensor for prolate spheroid under shear

Mura (1987)

$$S_{1212} = \frac{\pi\eta_{struc}{}^{2} + \left(\eta_{struc}{}^{2} - 1.75 - 2\nu_p\eta_{struc}{}^{2} + 2\nu_p\right)C_{I2}}{8\pi\left(1-\nu_p\right)\left(\eta_{struc}{}^{2}-1\right)} \qquad C_{I2} = \frac{2\pi\eta_{struc}\left(\eta_{struc}\sqrt{\left(\eta_{struc}{}^{2}-1\right)} - \cosh^{-1}\left(\eta_{struc}\right)\right)}{\sqrt{\left(\eta_{struc}{}^{2}-1\right)^{3}}}$$

S_{1212} varies from 0.3215(PSB) to 0.238 (Cell)

$$f_{Hill} = (1-f_w)\frac{3}{2}\frac{\dot{\varepsilon}_{eff}}{\dot{\sigma}_{eff}}$$

$$\mu_p = \frac{\mu}{1+2\mu f_{Hill}}$$

Hill (1965)

$$\nu_p = \frac{\nu + \frac{2}{3}\mu\left(1+\nu\right)f_{Hill}}{1+\frac{4}{3}\mu\left(1+\nu\right)f_{Hill}}$$

$$fw = f_{inf} + \left(f_0 - f_{inf}\right)\exp\left(\frac{-\Delta\gamma_p/2}{g_p}\right)$$

Estrin (1998)

Mesoscale-Sensitive Crystal Plasticity

Sandia National Laboratories

$\Delta\gamma^{max} < \gamma_M^{pl}$ → Yes → $\eta = \eta_{veins}$

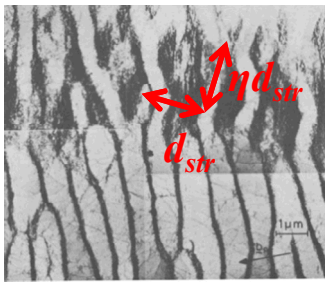

No

$\Delta\gamma^{max} > \gamma_{PSB}^{pl}$ → Yes → $\eta = \eta_{cell}$

No

$\Delta\gamma^{2^{nd}max} > \gamma_M^{pl}$

$\Delta\gamma^{CrossS(max)} < \gamma_M^{pl}$ → Yes → $\Delta\gamma^{Hirth(max)} > \gamma_M^{pl}$ → No → $\eta = \eta_{cell}$

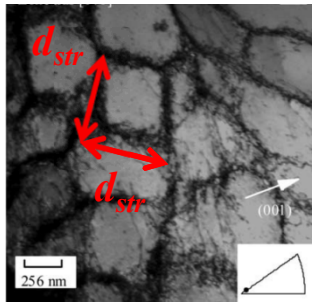

No

$\eta = \eta_{PSB}$

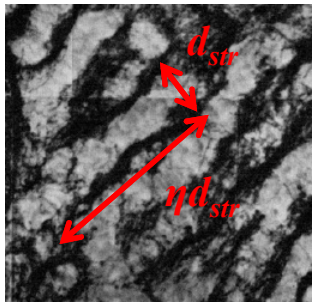

Yes

$\eta = \eta_{labyr}$

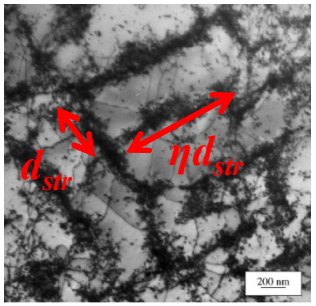

Integrated Computational Materials Engineering

How long does it take to envision, design and put on the market a new product?

Examples:
- Nuclear submarines: Multiple decades.
- Space satellite or rocket: About a decade.
- F35: About a decade

Commercial products can develop much faster:
- Medical devices: Years
- Electronic components: Months

The key to success is to integrate knowledge into efficient design strategies

Mesoscale Fatigue Model

Calibration: Mesoscale experimental data

Nucleation

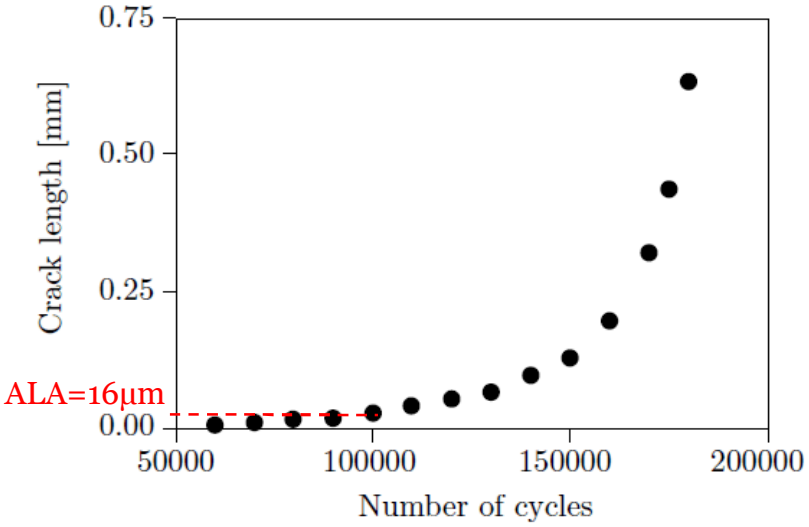

MSC

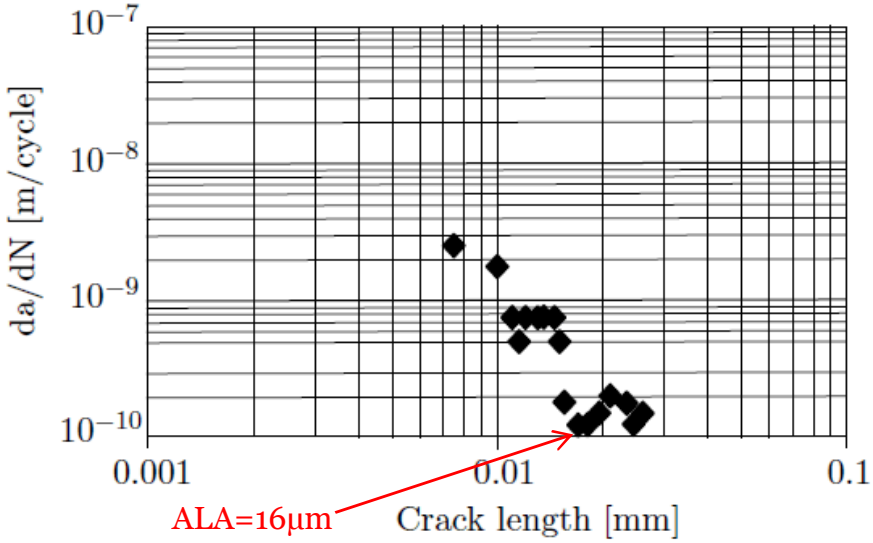

$$N_{nuc} = \frac{\alpha_g}{d_{gr}} \Delta\gamma^{-2}$$

$$\left.\frac{da}{dN}\right|_{msc} = \phi \left\langle \Delta CTD - \Delta CTD_{th} \right\rangle$$

Pang, H. T., PhD thesis, University of Southampton, UK, 2003.

Mesoscale Fatigue Model

Sandia National Laboratories

Implementation: Abaqus subroutines

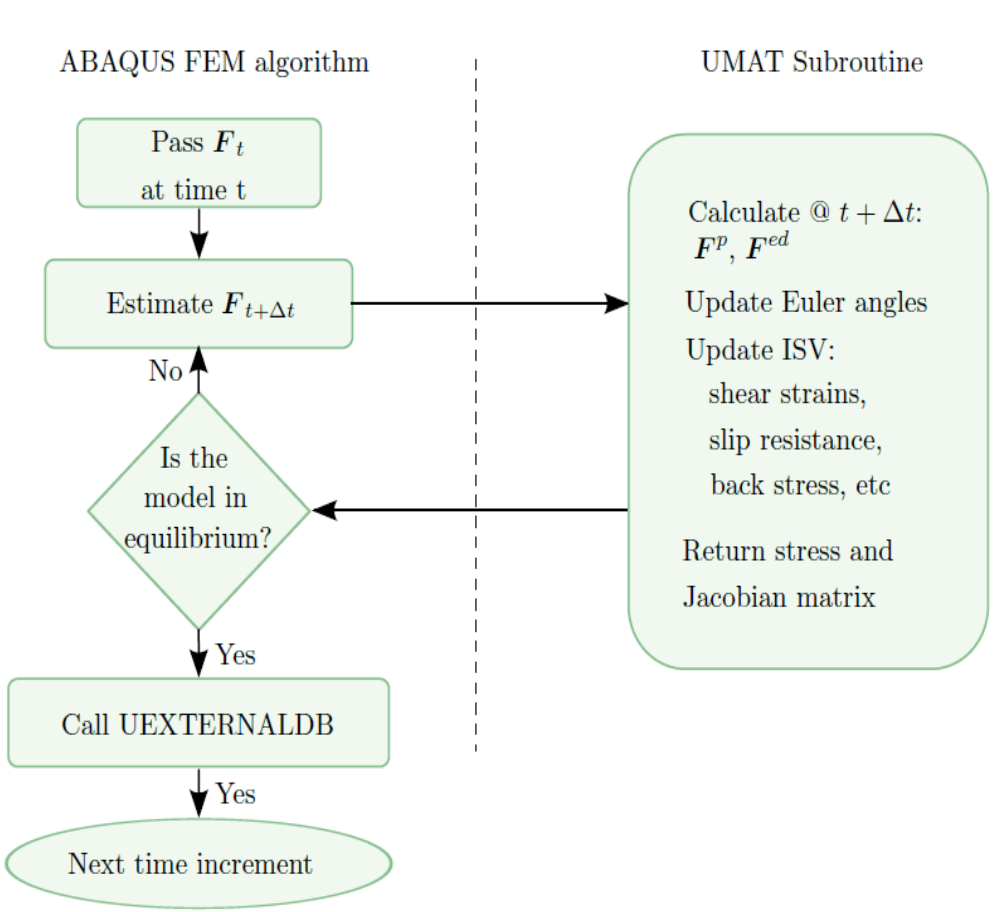

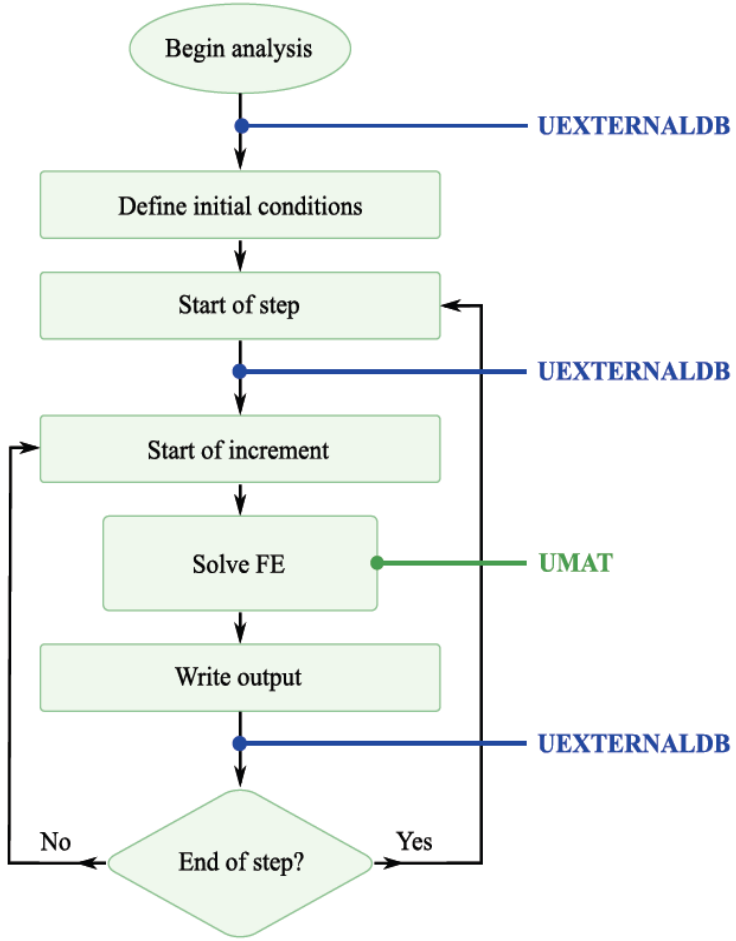

Mesoscale Fatigue Model

Normalized FIP within grains in polycrystals

Initial value for next uncracked grain

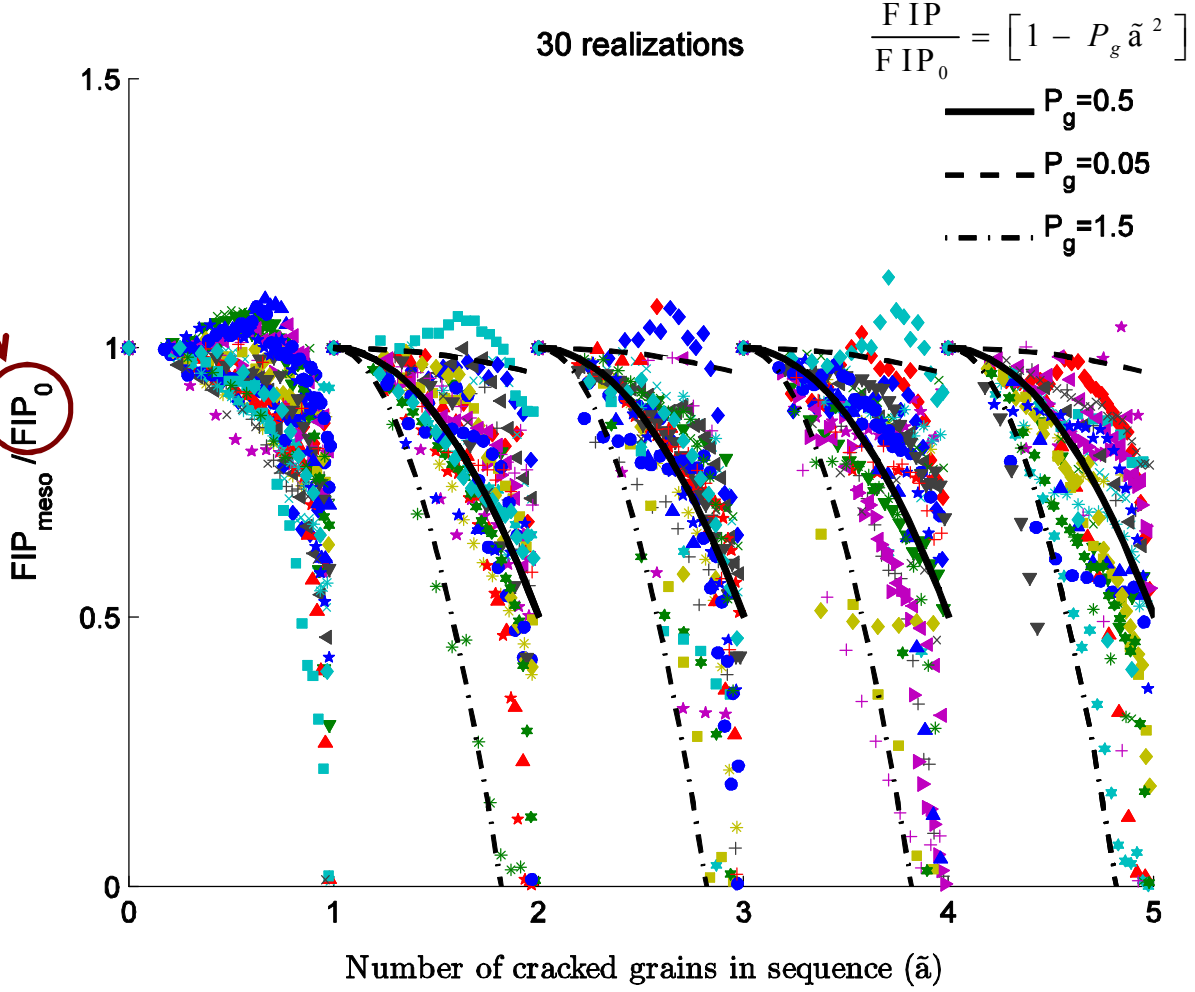

Mesoscale Fatigue Model

Sandia National Laboratories

Implementation: Abaqus subroutines

UMAT

- Contains RR1000 constitutive model.
- Degrades the elastic stiffness for cracked elements.

UEXTERNALDB

- Controls averaging volume and grain connectivity.
- Calculates local and non-local FIPs and life.
- Keeps track of failed grains and crack extension.

Mesoscale Fatigue Model

- 1% shear strain
- R_ε=0.1
- Oriented for single slip
- FIP averaged along bands

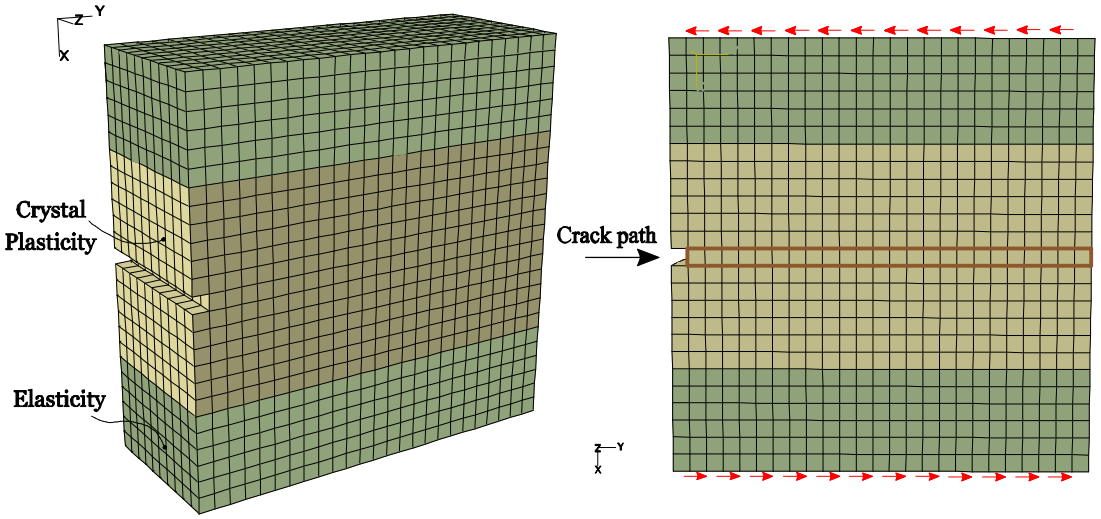

Fatigue driving force with and without crack growth in single crystals

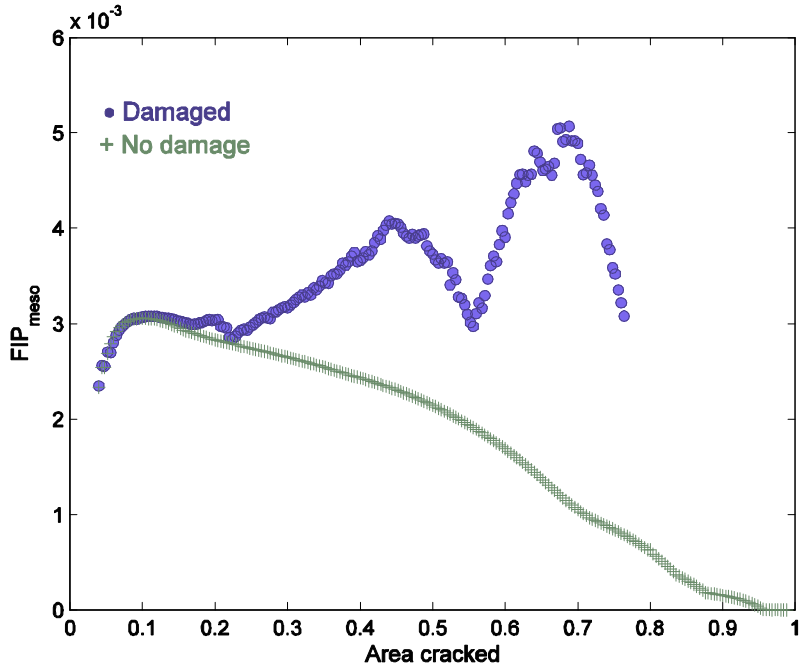

Mesoscale Fatigue Model

Sandia National Laboratories

FIP variability across grains prior to cracking

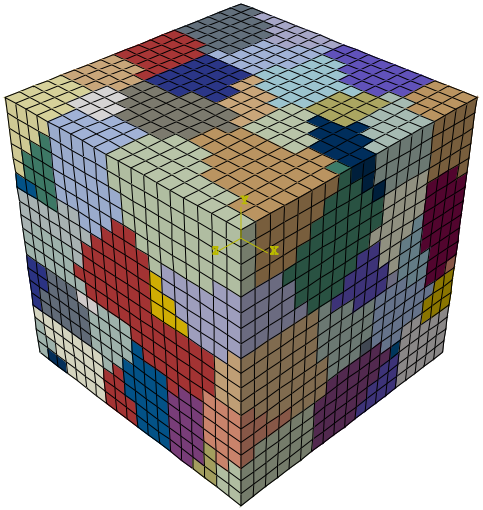

- $\Delta\varepsilon$=0.8
- R_ε=0

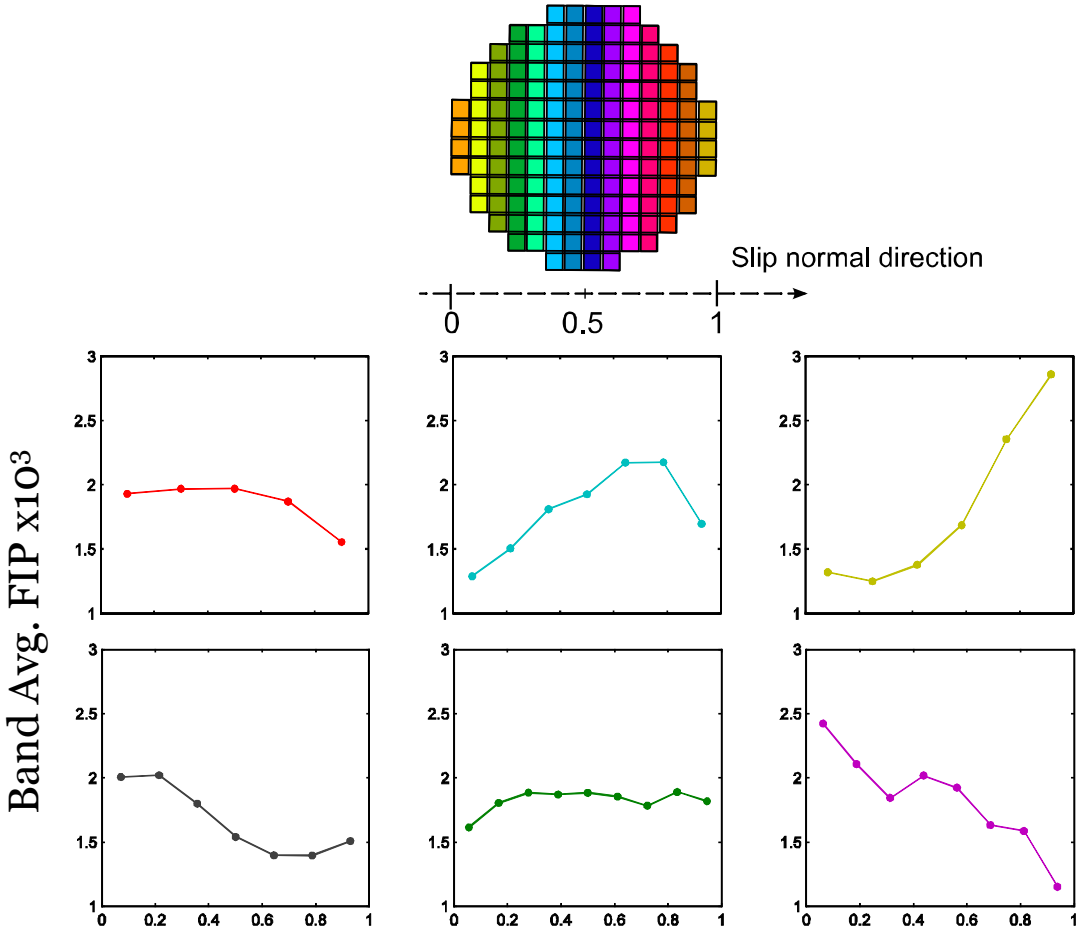

Early Stages of Fatigue Damage

Previous models

Navarro and de los Rios (1987)

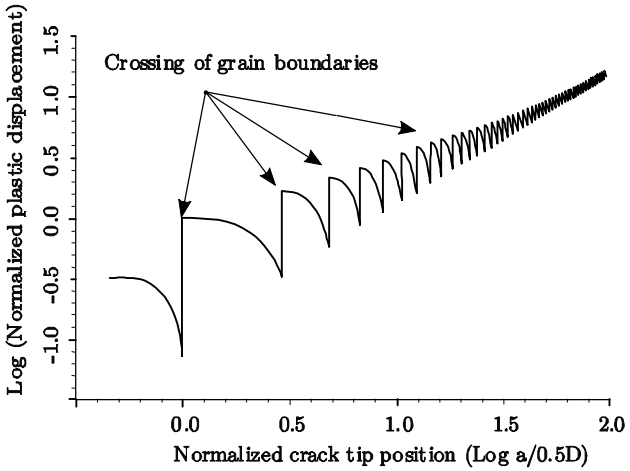

Hobson et al. (1982,1986)

$$da/dn = C(\gamma,\sigma)(d-a)^{\alpha} a^{\alpha}$$

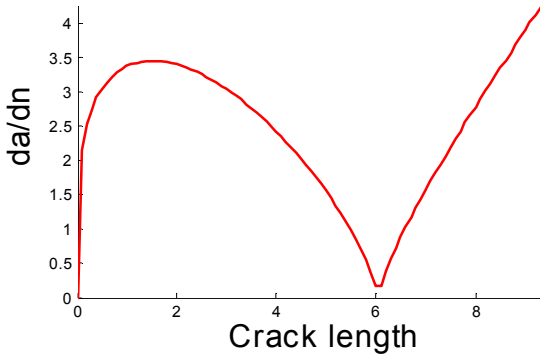

Miller's regimes (1997)

MFM

$$\frac{da}{dN} = A\Delta\gamma^{\alpha}(d-a)$$

EPFM

$$\frac{da}{dN} = B\Delta\gamma^{\beta} a - D$$

LEFM

$$\frac{da}{dN} = C(\Delta\gamma\sqrt{\pi a})^{n}$$

Multiaxial loading

Sandia National Laboratories

Smooth specimen

Dimensions:
95x95x95μm

Mean grain size:
18μm

Element size:
5μm

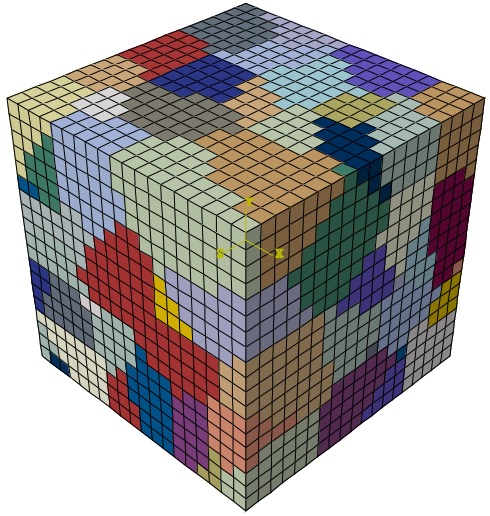

Stress concentration specimens

Notch radius:
72μm

Dimensions:
432x432x108μm

Mean grain size:
18μm

Element size:
5μm

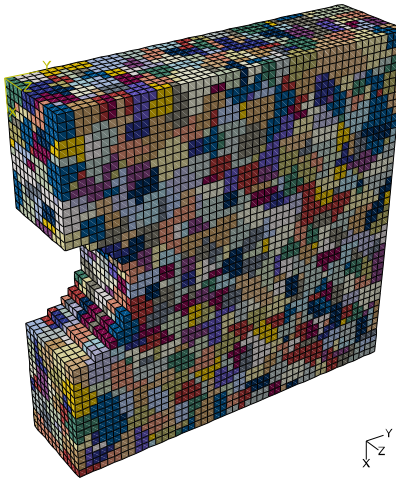

Hole radius:
72μm

Dimensions:
432x432x108μm

Mean grain size:
18μm

Element size:
5μm

Multiaxial loading

Smooth specimens

Notched specimens

Through-hole specimens

10 realizations for each loading condition

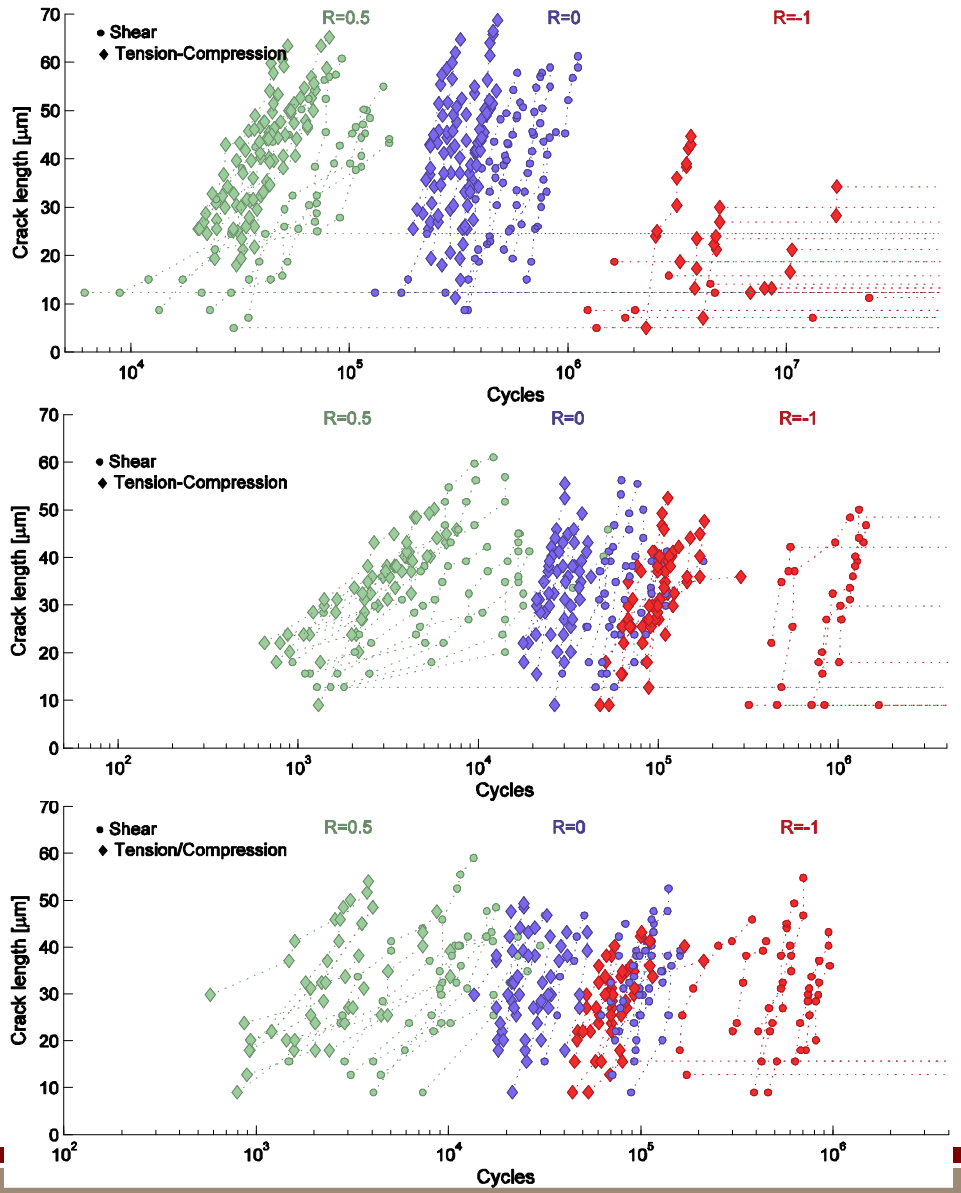

Multiaxial loading

Nominal mean stress effect on crack nucleation

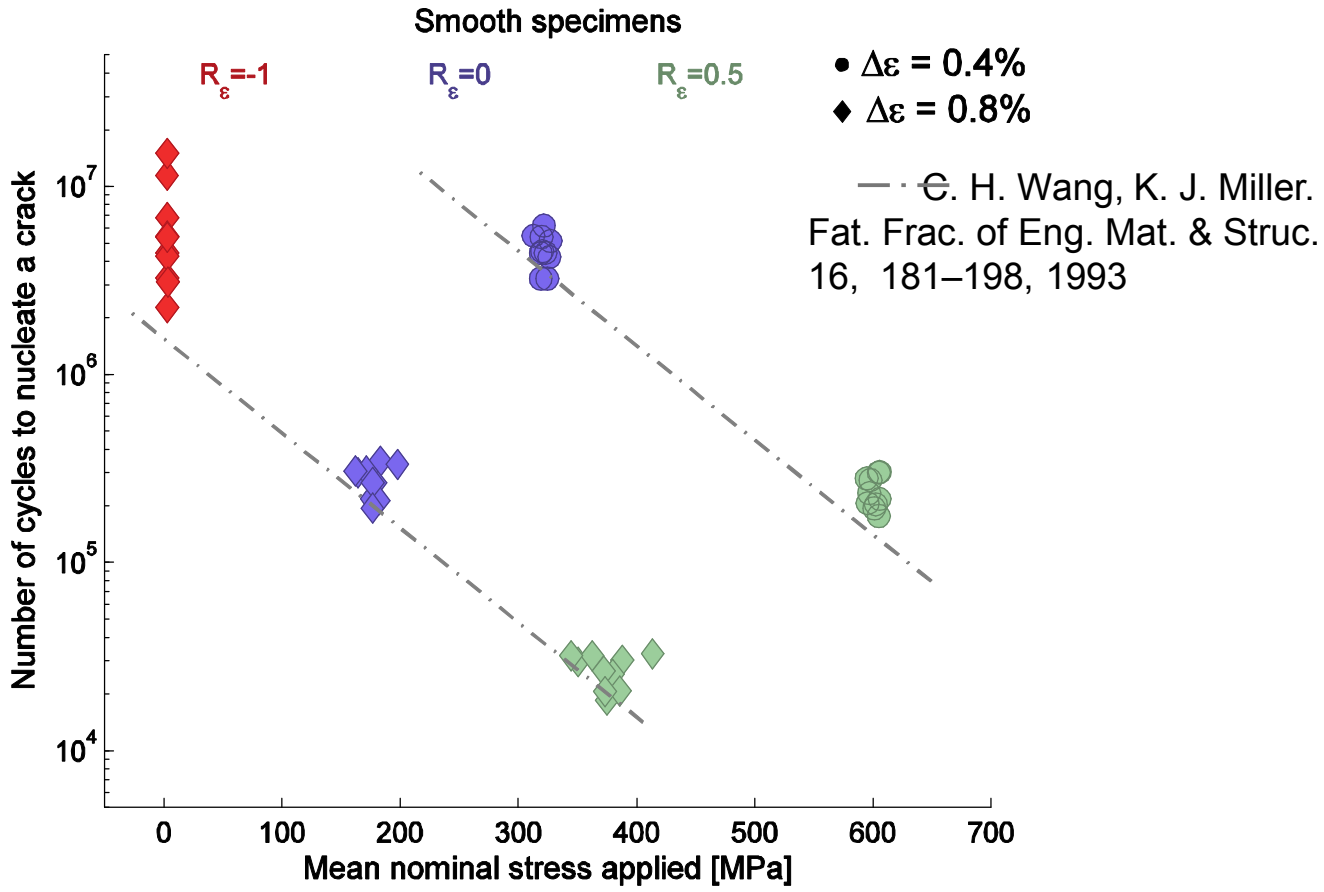

Multiaxial loading

Smooth specimens stress-strain curves

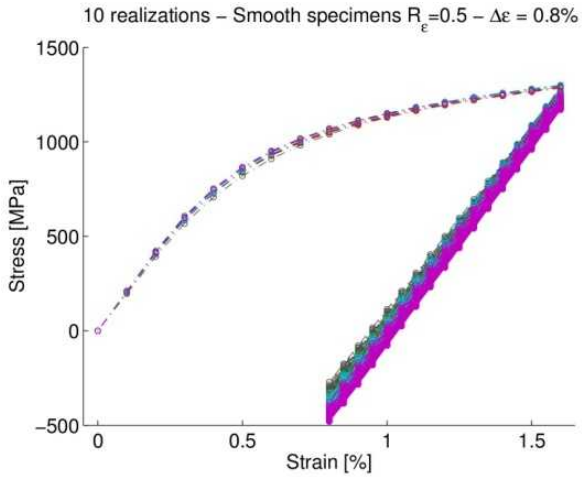

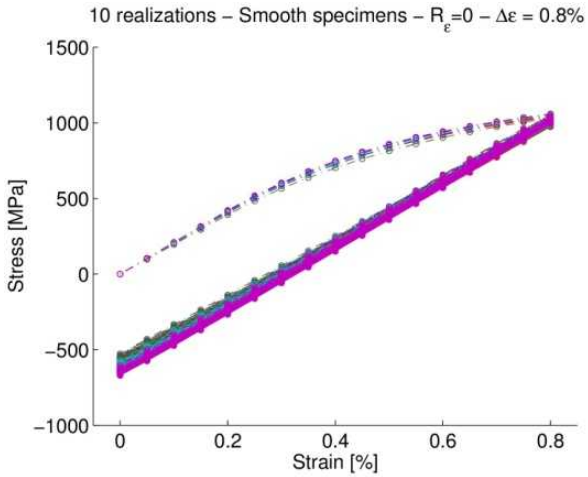

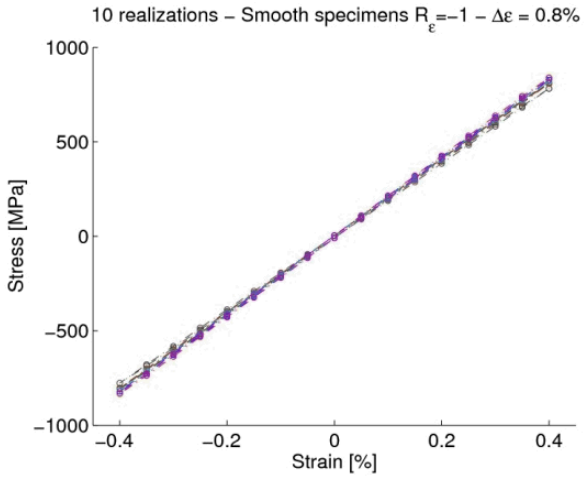

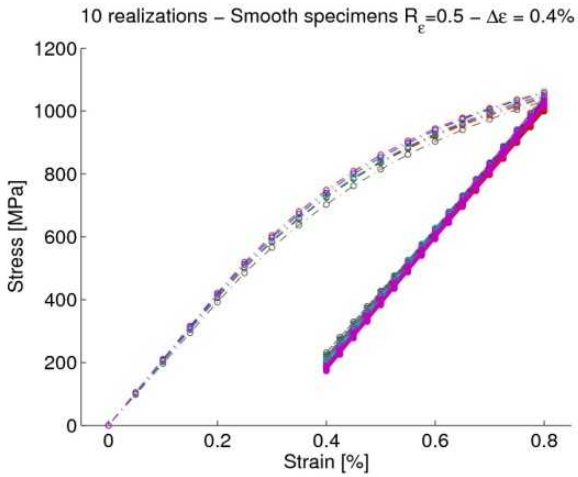

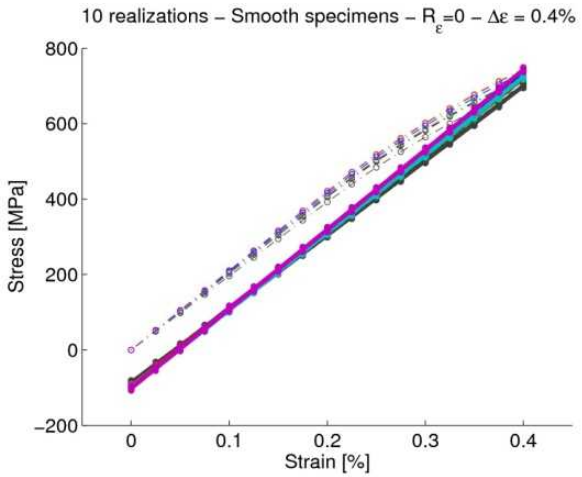

Computing the Crack Path

Sandia National Laboratories

Element-by-element cracking

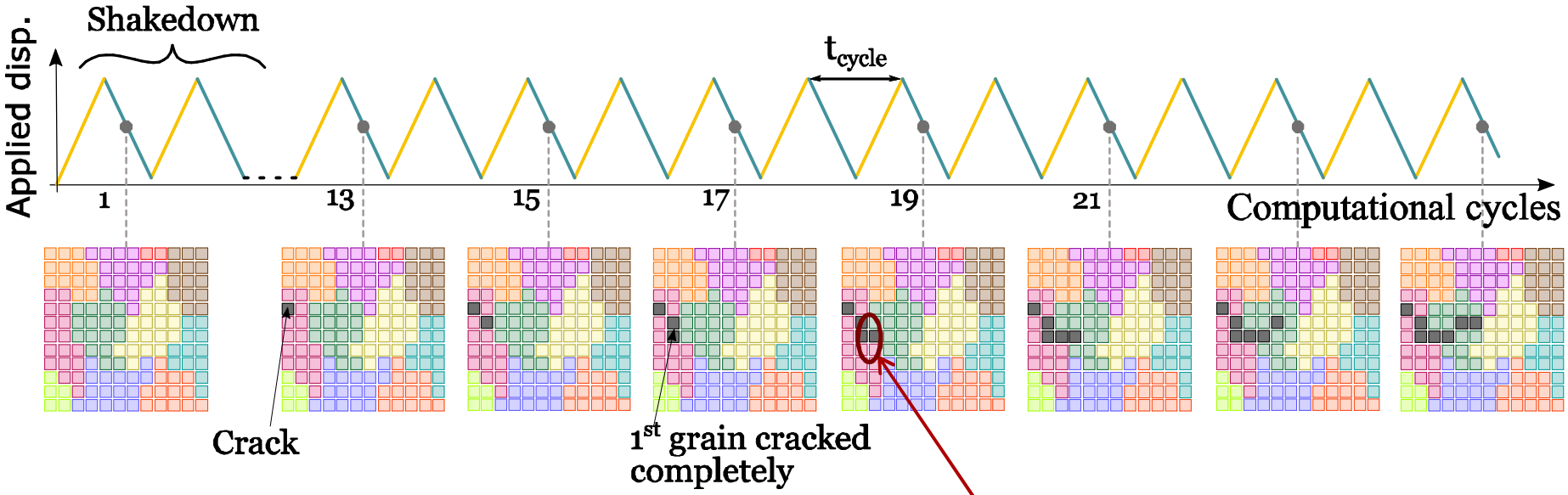

The bands intersect at least in one element along the grain boundary

Computing the Crack Path

Band-by-band (mesoscale) cracking

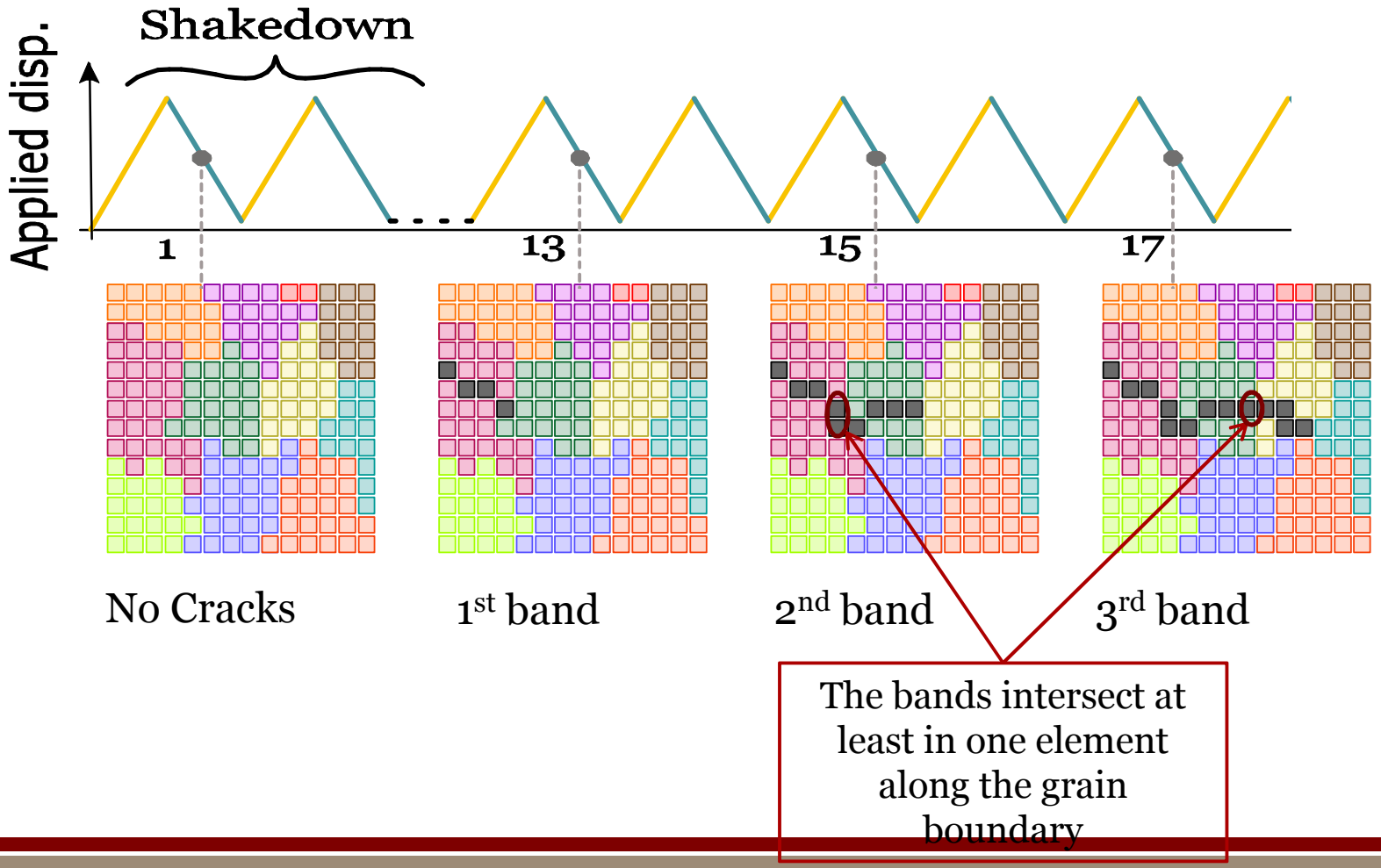

Computing Fatigue Crack Driving Force

Sandia National Laboratories

Element-by-element vs. Mesoscale cracking

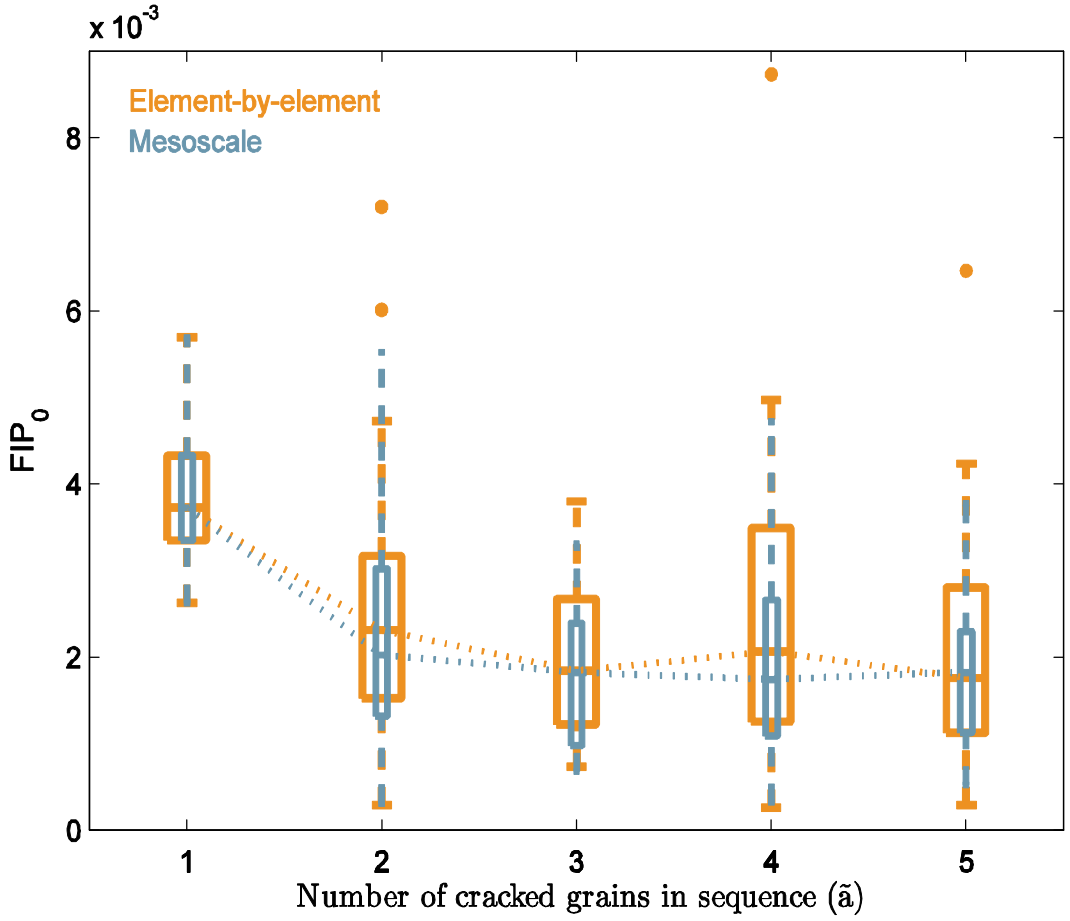

Main Assumptions

- Calibration of the irreversibility constant.

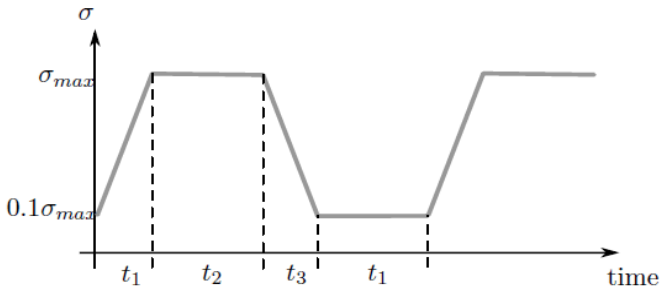

$$\phi = \phi_0 e^{\left(-Q/RT\right)} \left(0.9t_1 + t_2 + 0.1t_3\right)^{\left(1/2 - \xi\right)}$$

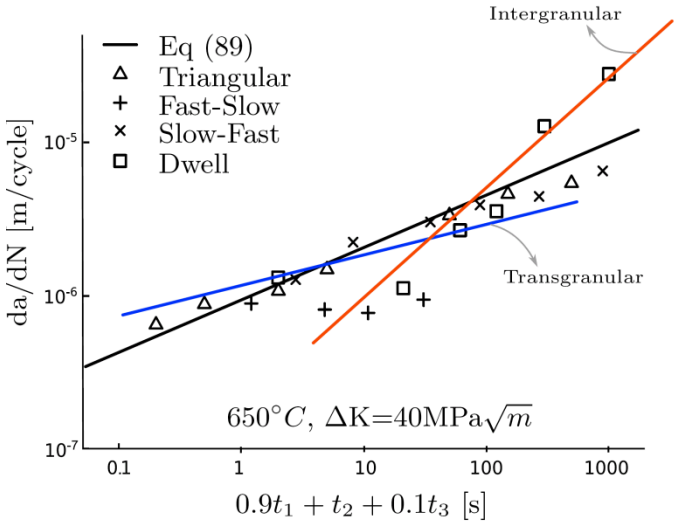

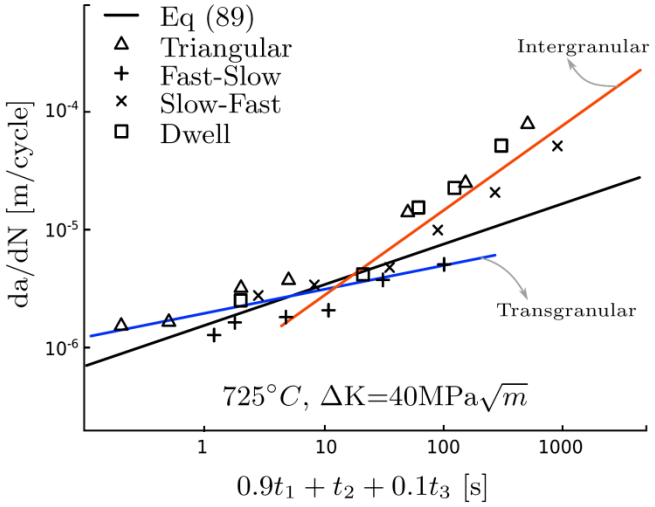

Tong, J., Dalby, S., and Byrne, J., J. Mat. Sci., 40, **5**, 1237-1243, 2005.

Computing Fatigue Crack Driving Force

Intergranular life is assessed for each grain boundary sector

Accumulated plastic strain

Stress normal to the GB

$$\mathrm{FIP}_{\mathrm{int}} = \left[\sum_{\alpha} \left[\frac{\gamma_p^{\alpha}}{2} \left(1 + k_{trans} \frac{\sigma_n^{\alpha}}{\sigma_y} \right) \right] \right]^{\lambda_1} \left(\frac{\sigma_n^{GB}}{\sigma_y} \right)^{\lambda_2}$$

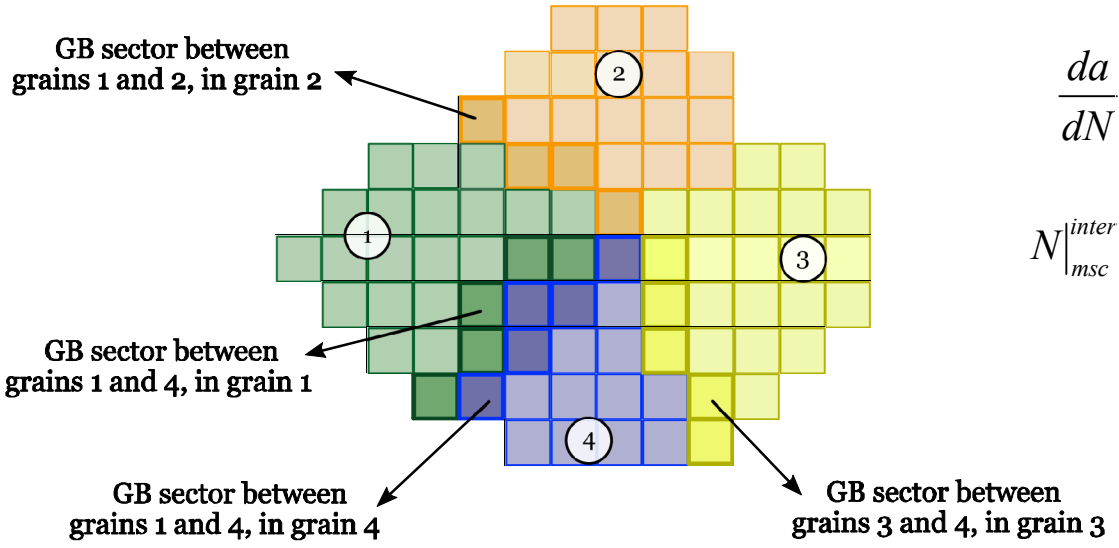

$$\left. \frac{da}{dN} \right|_{msc}^{inter} = \phi_{int} exp\left\{ -\frac{Q - B\langle PS \rangle}{RT} \right\} \Delta t^{(1/2-\xi)} \mathrm{FIP}_{\mathrm{int}}$$

$$N\Big|_{msc}^{inter} = \frac{l_{elem}}{\left[\phi_{int} exp\left\{ -\frac{Q - B\langle \sigma_{max}^{GB} \rangle}{RT} \right\} \Delta t^{(1/2-\xi)} \mathrm{FIP}_{\mathrm{int}} \right]}$$

Duplex Microstructures

Transgranular-Intergranular transition of ALA grains

50 realizations

Periodic Boundary Conditions

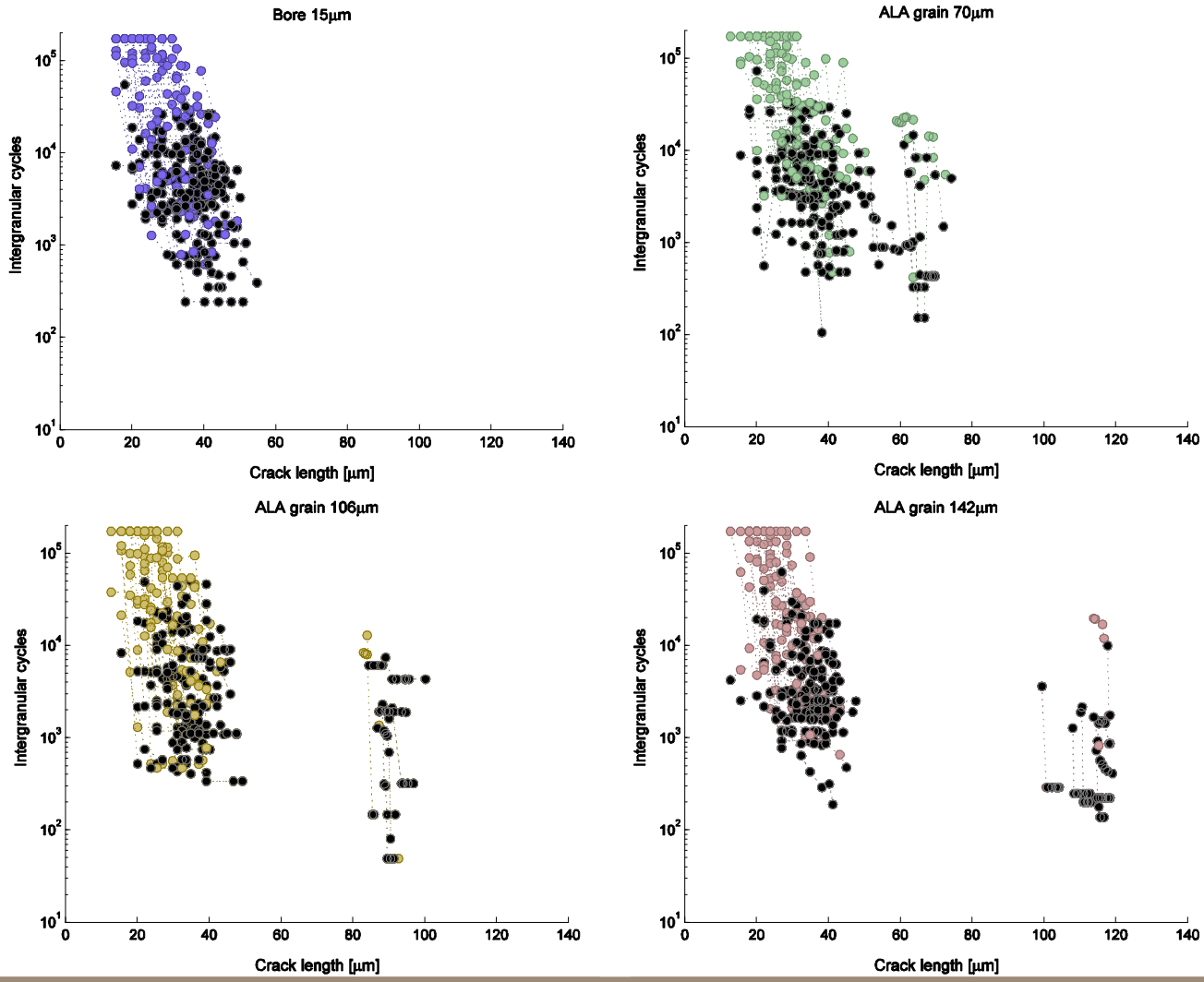

Computing Fatigue Crack Driving Force

Sandia National Laboratories

Smooth specimens – Displacement controlled

Dimensions:
95x95x95μm

Mean grain size:
18μm

Element size:
5μm

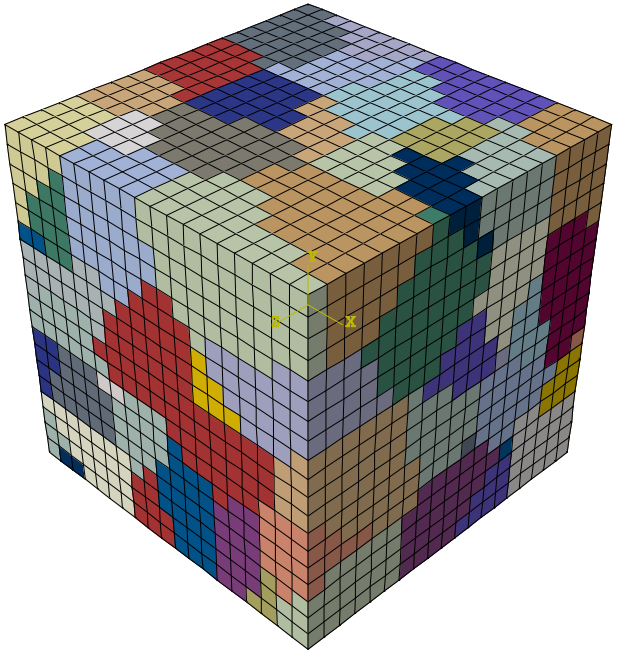

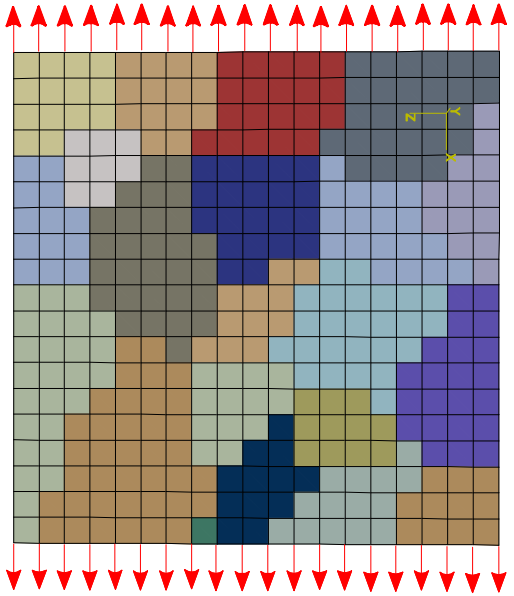

Computing Fatigue Crack Driving Force — FIP Averaging Volume Effects

Variability of the band averaged FIP within grains prior to crack nucleation

Width of averaging band = element size: fine 2 μm, coarse 5 μm)

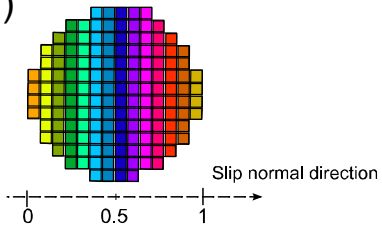

- Coarse and refine meshes compared.
- All plots correspond to different microstructural realizations.

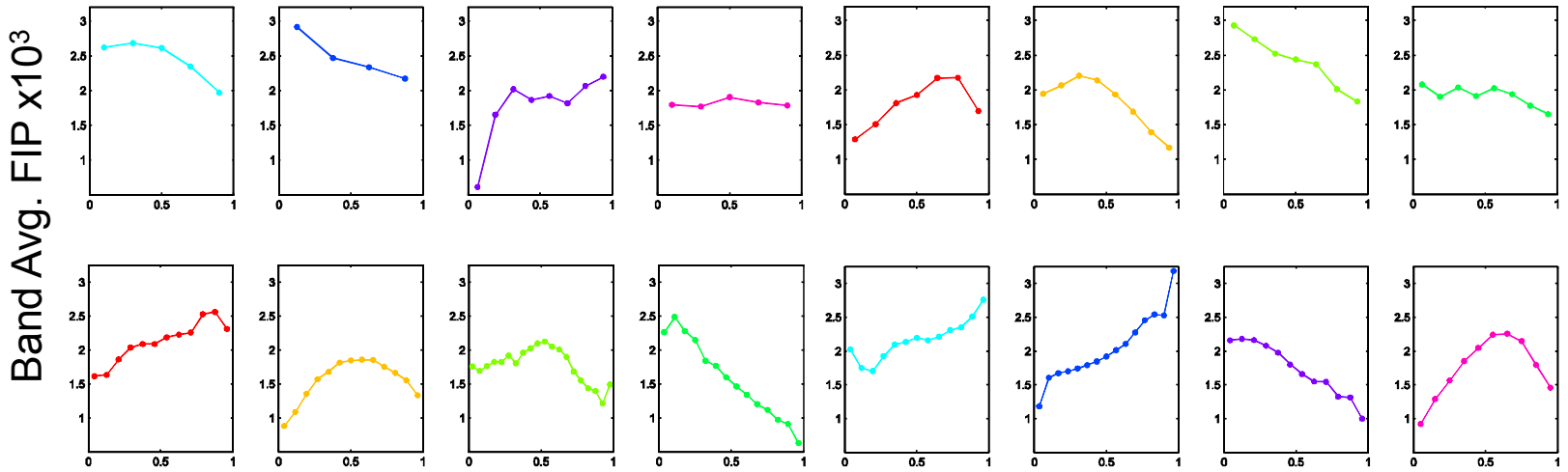

Highest FIPs in various realizations

Computing Fatigue Crack Driving Force

FIP distributions after 3 loading cycles - 50 realizations

Element

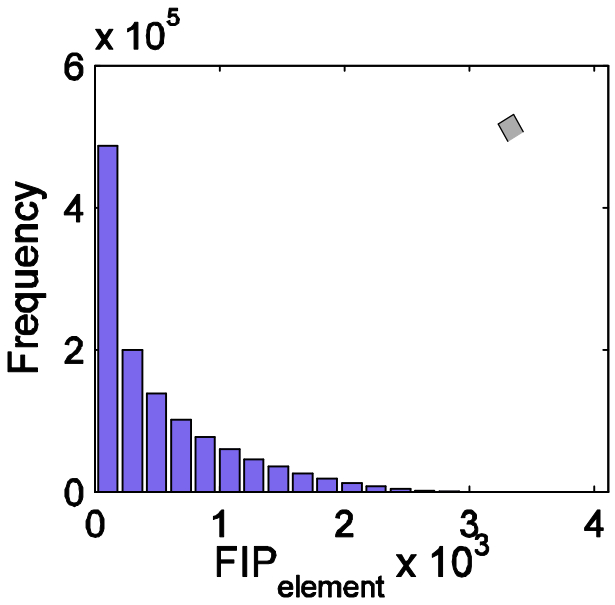

Band avg.

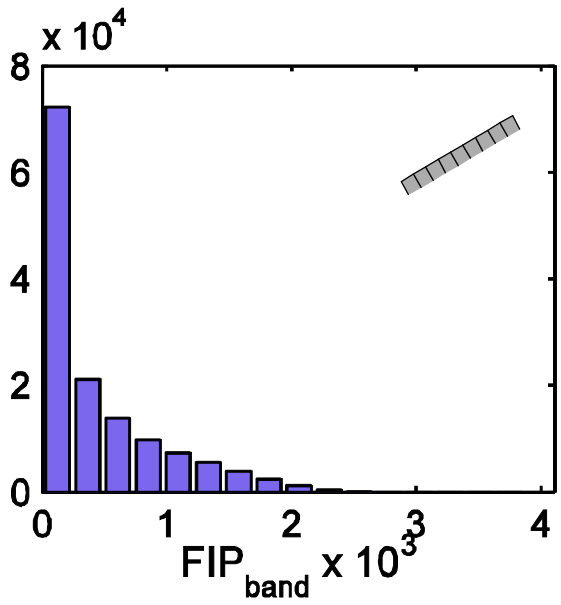

Grain avg.

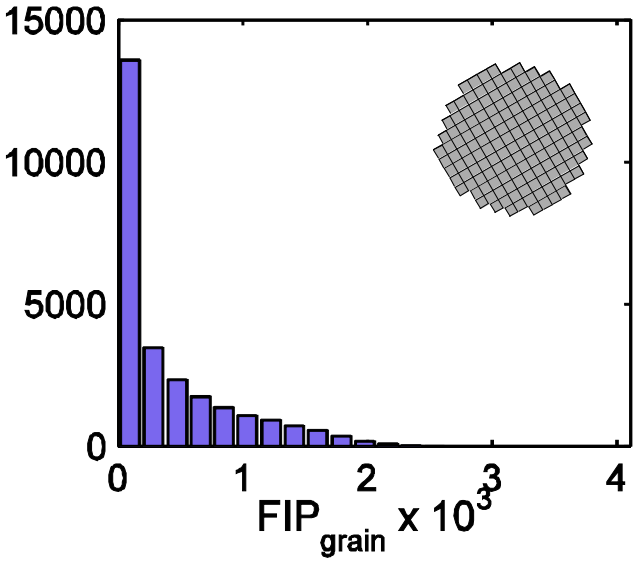

Computing Fatigue Crack Driving Force — FIP Averaging Volume Effects

FIP averaged along bands prior to crack nucleation

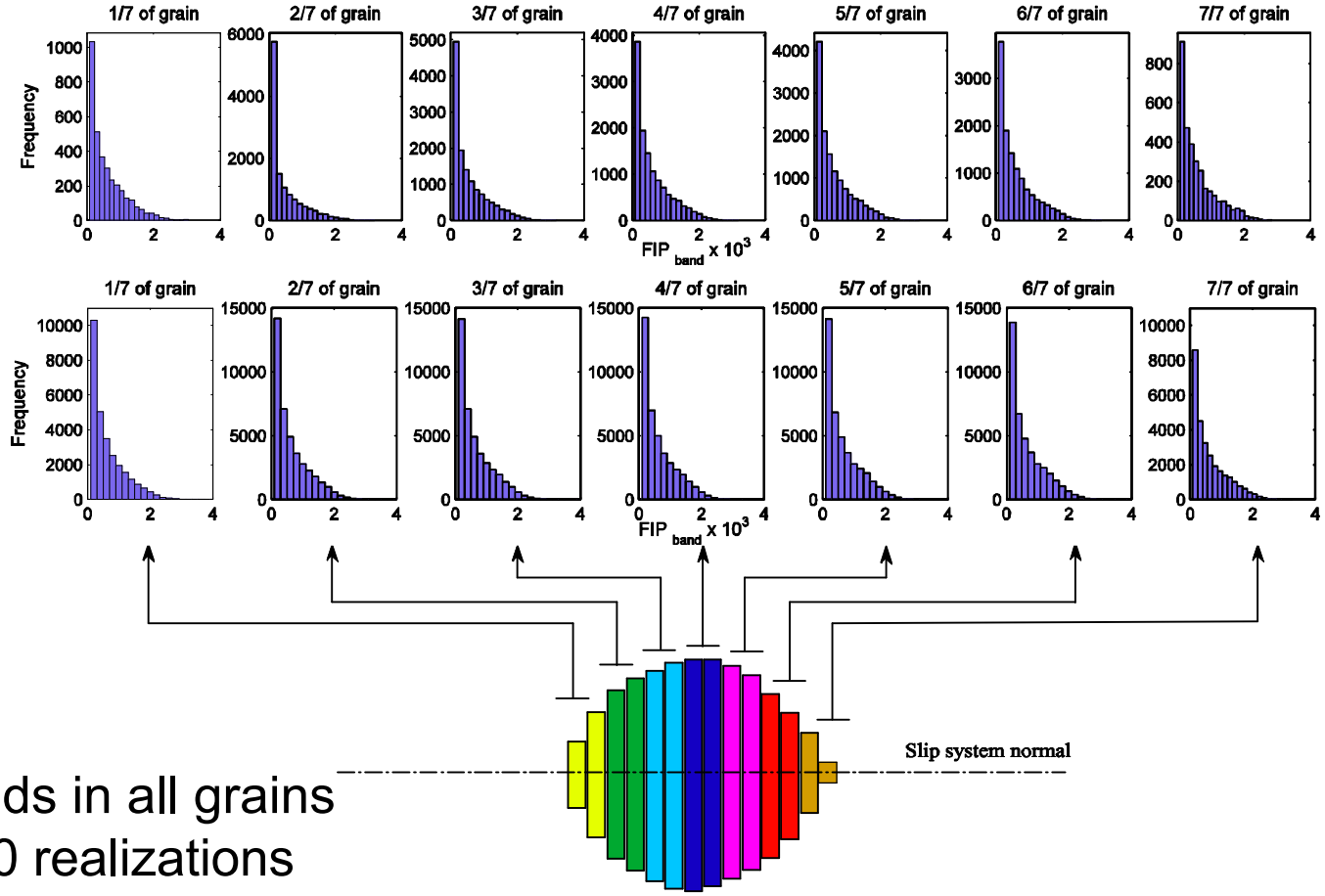

Coarse Mesh 5 μm

Fine Mesh 2 μm

All bands in all grains from 50 realizations

Computing Fatigue Crack Driving Force

Band avg.
vs
Grain avg.

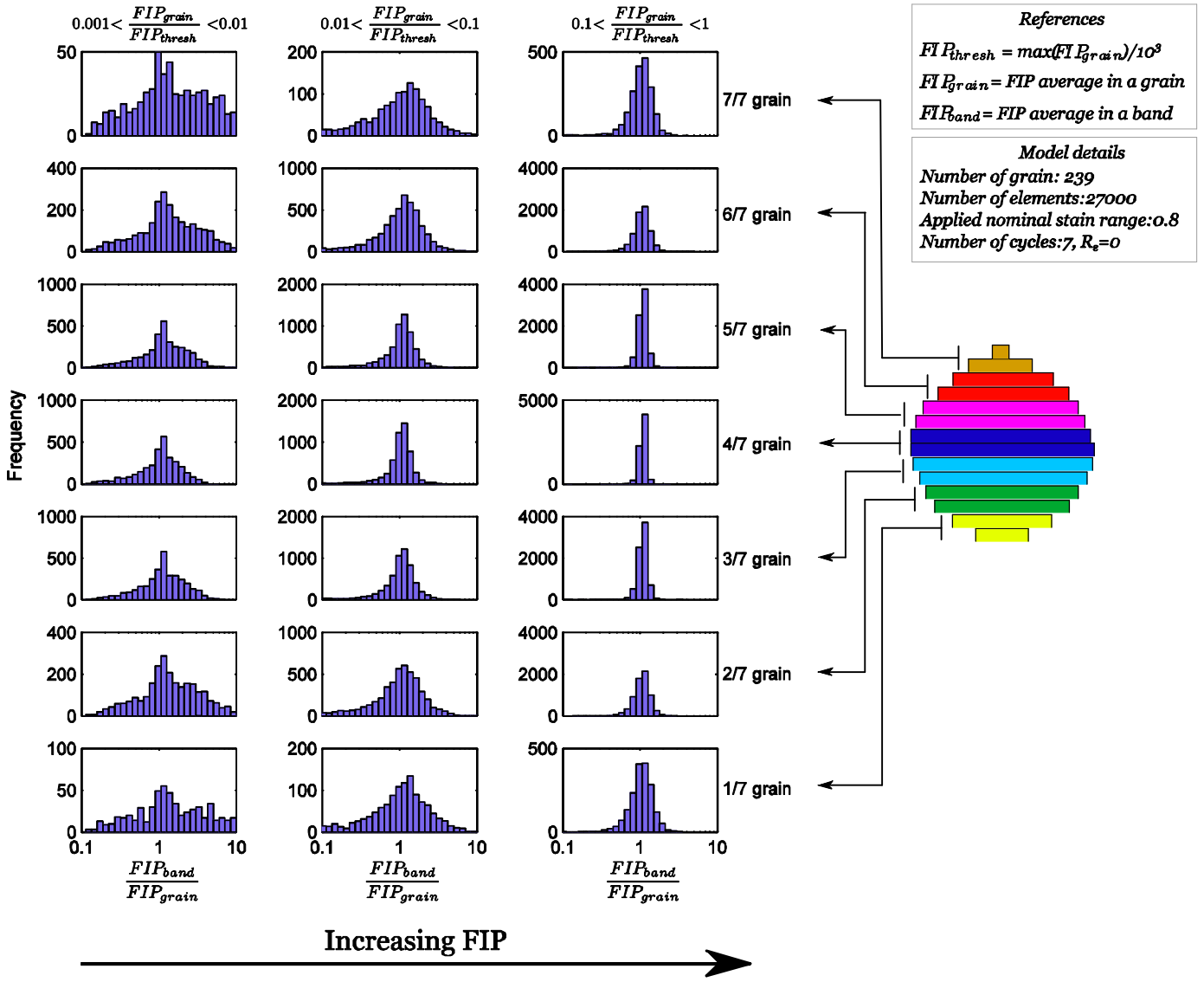

Appendix

Band avg.

$$d_{gr} = \sqrt{Cross\ Section}$$

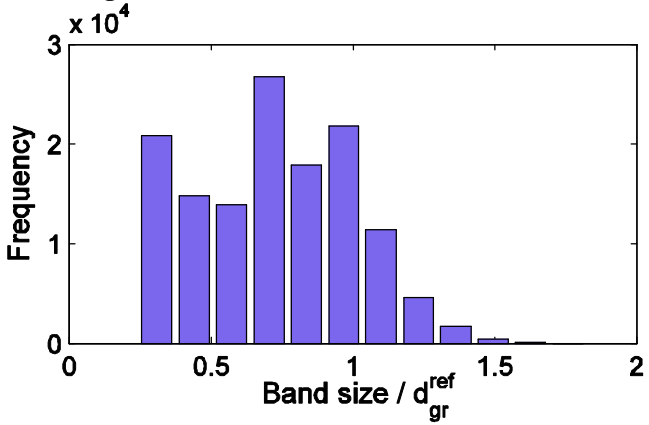

Grain avg.

$$d_{gr} = \sqrt[3]{Grain\ volume}$$

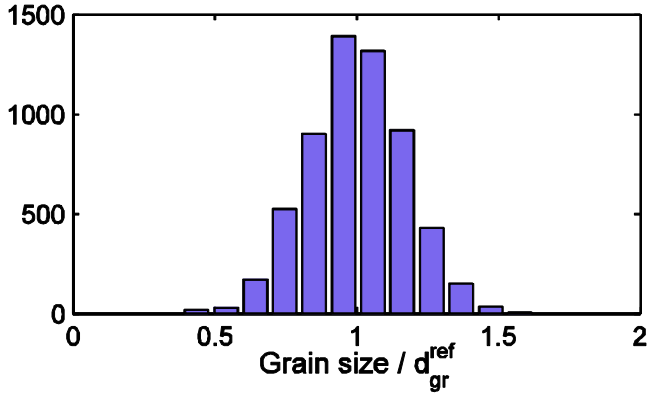

$$FIP_{Normalized} = d_{gr} / d_{gr}^{ref}\ FIP$$

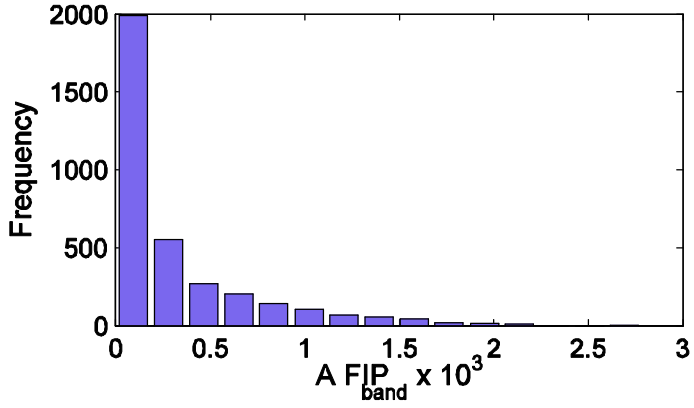

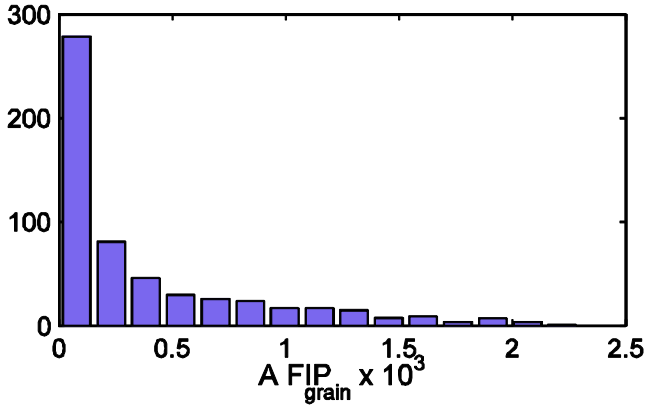

Appendix

Sandia National Laboratories

• 50 microstructural realizations, but the same crystallographic orientation and location is imposed to grain #1.

• Crack nucleation is assessed for the different bands in grain #1.

• Nominal tensile applied strain: $\Delta\varepsilon=0.8$, $R_\varepsilon=0$.

• Case 1: Grain #1 oriented for multiple slip.
Max. Schmid factor=0.408

• Case 2: Grain #1 oriented for single slip.
Max. Schmid factor=0.487

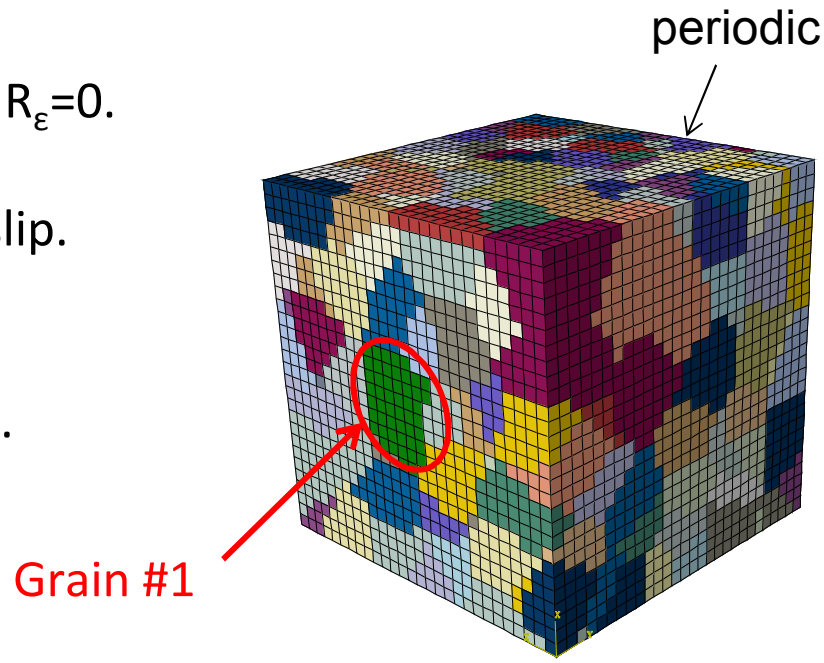

All sides free except top and bottom

Appendix

Maximum FIPs in Grain #1 out of 50 realizations

Case 1 | Case 2

Nucleation FIPs (Elements)

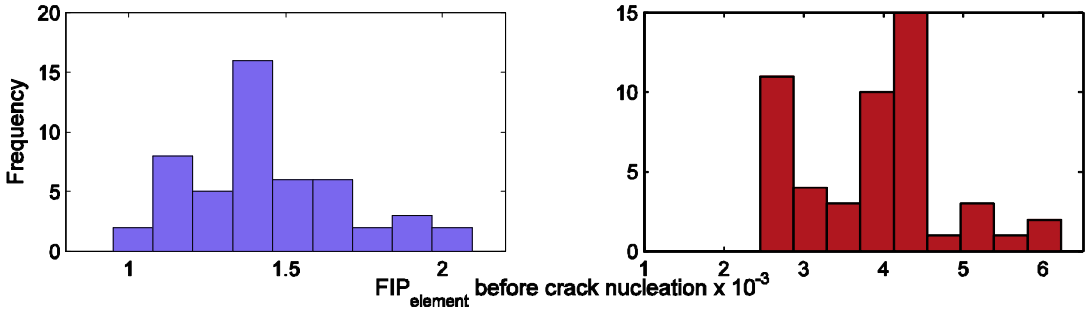

Nucleation FIPs (band avg.)

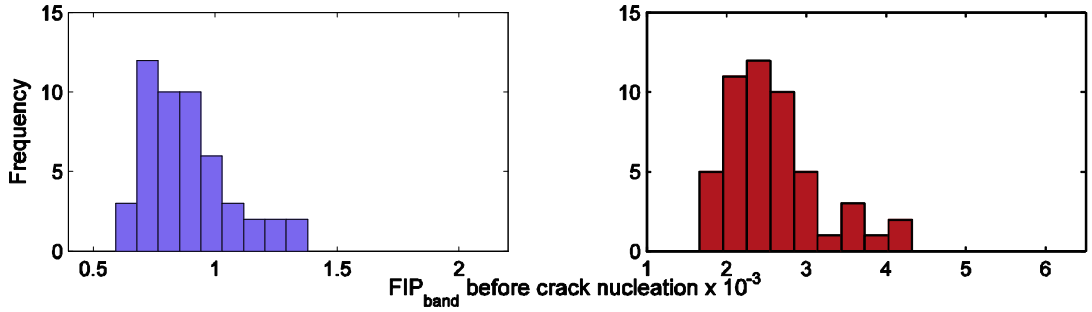

Nucleation FIPs (grain avg.)

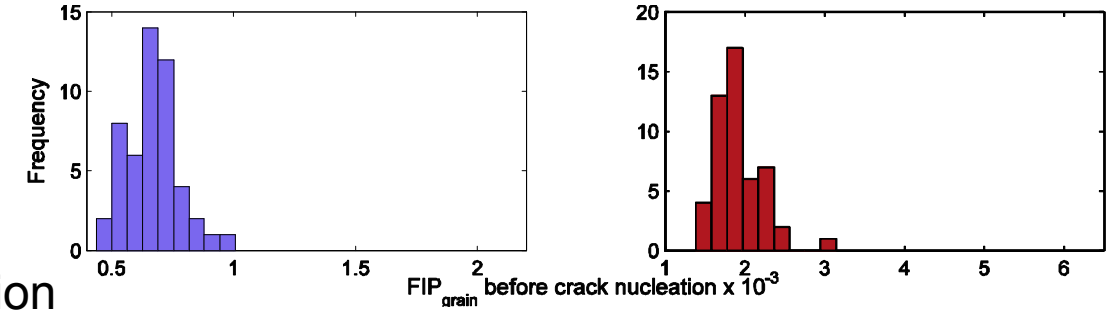

Grain is fixed in orientation and neighbors are changed

Multiple slip

Single slip

Early Stage Fatigue Processes

Sandia National Laboratories

Microstructurally Small Cracks (MSCs)

Small cracks

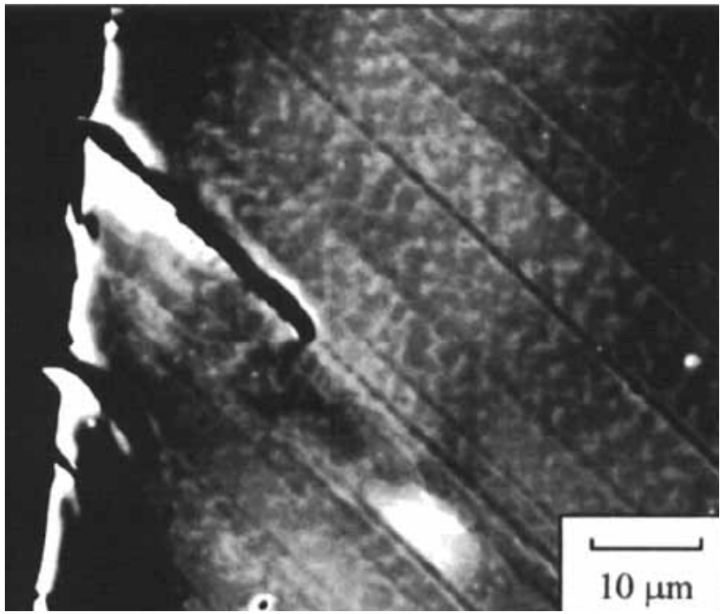

Long cracks

ECCI, contrast represents dislocation structures

Ahmed J. et al.. Philos. Mag. A, 81, 6, (2001), 1473-1488.

Early Stage Fatigue Processes

CTD as a fundamental magnitude

Dislocation emission-annihilation

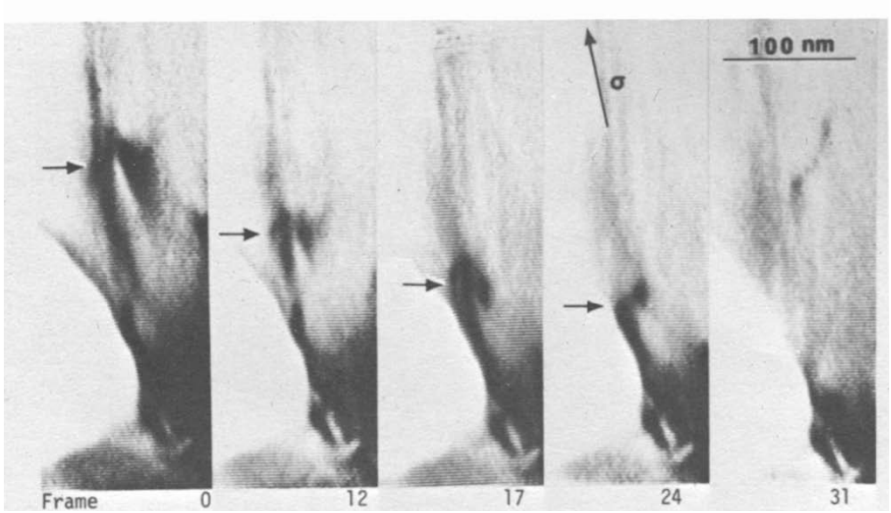

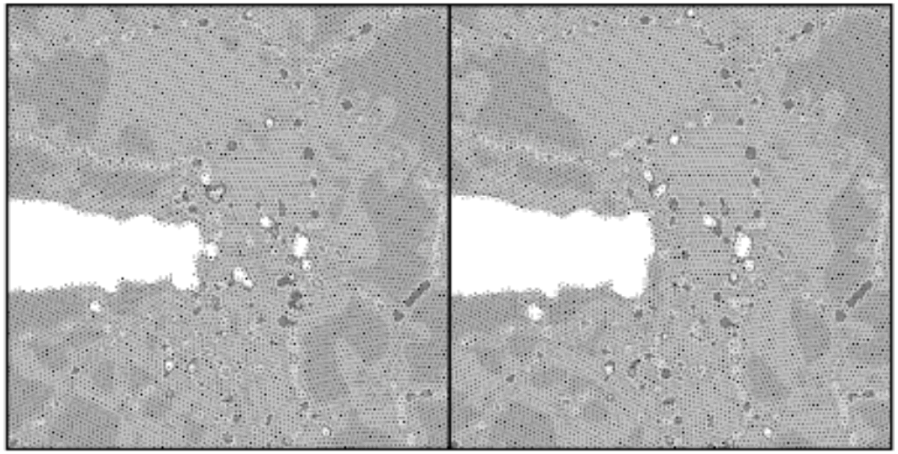

Horton J. A. and Ohr S. M., Scr. Metall., 16, (1992), 621-626.

Farkas D. et al. Phys. Rev. Lett. 94, 16 (2005),165502 1-4.

Material System

RR1000 Ni-base superalloy for turbine disks @650C:

- Extended fatigue Stage I crack growth
- Octahedral slip dominant
- Planar slip

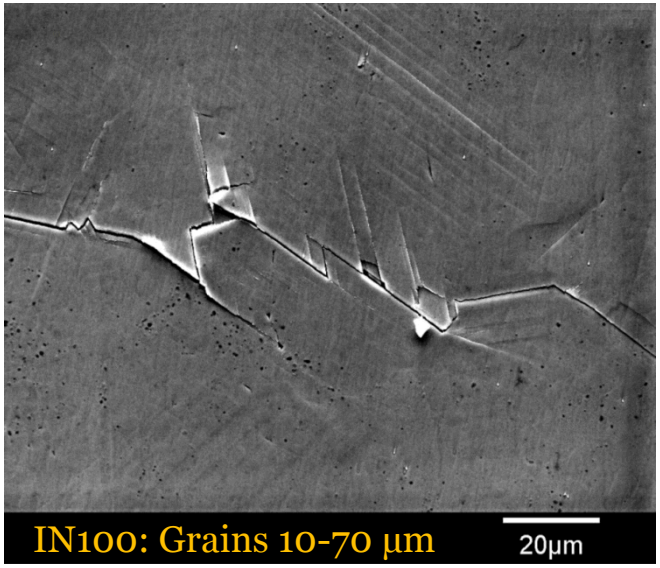

Li, K., Ashbaugh N. E., and Rosenberger A. H. Superalloy conf. 251–258, 2004.

A method to extend the crack

Sandia National Laboratories

• Crack growth is modeled by degrading the elastic stiffness tensor element-by-element.

$$\overline{\mathbf{C}} = (1 - d_1)\mathbf{C}, \qquad 0 < d_1 < 0.99$$

• The elastic stiffness is fully degraded independently from the fatigue crack driving force:

$$d_1^{(i+1)} = d_1^{(i)} \pm \nu \Delta t^i$$

• Also, an anisotropic damage model has been developed and partially implemented.

Computing the Crack Path

Sandia National Laboratories

Example of the elastic stiffness degradation

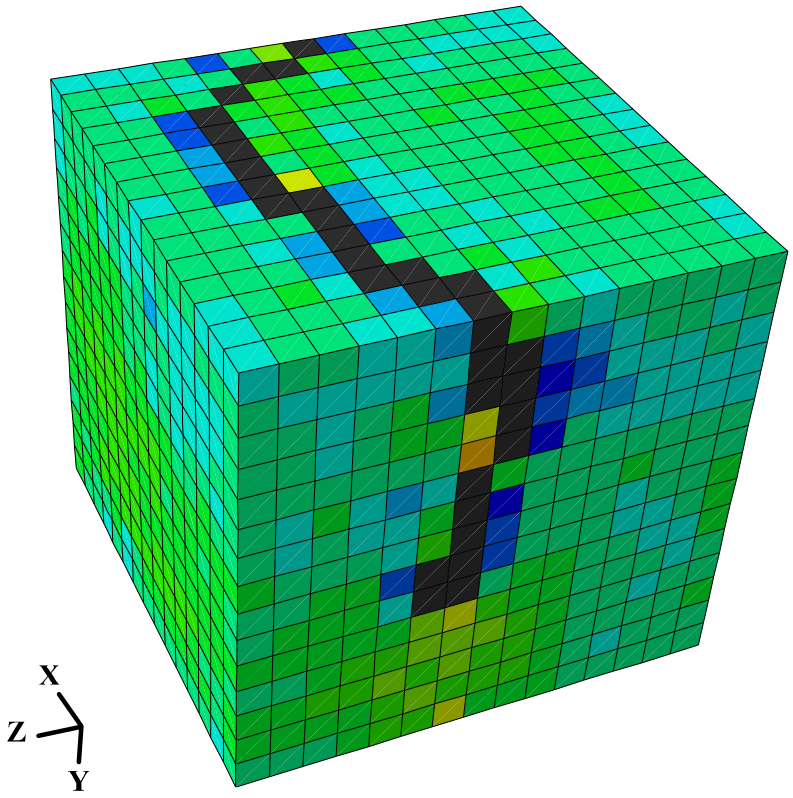

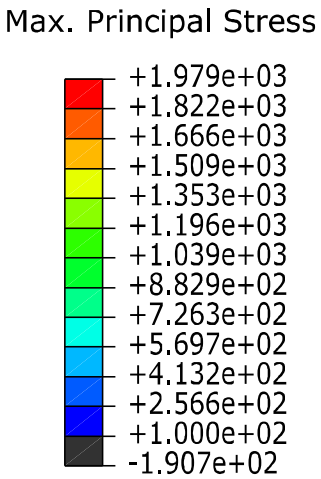

$$\bar{\mathbf{C}} = (1 - d_1)\mathbf{C}$$

$$0 < d_1 < 0.99$$

Appendix

FIP calculation

$$\mathrm{FIP}^{\alpha} = \frac{\Delta\gamma_p^{\alpha}}{2}\left(1 + k\frac{\sigma_n^{\alpha}}{\sigma_y}\right)$$

σ_n^{α} : Stress normal to the slip plane

γ_p^{α} : Plastic shear strain in slip plane α

$$\Delta\gamma^{\alpha}\Big|_{cyc} = \Delta\gamma^{\alpha}\Big|_{\substack{\max \\ \text{over cycle}}} - \Delta\gamma^{\alpha}\Big|_{\text{ratch}}$$

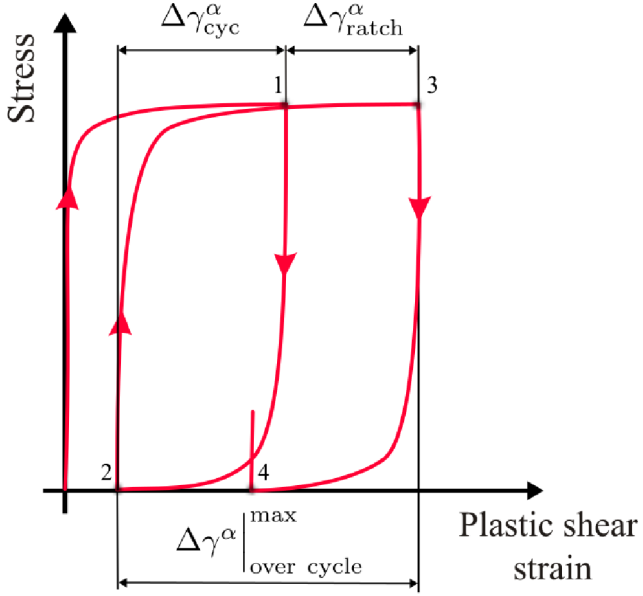

Appendix

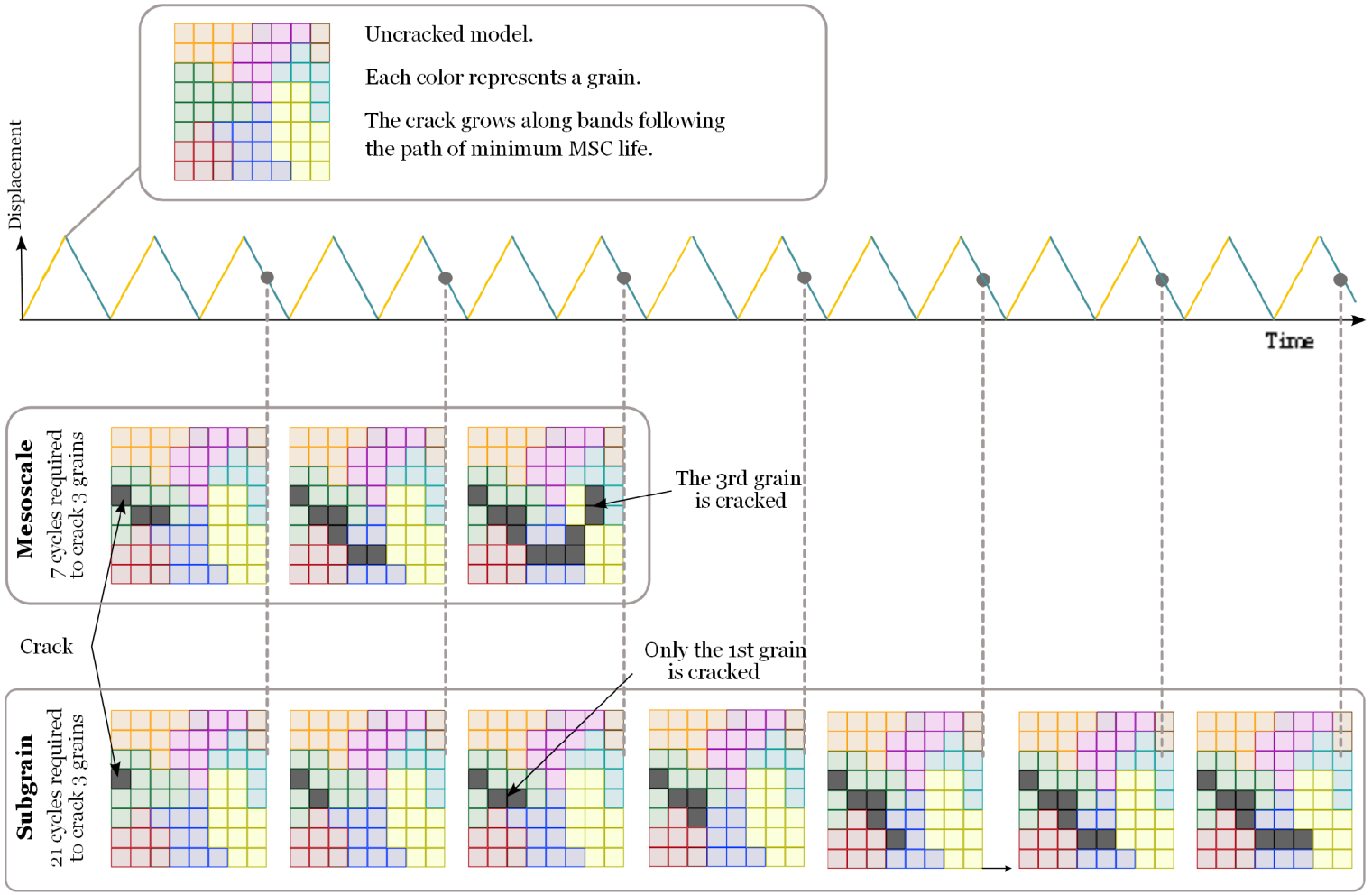
Uncracked model.
Each color represents a grain.
The crack grows along bands following the path of minimum MSC life.
Displacement
Time
Mesoscale
7 cycles required to crack 3 grains
The 3rd grain is cracked
Crack
Only the 1st grain is cracked
Subgrain
21 cycles required to crack 3 grains

Appendix

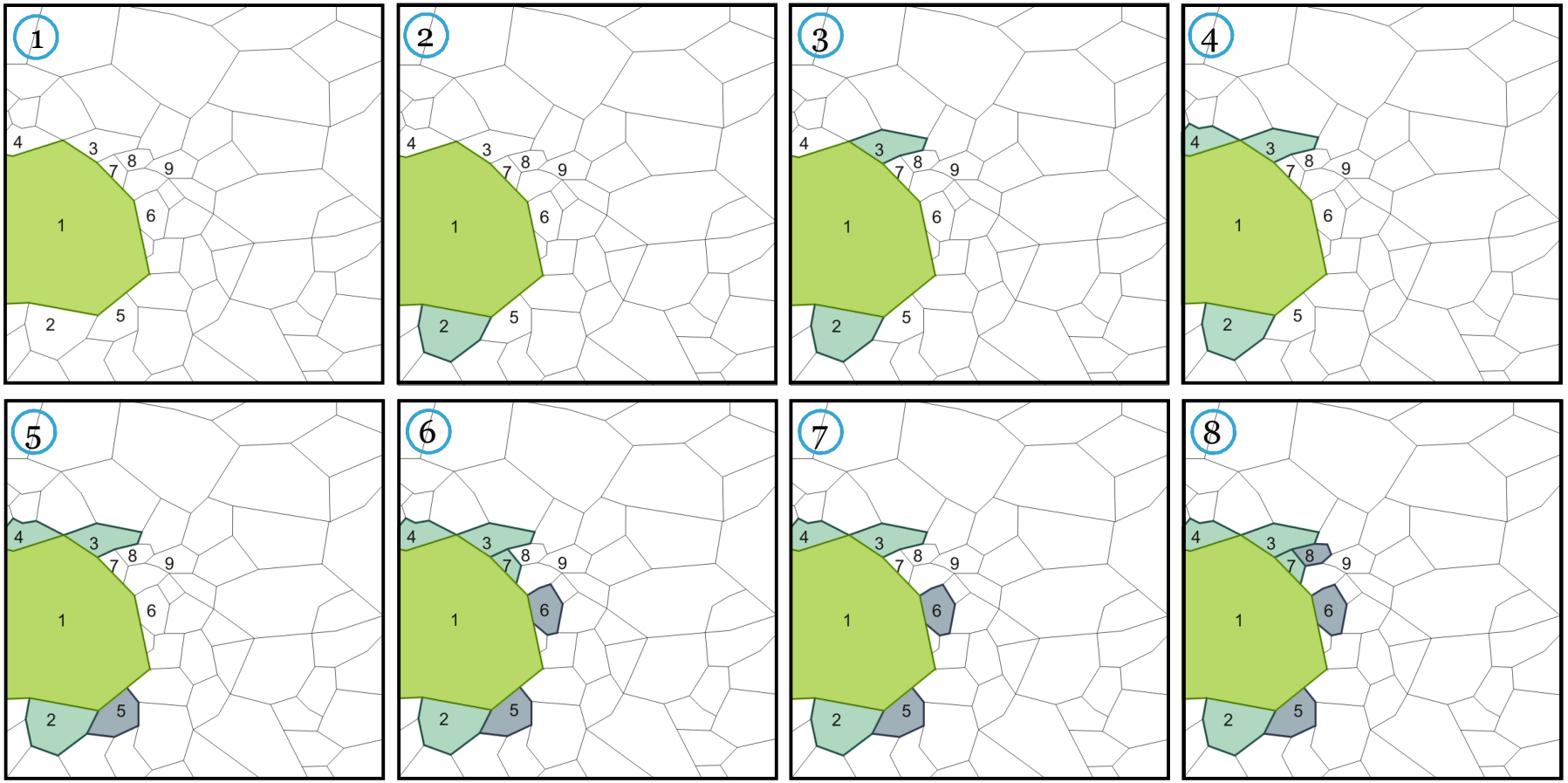
1
4
3
7
8
9
6
1
2
5
2
4
3
7
8
9
6
1
2
5
3
4
3
7
8
9
6
1
2
5
4
4
3
7
8
9
6
1
2
5
5
4
3
7
8
9
6
1
2
5
6
4
3
7
8
9
6
1
2
5
7
4
3
7
8
9
6
1
2
5
8
4
3
7
8
9
6
1
2
5

Appendix

The crack length is estimated as the square root of the total number of elements damaged, i.e., semicircular crack (Murakami, 2002)

Y. Murakami, Metal fatigue: effects of small defects and nonmetallic inclusions, Elsevier, 2002.

Appendix

Crack growth is the result of an irreversible change of crack tip displacement (CTD)

$$\frac{da}{dn} = \beta \cdot \Delta CTD$$

Driving force

Crack tip irreversibility

Based on Tanaka (1984,86,99) and related to dislocation emission via J-integral Rice (1992)

Appendix

Crystal plasticity for RR1000 Ni-base superalloy @ 650C

B. Lin et al. Mater. Sci. Eng. A, 527, 3581-87, 2010

$$\dot{\gamma}^{(\alpha)} = \dot{\gamma}_0 exp\left[-\frac{F_0}{\kappa\theta}\left\langle 1-\left\langle \frac{\left|\tau^{(\alpha)}-B^{(\alpha)}\right|-S^{(\alpha)}\mu/\mu_0}{\hat{\tau}_o\,\mu/\mu_0}\right\rangle^{p}\right\rangle^{q}\right] sgn(\tau^{(\alpha)}-B^{(\alpha)})$$

$$\dot{S}^{(\alpha)} = \left[h_S - d_D\left(S^{(\alpha)}-S_0^{(\alpha)}\right)\right]\left|\dot{\gamma}^{(\alpha)}\right|$$

$$\dot{B}^{(\alpha)} = h_B\dot{\gamma}^{(\alpha)} - r_D^{(\alpha)}B^{(\alpha)}\left|\dot{\gamma}^{(\alpha)}\right|$$

$$r_D^{(\alpha)} = \frac{h_B\mu_0}{S^{(\alpha)}}\left\{\frac{\mu_0'}{f_c\lambda}-\mu\right\}^{-1}$$

	Oct.	Cube
F_o	295	295
P	0.31	0.99
q	1.8	1.6
$\gamma_0 (s^{-1})$	120	4
$\tau_0 (GPa)$	810	630
$S_o (MPa)$	350	48
f_c	0.42	0.18
$h_B (GPa)$	400	100
$h_S (GPa)$	10	4.5
$d_D (MPa)$	6024	24
$\mu'_0 (GPa)$	72.3	28.6

Appendix

Grain size distributions

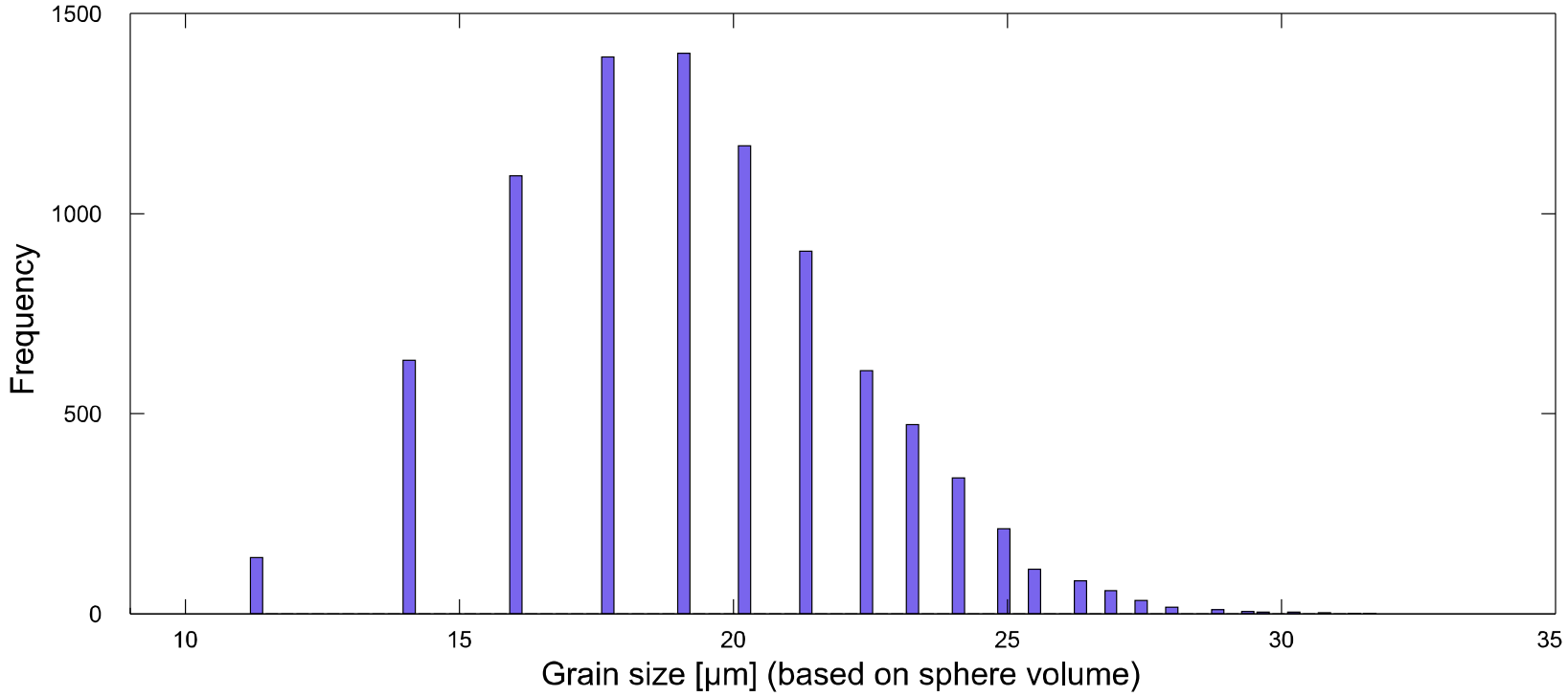

Appendix

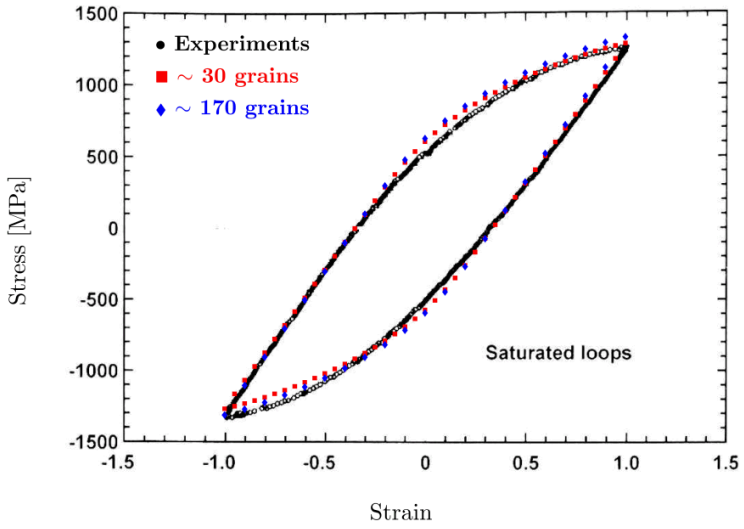

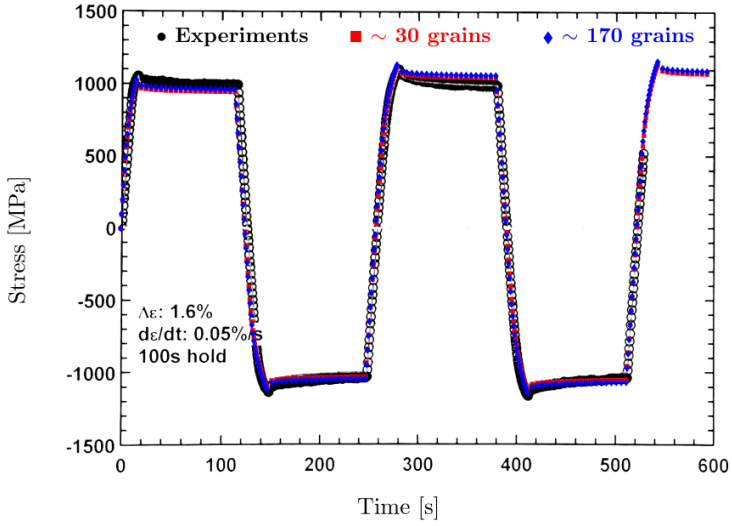

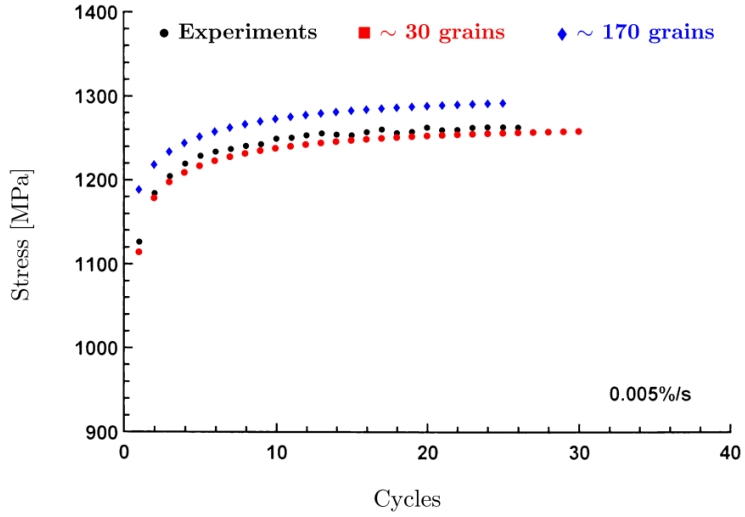

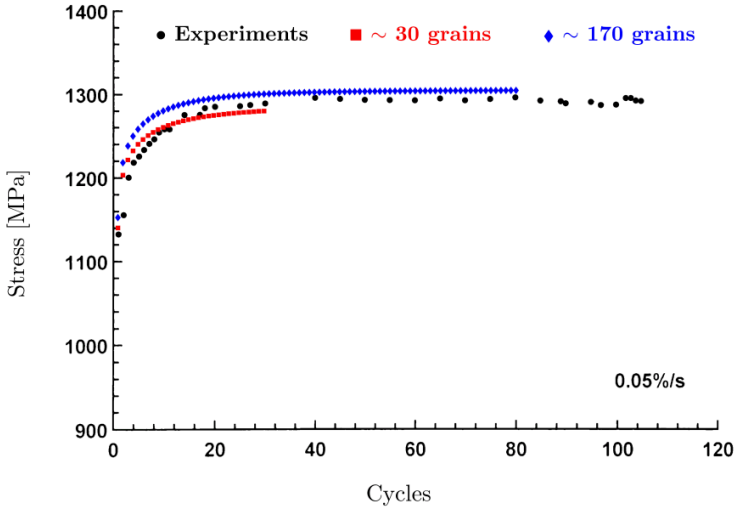

Zhan, Z., PhD thesis, University of Portsmouth, UK, 2004.

Strain localization

Mesoscale structures

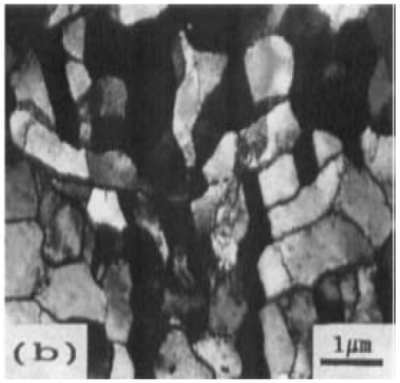

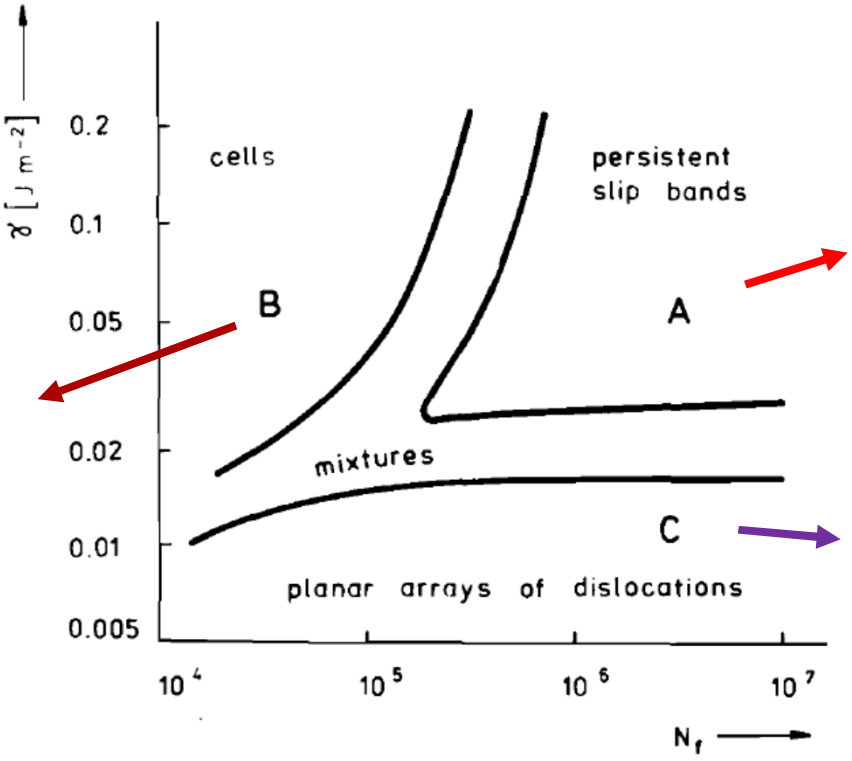

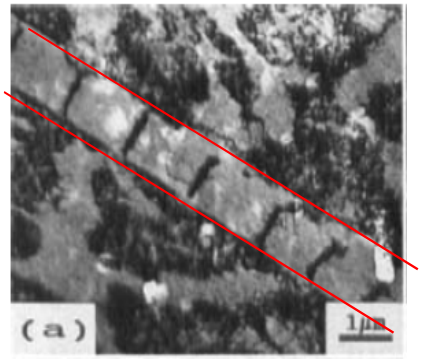

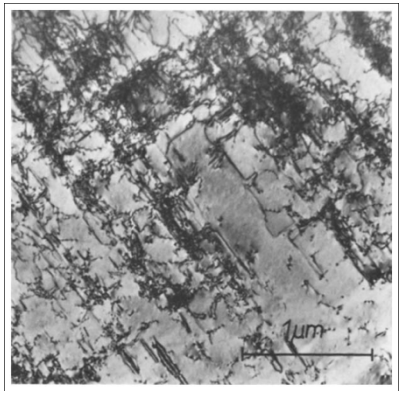

Adapted from **Klesnil M. and Lukas P**. Fatigue of Metallic Materials, Elsevier, (1992).

Appendix

The open literature seems to agree that in Ni base superalloys, cube slip is mainly due to zig-zag cross slip in octahedral planes, and starts at around 700°C.

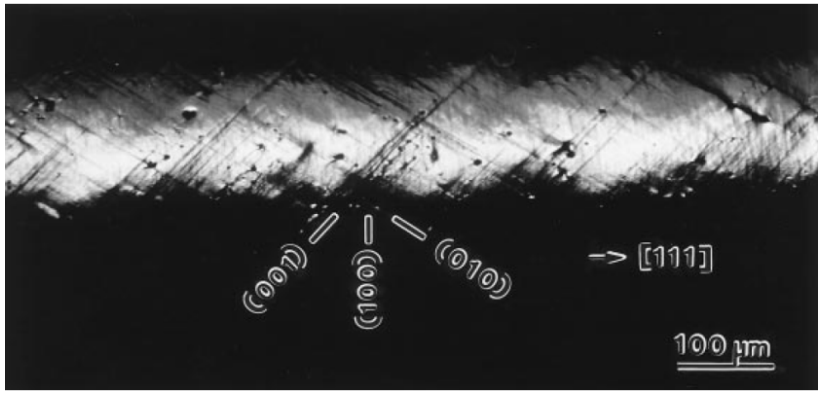

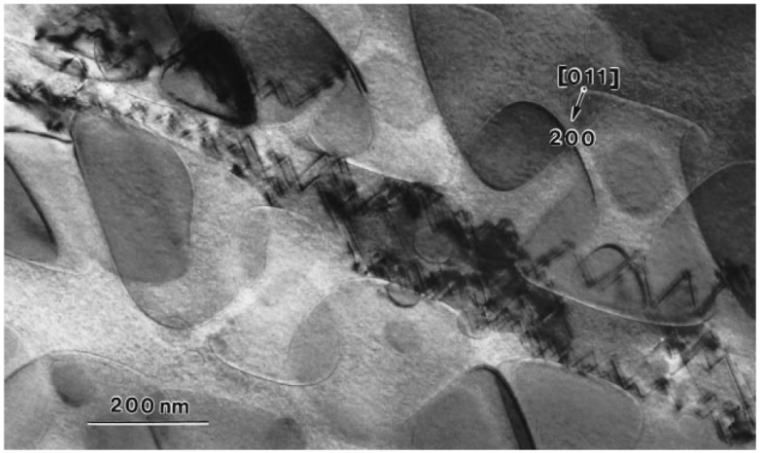

D. Bettge and W. Osterle, Scripta Materialia 40, 4, 1999: 389-395.

Appendix

Cross slip can occur when the following is satisfied:

1. Two slip systems must have the same slip direction.
2. The resolved shear stress should have the same direction on both slip systems.

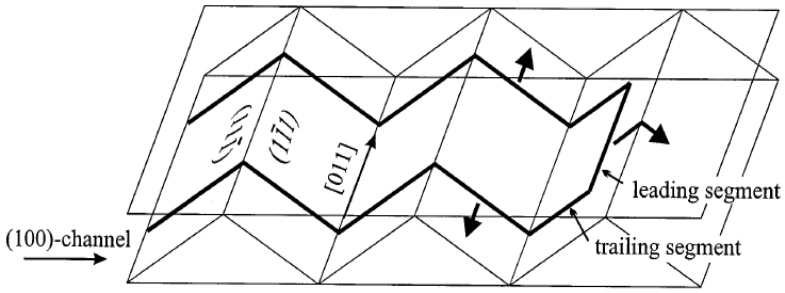

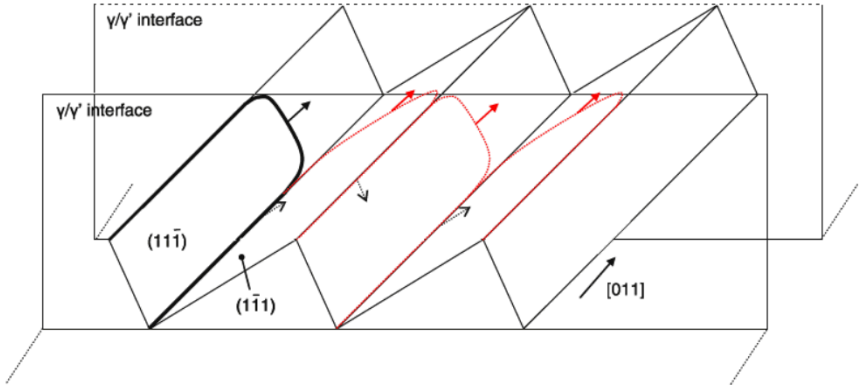

T. Tinga et al, Cube slip and non-Schmid effects in single crystal Ni-base superalloys, Modell. Simul. Mater. Sci. Eng 18, **1** (2010): 015005.

Appendix

U-notch specimen under bending

- Bending load 10.4KN (12.5x12.5x80 mm)
- 60 realizations
- Irregular mesh
- RR1000 alloy
- R=0.1

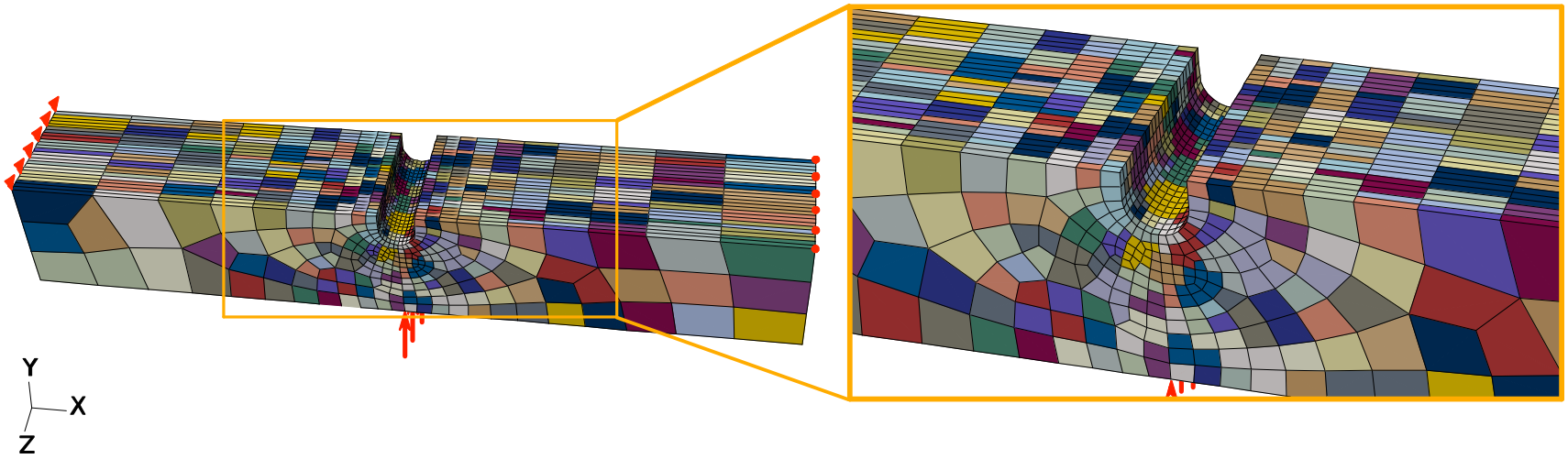

Computing the Crack Path

Mesoscale model - Mesh refinement

50 realizations

Element size:
- Refined: 5μm
- Coarse: 9μm

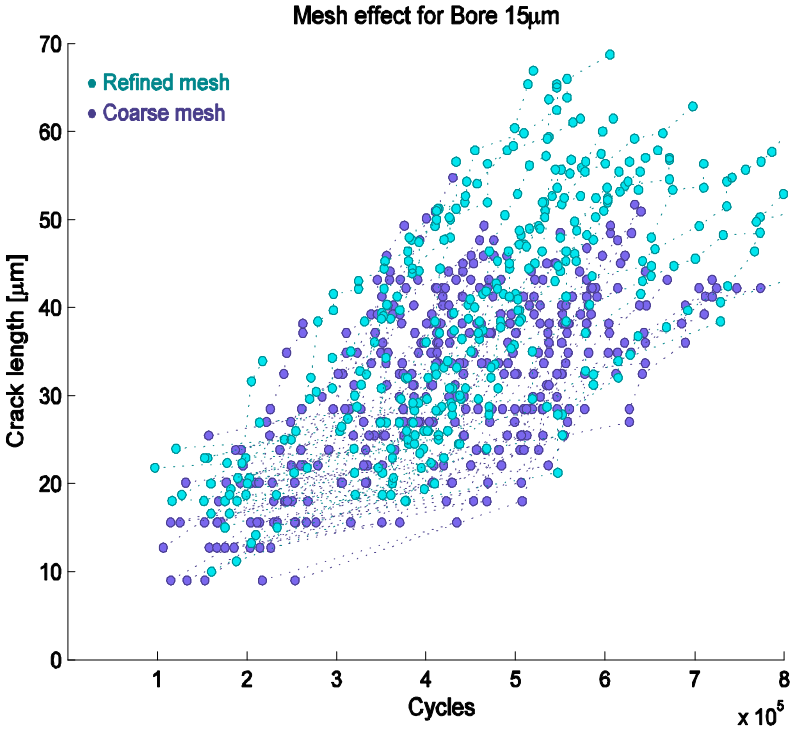

$$\ln(a) = c_1 N$$

Refined simulations have an average correlation coefficient of R=0.9127 with the crack length logarithm!!

Duplex Microstructures

Sandia National Laboratories

As large as (ALA) grains

50 realizations

Periodic Boundary Conditions

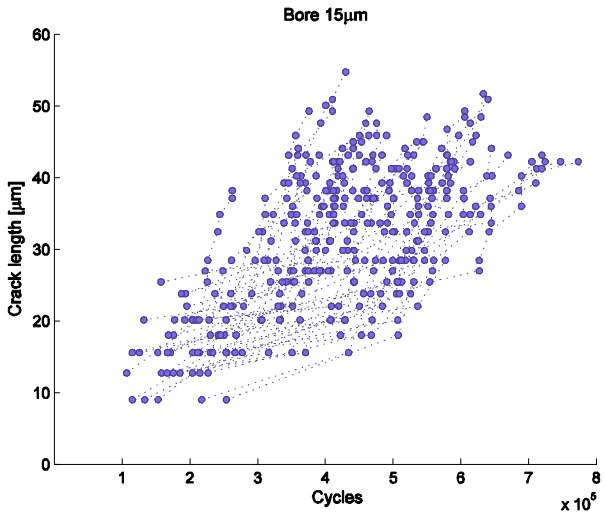

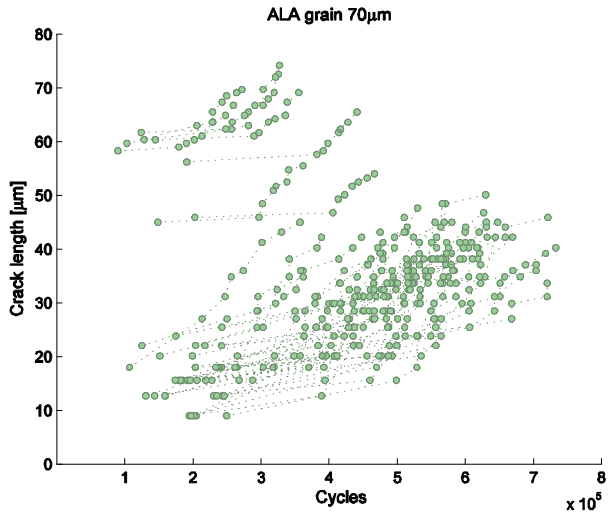

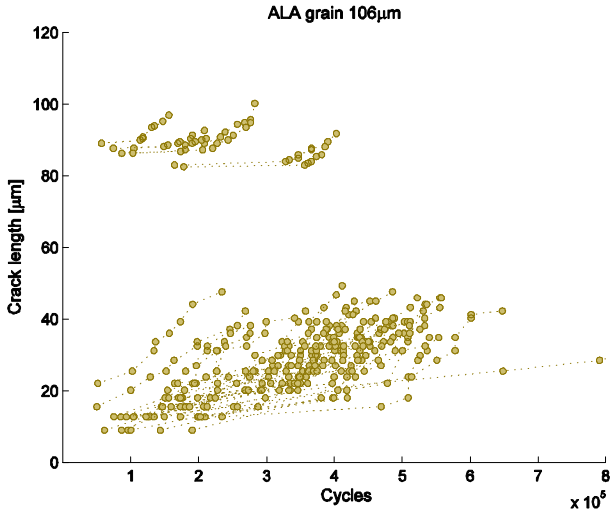

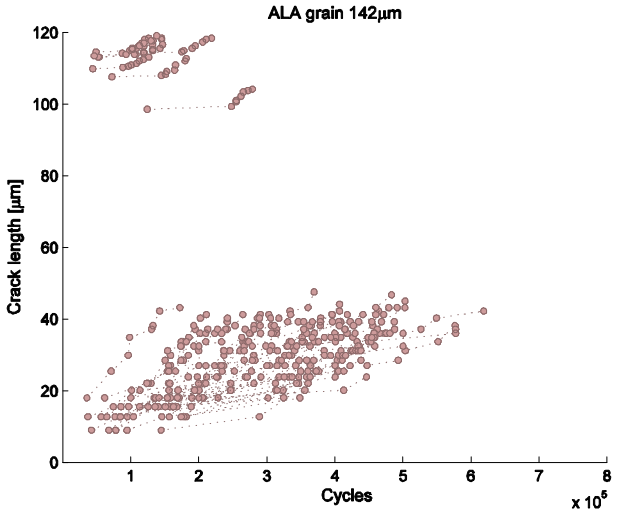

Appendix

Transgranular-Intergranular transition of ALA grains

50 realizations

Periodic Boundary Conditions

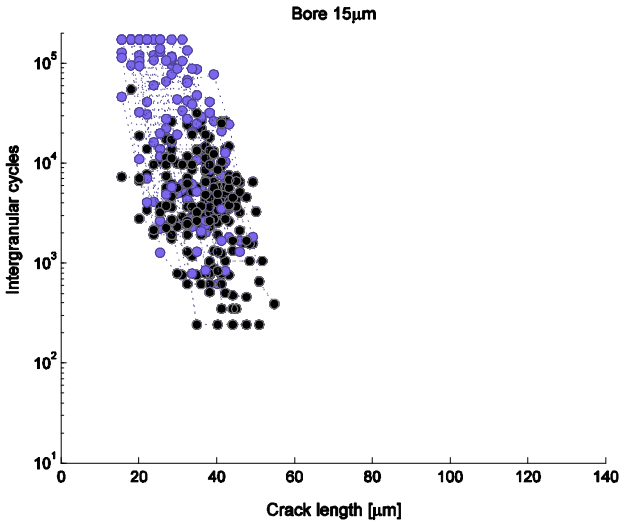

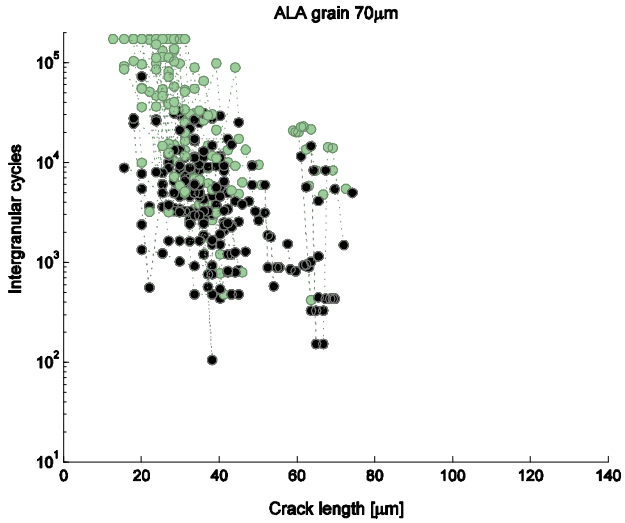

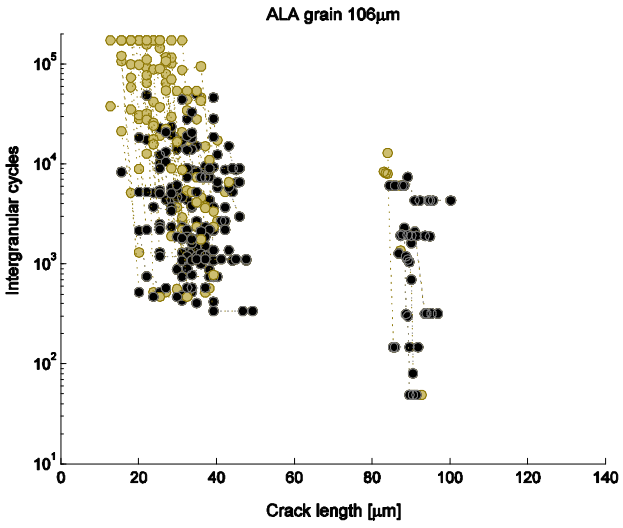

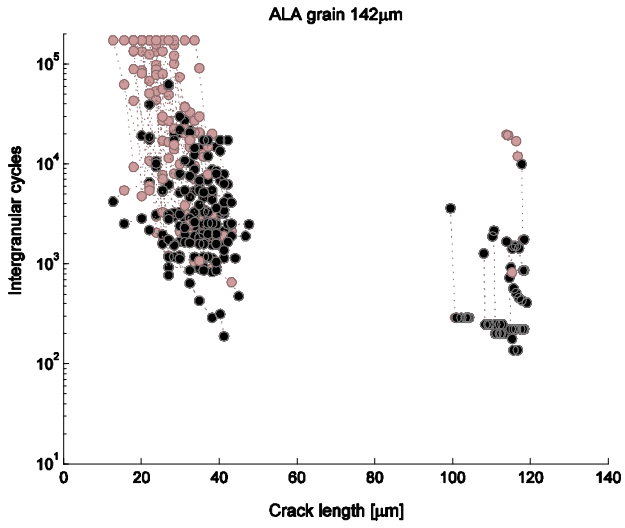

Appendix

FIP evolution within grains

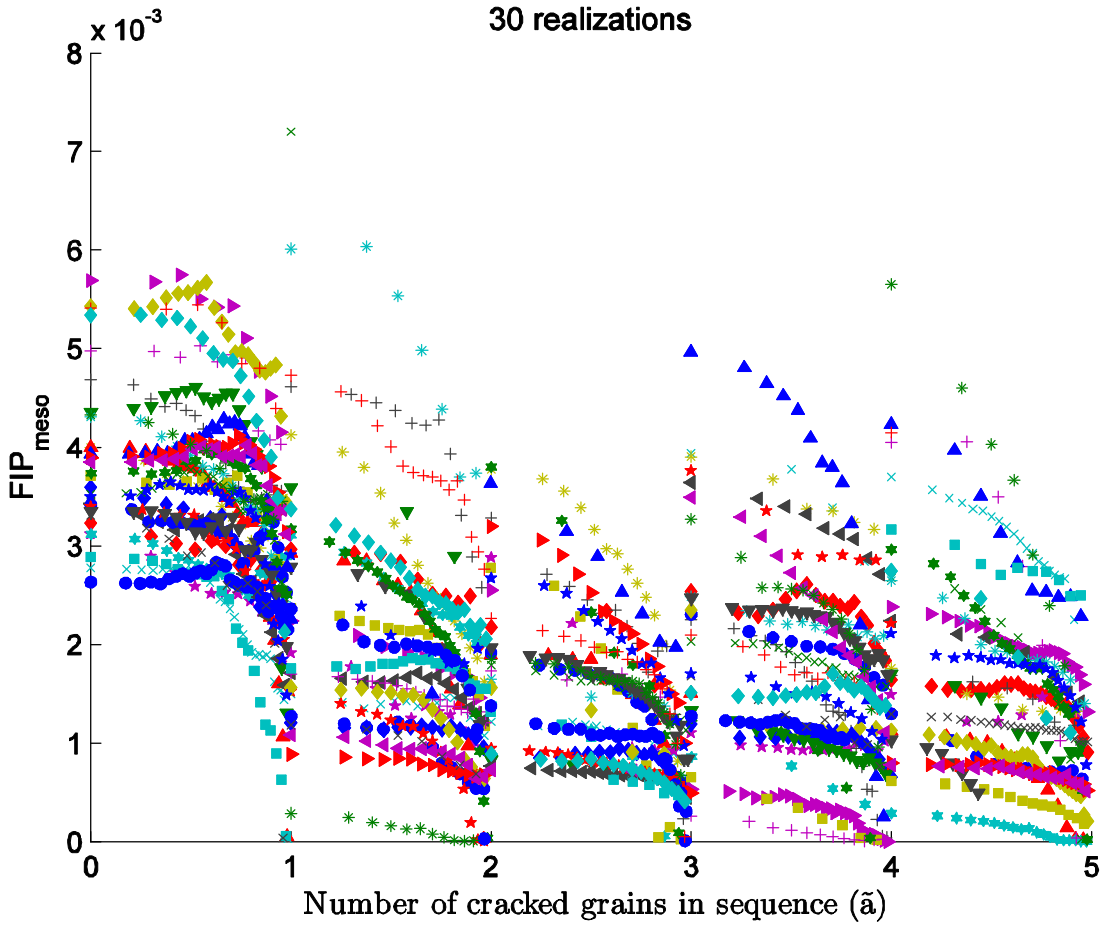

Computing the Crack Path

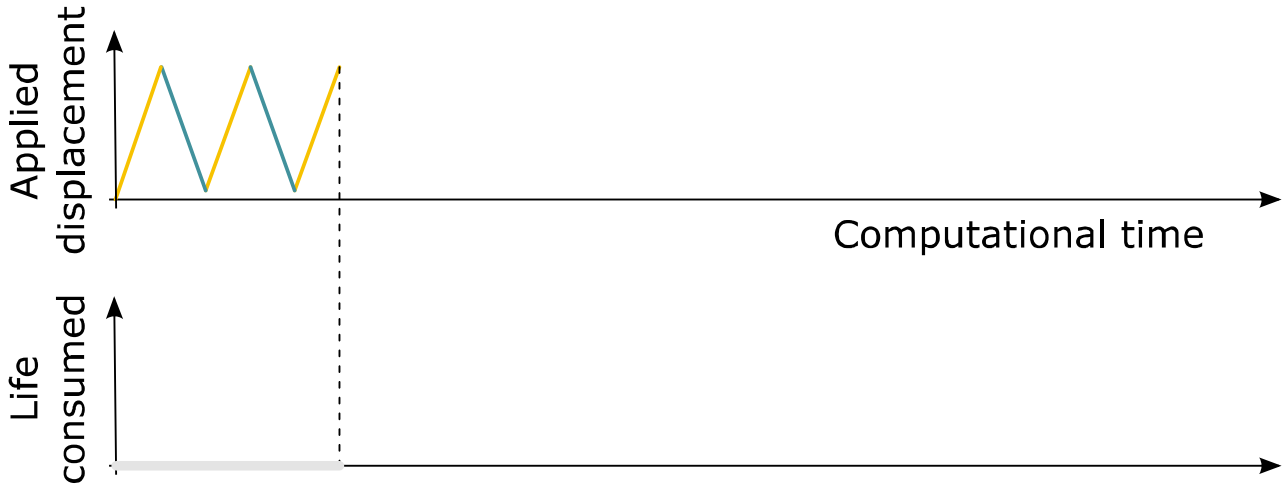

Computing the Crack Path

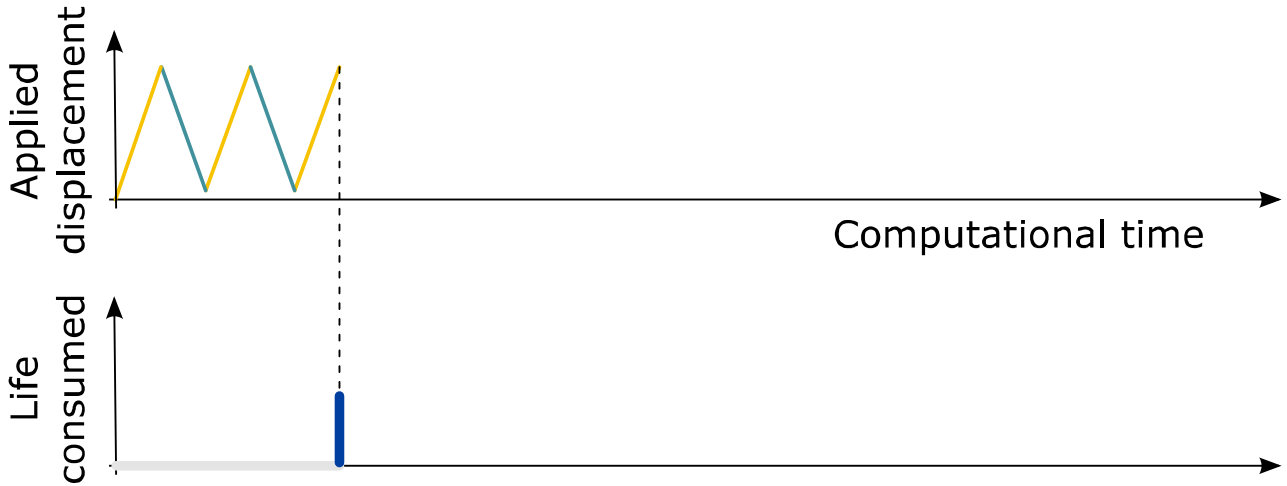

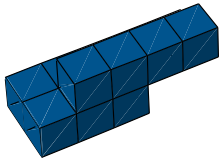

1st band (Nucleation)

Computing the Crack Path

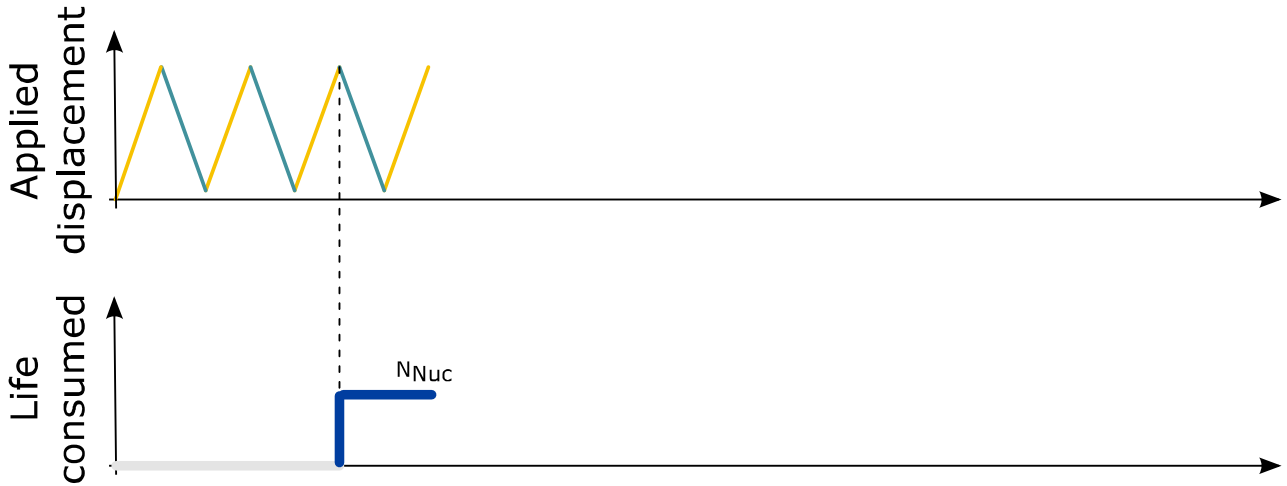

Degrade the elements in the band with shortest nucleation life

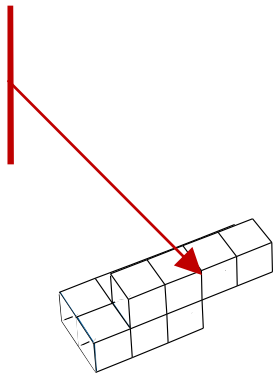

1st band (Nucleation)

Computing the Crack Path

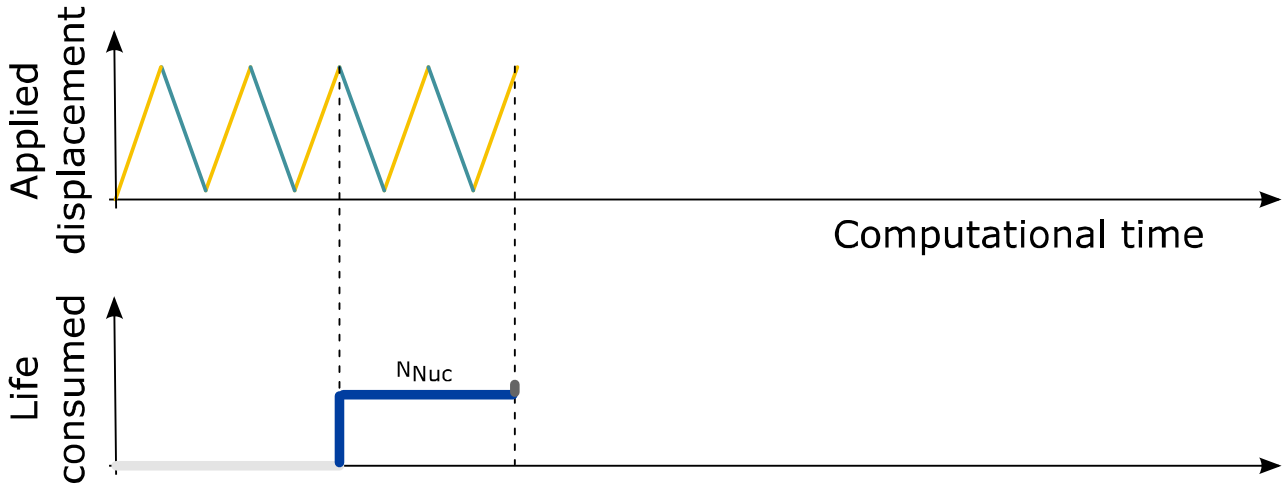

Find the band that intersects the crack front with shortest MSC life

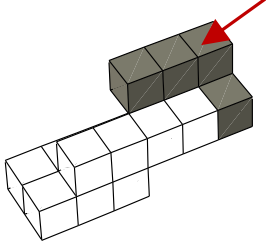

2nd band (MSC)

Computing the Crack Path

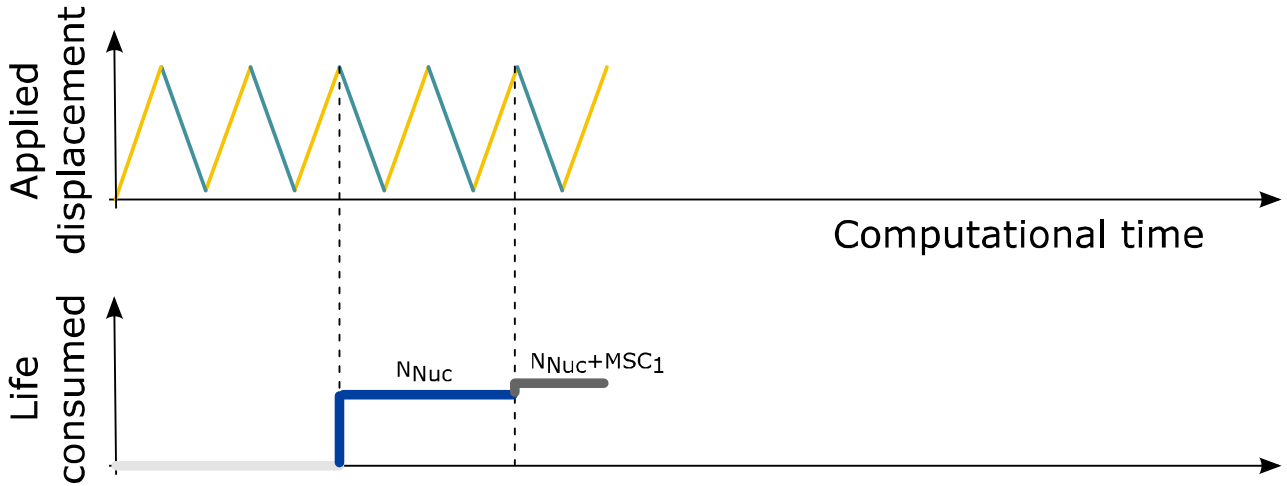

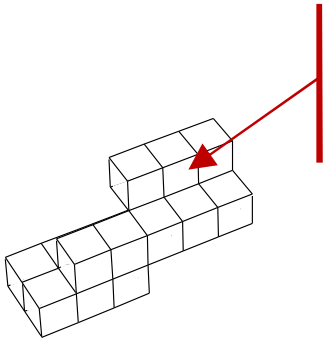

2nd band cracked

2nd band (MSC)

Computing the Crack Path

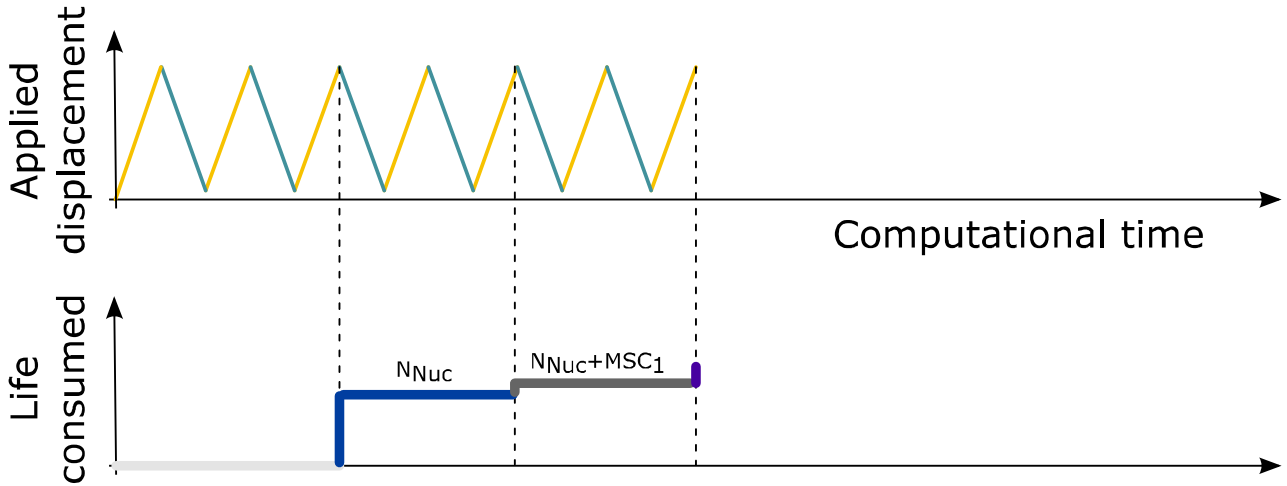

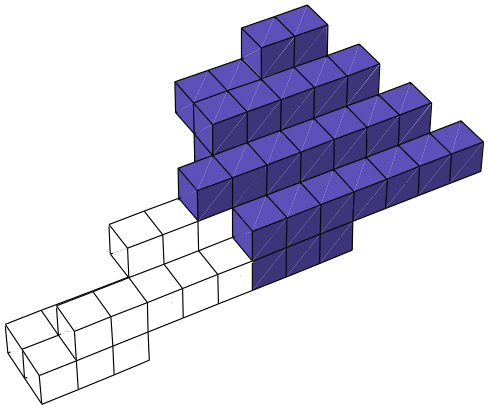

3rd band (MSC)

Computing the Crack Path

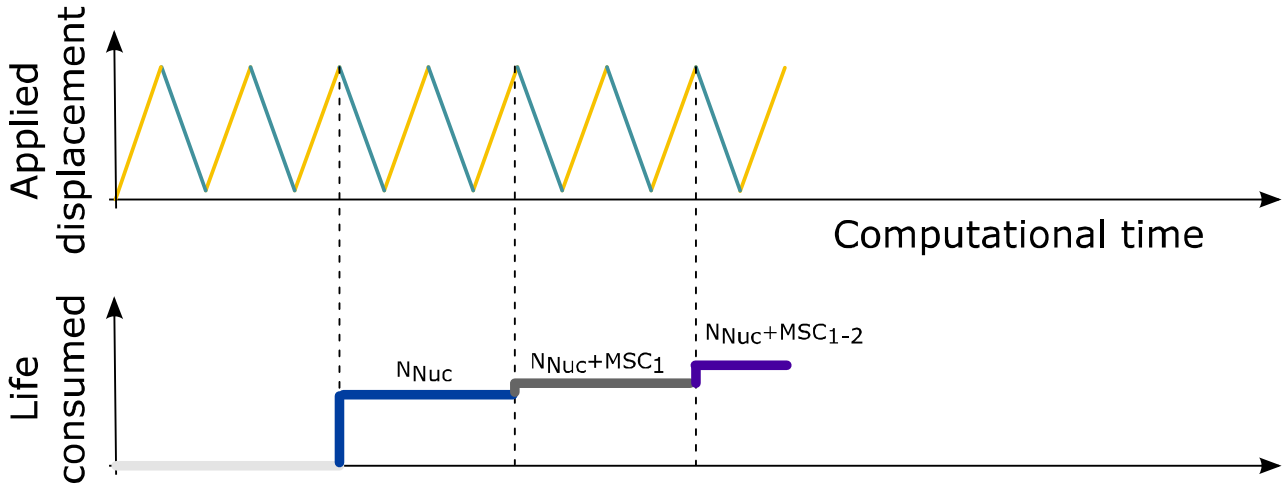

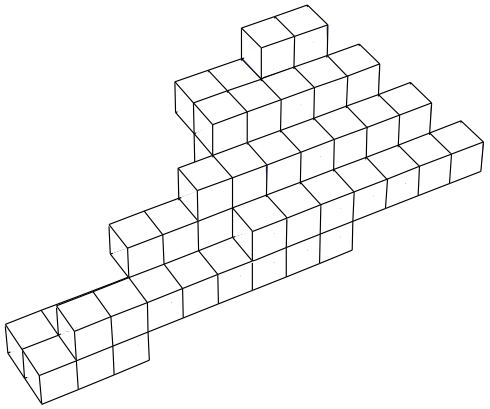

3rd band (MSC)

Computing the Crack Path

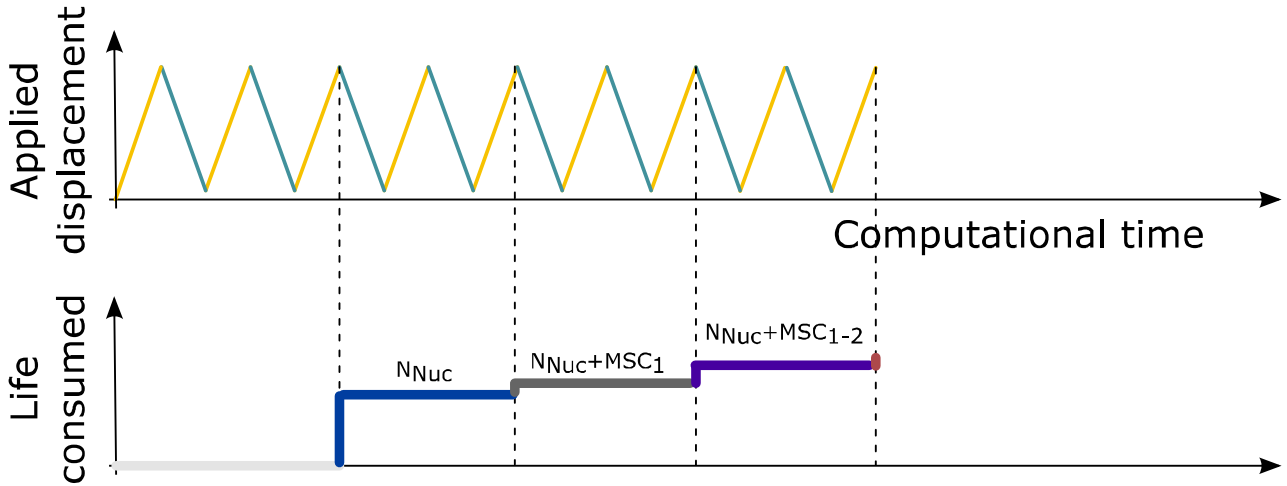

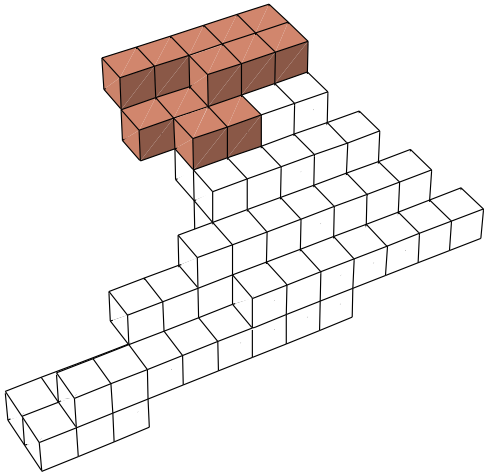

4th band (MSC)

Computing the Crack Path

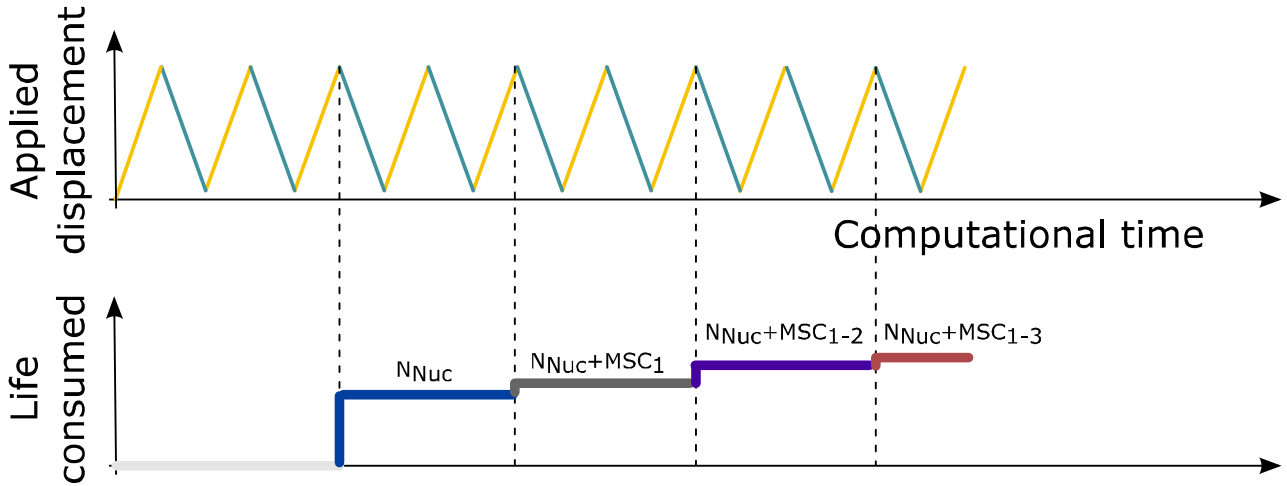

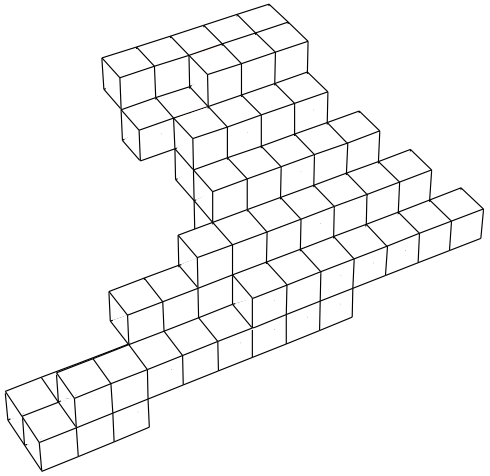

4th band (MSC)

Computing the Crack Path

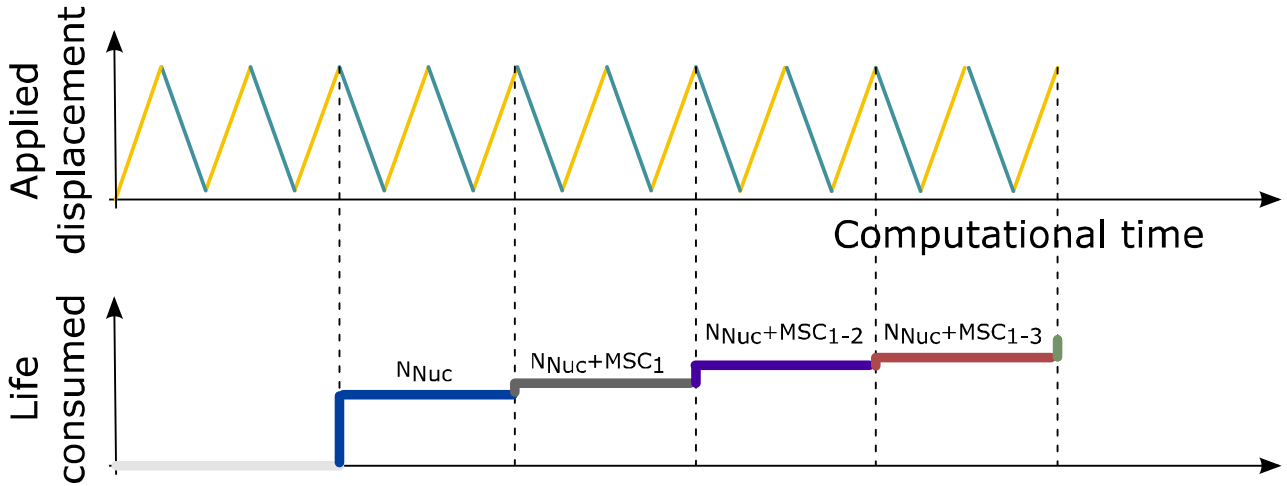

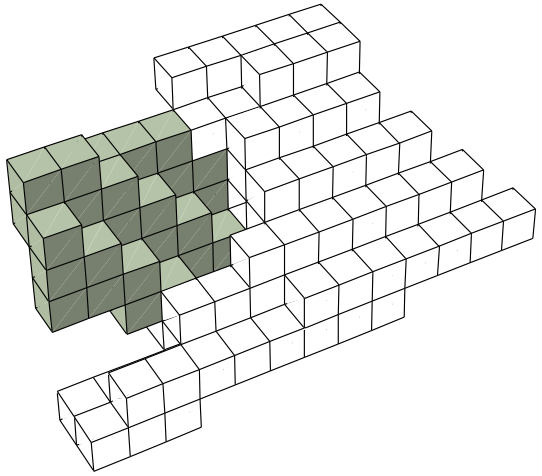

5th band (MSC)

Computing the Crack Path

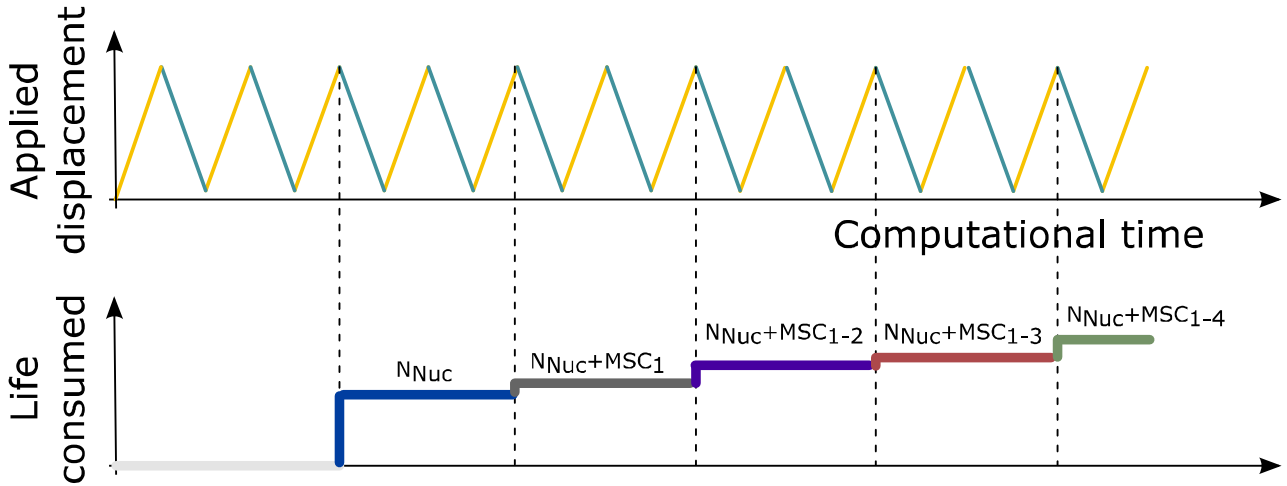

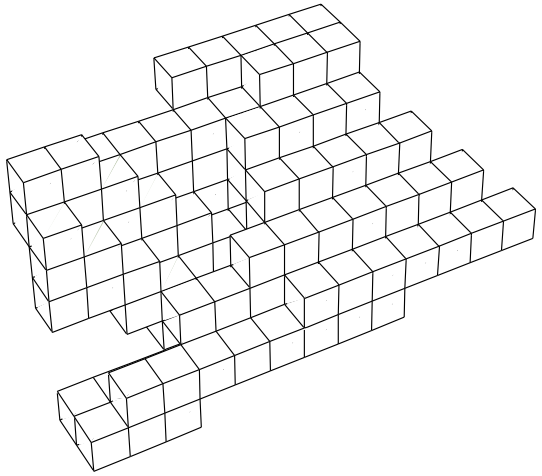

5th band (MSC)